Development of methodologies to identify polysialylated proteins and to visualize receptors for polysialic acid in biological samples

by

Muhammad Idrees

A thesis submitted in partial fulfillment of the requirements for the degree of

Master of Science

in

Physiology, Cell, and Developmental Biology

Department of Biological Sciences
University of Alberta

Abstract

Polysialic acid (polySia) is a homo polymer made of Sialic acid monomers linked to each other through α-2-8 linkages in humans. Its expression on cellular surfaces is limited to nervous, immune, and reproductive systems in a healthy adult human. It is overexpressed in certain tumors and results in higher invasion and metastasis. It increases cancer progression and severity and is associated with higher mortality and decreased survival rates. Only a handful of polysialylated proteins have been discovered so far. Willis's lab has confirmed the presence of more such proteins that need to be identified. Research has also shown that polySia is an immunomodulatory ligand, but additional studies are required to identify its receptor(s). To explore the polySia role further, the development of reliable and sensitive methods is essential as limited methodologies are available to work with polySia.

We propose two tactics to enhance polySia research. Firstly, we have developed a biotin-modified sialic acid that can be incorporated onto the polySia chain of polysialylated protein and subsequently extracted using streptavidin beads. Secondly, we propose employing a polysialylated fluorescent protein as a ligand to detect the presence of polySia receptors on immune cells.

The modified sialic acid with an attached biotin though disulfide linkage (CMP-Sia-S-S-Biotin) has been synthesized and successfully added to polySia chains on small molecules and cell surface polySia. We could also effectively extract biotin-polySia-protein with streptavidin beads and reduce the disulfide bond. To confirm the presence of polySia receptor(s), a fluorescent ligand was designed and incubated with Jurkat T cells. Later, the ligand was modified to enhance its avidity. These methods lay the groundwork for future research and development.

Preface

This thesis is an original work by Muhammad Idrees. No part of this thesis had been previously published.

List of conferences and presentations attended.

MCS Seminar 2021
Oral presentation on “Identification of receptors for polysialic acid on T and NK cells”.

ImmunoNet Research Day 2022
Poster presentation on “Identification of receptors for polysialic acid on T and NK cells”.

ImmunoNet Research Day 2023
Poster presentation on “Identification of receptors for polysialic acid on T and NK cells”.

Acknowledgment

الْحَمْدُ لِلَّهِ رَبِّ الْعَالَمِينَ

During my academic journey, I received unrelenting support, guidance, and encouragement from my supervisor, Dr. Lisa Willis, without whom I would not have been able to complete my degree. Dr. Willis has been a constant companion and mentor throughout my research work. She has generously invested her time and effort in my growth and development, both personally and professionally. Her expertise in the field of glycobiology and her comprehensive knowledge of research methodologies have helped me shape my research work and provided me with invaluable lessons beyond my academic field. Under her supervision, I have acquired skills that will undoubtedly be helpful in the future.

Furthermore, I would also like to express my sincere gratitude to my committee members, Dr. Matthew Macauley, Dr. Daniel Barreda, and Dr. Glen Uhrig. Their valuable advice, insightful feedback, and constructive criticism have significantly contributed to my success. Their support and guidance have helped me shape my research work, and their inputs have challenged my thinking and helped me develop a broader perspective. I am incredibly thankful for their time, effort, and commitment throughout my academic journey.

I would like to express my gratitude to all the talented and dedicated individuals who have been a part of the Willis lab, both past and present. I am truly appreciative of the valuable contributions made by Dr. Carmanah Hunter, Sogand Makhsous, Ellen Hayhoe, Bill Vouronikos, and the numerous undergraduate students who have worked with us over the years. Their hard work and commitment have been instrumental in advancing our research and achieving our goals. Thank you all for your dedication and contributions to the Willis lab.

Table of Contents

List of tables

List of figures

List of abbreviations

Acetonitrile	:	ACN
Adenine monophosphate	:	AMP
Adenine triphosphate	:	ATP
Alpha-1-antitrypsin	:	A1AT
Ascorbate peroxidase	:	Apex
Bacterial polysialyltransferase	:	bPST109
Bicinchoninic acid	:	BCA
Brain-derived neurotrophic factor	:	BDNF
Bovine serum albumin	:	BSA
B1 domain of protein G	:	GB1
Chemokine (C-C motif) ligand 2	:	CCL21
Chinese hamster ovary	:	CHO
C-C chemokine receptor type 7	:	CCR7
Colominic acid	:	CA
Cytidine monophosphate	:	CMP
Cytidine triphosphate	:	CTP
Disulfide	:	S-S
Deaminated neuraminic acid	:	KDN
Degrees Celsius	:	°C
Degree of polymerization	:	DP
Dithiothreitol	:	DTT
Double mutant	:	DM
Electroscopy ionization	:	ESI
Enzyme linked immuno-assay	:	ELISAs
Escherichia coli	:	*E. coli*
Endosialidase	:	EndoN
Fibronectin	:	FN
Fluorinated boron-dipyrromethene	:	BODIPY
Galactose	:	Gal
Glucose	:	Glc
Glycosaminoglycans	:	GAGs)
Green fluorescent protein	:	GFP
Heparin sulfate	:	HS
High Performance Liquid Chromatography	:	HPLC
Immobilized metal affinity chromatography	:	IMAC
Immunoglobulin	:	Ig
Interleukin-2	:	IL-2
Invasive cytotrophoblasts	:	iCTBs
Isoform-Specific O-Glycosylation Prediction	:	IsoGlyP
Lysogeny broth	:	LB
mAB735	:	Anti polySia monoclonal antibody
Matrix assisted laser desorption/ionization	:	MALDI
N-acetylmannosamine	:	ManNAc
N-acetylneuraminic acid	:	Neu5Ac

N-acetyl-9- phosphoneuraminic acid	:	Sia9P
Natural killer cells	:	NK cells
Neuropilin-2	:	NRP-2
New Zealand Black	:	NZB
Neural cell adhesion molecule	:	NCAM
Neuraminic acid	:	Neu
N-Glycolylneuraminic acid	:	Neu5Gc
Phosphate buffer saline	:	PBS
Phosphate buffer saline with tween	:	PBST
Peanut agglutinin	:	PNA
Polysialic acid	:	polySia
Quiescin Sulfhydryl Oxidase 2	:	QSOX2
Relative centrifugal force	:	RCF
Secondary horseradish peroxidase	:	HRP
Sialic acid	:	Sia
Sialic acid Azide	:	SiaAz
Sialic acid disulfide biotin	:	Sia-S-S-Biotin
Sialic acid binding Ig like lectin	:	Siglec
Sodium dodecyl-sulfate polyacrylamide gel electrophoresis	:	SDS-PAGE
Synaptic cell adhesion molecule	:	SynCAM
Systemic sclerosis	:	SSc
Thin layer chromatography	:	TLC
Tris(2-carboxyethyl)phosphine	:	TCEP
Tris-hydroxy propyl triazolyl methyl- amine	:	THPTA
Uridine diphosphate *N*-acetylglucosamine	:	UDP-GlcNAc
3′-3-5′-5-tetramethylbenzidine	:	TMB
4',6-diamidino-2-phenylindole	:	DAPI

Chapter 1: Introduction

1.1. Overview

Glycans are present on the surface of all eukaryotic and prokaryotic cells, forming a dense coating known as, the glycocalyx[1]. These glycans are typically bound to proteins and lipids through covalent bonds, resulting in glycoproteins and glycolipids, respectively[2]. The biological functions of glycans can be broadly categorized into three areas: structural support, energy metabolism, and information transmission. However, determining the specific role of a particular glycan is not that straightforward as a single glycan can serve multiple functions, and their structural diversity can add complexity to their functions[2, 3].

There are many types of glycans, but we are particularly interested in sialic acid (Sia) and its polymer, polysialic acid (polySia). PolySia plays a crucial role in both health and disease. In healthy adults, polySia is limited to the nervous, immune, and reproductive systems, and it is essential for fundamental processes such as synaptogenesis and cell migration[4]. In addition, it is expressed on the surface of most of the leukocytes and is a potent immunonmodulator[5]. However, polySia is overexpressed on cellular surfaces in certain cancers, and is associated with higher invasion and metastasis rates[6]. Unfortunately, the mechanisms behind these effects are not well understood, primarily due to a lack of research methods to study polySia and its interaction partners. To address this, we have been working on two potential methods to identify polysialylated proteins, as well as ways to confirm the presence of polySia receptors.

1.2. Sialic acid

In mammals, the most common terminal sugars are Sias which are important determinants of the biological functions of glycans[7]. Sias are also found on the surface of cells in all vertebrates and some invertebrates but not in plants[8, 9]. Based on side chains at carbon number 5, Sias are of four different types (Figure 1)[3]. These are, *N*-acetylneuraminic acid (Neu5Ac), *N*-glycolylneuraminic acid (Neu5Gc), deaminated neuraminic acid (KDN), and neuraminic acid (Neu)[10].

Although sialic acid refers to any number of this family, it is mostly commonly used for Neu5Ac which is the most abundant type of Sia in humans. The carboxylic acid group at carbon number 2 makes it acidic with the pKa value of 2.6[11] (Figure 1). In addition, the glycerol side chain results in formation of hydrogen bonds with the target while the *N*-acetyl group provides an interface for hydrophobic interactions[3, 12].

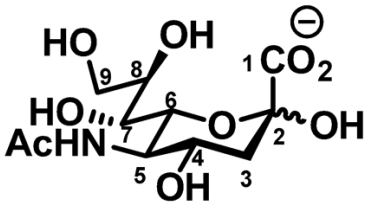

Neu5Ac

Figure 1. Structure of Neu5Ac

The initial stages of Neu5Ac biosynthesis occur within the cytoplasm and involve the synthesis of UDP-GlcNAc (uridine diphosphate *N*-acetylglucosamine) from glucose (Glc). UDP-GlcNAc 2-epimerase then converts UDP-GlcNAc into ManNAc (*N*-acetylmannosamine), which is the rate-limiting step (Figure 2)[13]. ManNAc kinase then phosphorylates ManNAc into ManNAc-6-phosphate[14]. Subsequently, Sia synthase combines ManNAc-6-phosphate with

phosphoenolpyruvate to form *N*-acetyl-9- phosphoneuraminic acid (Sia9P). Finally, Sia9P phosphatase carry out a de-phosphorylation step, resulting in the synthesis of free Sia[12,13].

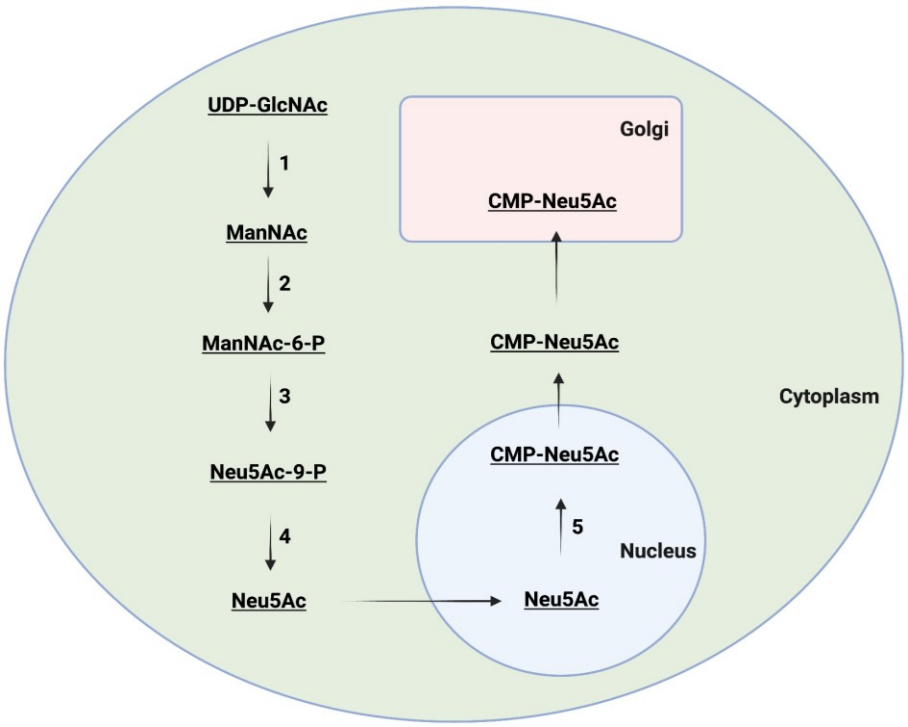

Figure 2. The process of Sialic acid biosynthesis.
The process of Sia biosynthesis initiates with the formation of UDP-GlcNAc from Glc which is then converted into ManNAc. ManNAc is phosphorylated into ManNAc-6-phosphate and is then converted into Neu5Ac-9-phosphate. A dephosphorylation step results in Sia. Sia undergoes activation and results in the synthesis of CMP-Sia. Enzymes; UDP-GlcNAc 2-epimerase (1), ManNAc Kinase (2), Sialic acid synthase (3), Neu5Ac-9-P phosphatase (4). CMP-Sia synthetase (5).

Sias cannot be utilized in glycan biosynthesis without their activation. This activation process is carried out by CMP-Sia synthetases using cytidine triphosphate (CTP) as a donor, resulting in the formation of CMP-Sia. However, this activation step occurs within the nucleus for reasons that remain unclear[12,13]. The newly activated CMP-Sia molecule is transported back

to the cytosol via an unknown mechanism before ultimately making its way to the Golgi lumen through the CMP-Sia transporter[12,13]. In the Golgi, CMP-Sia is enzymatically added to the terminus of underlying glycans through the anomeric carbon (C-2) of Sia by enzymes called sialyltransferases. CMP-Sias are covalently added to underlying galactose (Gal) through α-2,3 and α-2,6 linkages while linkage with *N*-acetylgalactosamine (GalNAc) could only be α-2,6. In addition, it is also covalently added to the underlying Sia through α-2,8[15].

Sia is a crucial player in various cellular processes, such as cellular signaling, migration, and intracellular interactions[15]. It plays a critical role in embryonic development[16]. Studies have shown that mice lacking Sia enzymes are unable to survive beyond the embryonic stage, indicating the essential role of Sia for survival during this stage[17]. Sia acts as a ligand for lectins, antibodies, enzymes, and receptors[18]. For example, during the development of B cells, a noticeable increase in the expression of α-2,6-linked Sia is observed. This coincides with the binding preference of the surface molecule Sia binding immunoglobulin like lectin 2 (Siglec-2) found on B cells, which plays a role in regulating the B cell response to antigen stimulation[10, 19]. On the other hand, it has also been observed that alterations in the expression of Sia are evident in several pathological conditions. Autoantibody production against Sia or antibodies that are improperly glycosylated are responsible for certain immune disorders[10, 20]. Changes in sialylation are also seen in many types of cancer and are linked to tumor progression[21]. Malignant cells tend to excessively express Sia on their surface, which may shield them from immune detection and elimination[21]. Additionally, certain pathogens employ molecular mimicry by coating their surfaces with Sia to evade recognition by the immune system[22]. In short, Sia expression plays a significant role in both the development of a healthy body and in the progression of diseases.

1.3. Polysialic acid

Polysialic acids (polySia's) are linear carbohydrate polymers that, in humans, consist of Sia residues linked by α-2,8 bonds[23]. The length of polySia chains can range from 8 to 400 monomer units, while chain length consisting of 2-7 is termed as oligoSia[24]. This categorization is based on anti-oligoSia/polySia antibodies. A minimum of eight Sias could make the required helical structure that is recognized by anti-polySia antibody while the anti-oligoSia could only bind to Sia chains that vary from 2-7[25]. The enzymes that synthesize polySia are called polysialyltransferases. In humans, two such enzymes ST8Sia2 and ST8Sia4 are the key enzymes for this process[26]. Both can synthesize polySia individually and their expression changes during development of a fetus and in adulthood[23]. The expression of ST8Sia2 decreases significantly, and that of ST8Sia4 decreases slowly after birth. Moreover, in adult humans, both have limited expression, but ST8Sia4 is the primary enzyme responsible for the presence of polySia[23, 27].

The most abundant, and well-studied polysialylated protein found in humans is neural cell adhesion molecule (NCAM). It is present in the nervous, immune, and reproductive systems in mammals[28, 29]. The extracellular domain of NCAM consists of five immunoglobulin (Ig) and two fibronectin (FN) domains[30] (Figure 3). Potential six glycosylation sites were marked but only two in Ig5 domain could be polysialylated[31]. PolySia chains when attached to NCAM, increase its hydrodynamic radius and affect its biological functions[32]. In addition, polySia could also mask proteins from their interaction partners because of its bulky structure[29] (Figure 3).

Aside from NCAM, synaptic cell adhesion molecule (SynCAM) and neuropilin-2 (NRP2) have also been identified that are polysialylated [33, 34]. Other putative polysialylated proteins exist but either await confirmation or are controversial. These proteins include C-C chemokine receptor type 7 (CCR7), voltage-gated sodium channel, and E-selectin ligand[35-37].

Furthermore, polysialyltransferase enzymes are also autopolysialylated, with ST8Sia4 displaying a greater extent of autopolysialylation compared to ST8Sia2[38]. The autopolysialylated ST8Sia4 covalently adds more polySia to NCAM, suggesting that this process could stabilize the interaction between enzyme and its substrate. Notably, a reduction in autopolysialylation negatively impacts the activity of these enzymes[38].

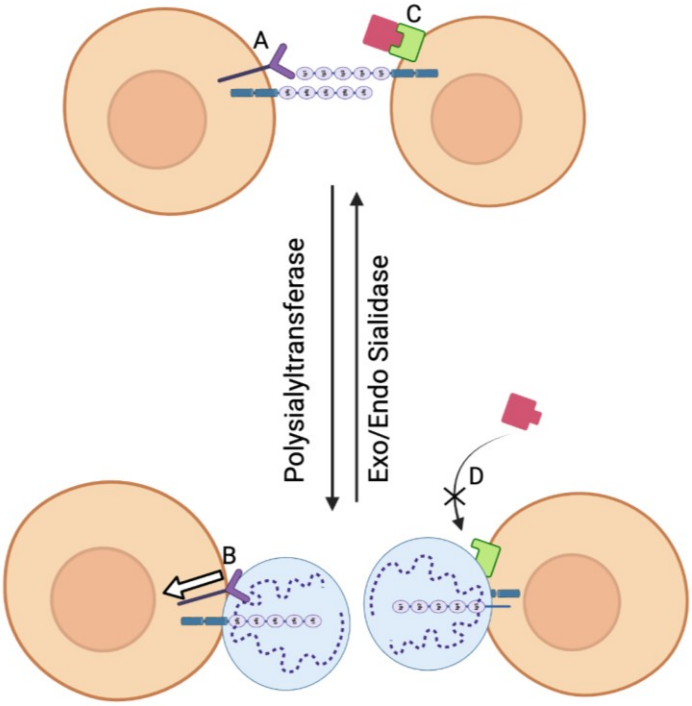

Figure 3. NCAM polysialylation and effects on its potential interactions.
Two cells appear near to each other in the absence of polySia, and the distance increases when polySia is present. By comparing "A" and "B," the polySia receptor effects could be observed, while by comparing "C" and "D," the polySia masking effects could be seen.

1.3.1. Interactions of polySia

The interactions of polySia on a molecular level are not well characterized. Because of its charged nature its interactions could be based upon the production of repulsive and attractive fields. Due to its bulky nature, negative charge, and hydration effect, it has been shown that

polySia affects interactions between cells and cell-extracellular matrix[39]. In one study, it was found out that the endosialidase reduced the distance between two polySia expressing cells by 10-15 nm when estimated with electron microscopy before and after endosialidase (EndoN) treatment[40]. PolySia when attached to NCAM, increases its hydrodynamic radius which results in higher intermembrane spaces and interferes with the adhesive properties of NCAM[41]. In addition, there is direct evidence proving that polysialylation of NCAM results in higher intermembrane repulsions and decreases homophilic interactions of NCAM[40]. Higher expression of polySia on cell surface has been observed in various cancers, such as neuroendocrine cancers, including glioblastomas and neuroblastomas[42],[51]. This has been linked to increased tumor progression, invasion, and metastasis resulting in a decrease in survival rates[42]. This could be the result of dissemination of cells from primary tumor mass because of the diminished cell-cell/matrix adhesion[42]. However, there are also cell lines which are heavily polysialylated and yet grow as clumps, suggesting that steric/charge repulsion is not the entire basis for polySia function[43].

In 2008, a study demonstrated that polySia not only possesses a repulsive field, but also an attractive field that enables it to capture biological molecules, for instance it binds to brain-derived neurotrophic factor (BDNF)[44]. Subsequent studies identified other biological molecules that could be captured by polySia, such as chemokine (C-C motif) ligand 21 (CCL21) and catecholamines[23, 45]. However, it is important to note that the binding of polySia to certain neurotransmitters and biological molecules like BDNF could be a receptor-ligand interactions. In addition to binding to polySia, BDNF also has the ability to bind to glycosaminoglycans (GAGs), like heparin sulfate (HS). When polySia and HS were immobilized and BDNF was introduced, the binding was nearly identical based on the K_D values[46]. However, when BDNF

was immobilized and polySia or HS was added, the K_D value of BDNF towards HS was almost unchanged, while the K_D value towards polySia decreased by two to three orders of magnitude[46]. This could suggest that the site used by BDNF to bind to polySia may already be inaccessible since it was likely utilized during immobilization.

PolySia may also act as a ligand for transmembrane receptors like the siglec-11 and siglec-16 proteins[47]. These interactions could result in inhibition or activation, depending on the receptor type[47, 48]. For example, binding of polySia to siglec-11 leads to the inhibition of microglial cells, whereas binding to siglec-16 causes activation of tissue macrophages. Interestingly, when both receptors are present on the same cell, they can neutralize each other's responses[49].

1.3.2. The Expression of PolySia

PolySia is prevalent during the developmental stages of mammals but diminishes rapidly postnatally or with maturity. In healthy adults, its cellular surface expression is limited to the nervous, immune, and reproductive systems. It is re-expressed in certain disease states e.g., Neuroblastoma and Glioblastoma etc[50, 51].

1.3.2.1. PolySia in Nervous System

In the nervous system, most polySia literature is related to polysialylation of NCAM, which was initially based primarily on the NCAM polySia research in murine models. In mice, polySia is expressed on the surface of cells throughout development with peak expression levels perinatally[52]. More than 95 % polySia perinatally is found on the isoforms of NCAM, i.e., NCAM-140 and 180[31]. During the first week of postnatal development, the amounts of polySia remain high, followed by a rapid decline (around 70 %) during postnatal days 9 to 17[53]. Approximately 10 % further decrease in polySia occurs during adulthood[53]. The expression of NCAM isoforms remains constant during the first three weeks of postnatal development, while

the decrease in polySia correlates with the appearance of polySia-free NCAM[34, 53, 54]. Both ST8Sia2 and ST8Sia4 are expressed in correlation with polySia expression during neurogenesis. In mice, when one polysialyltransferase is knocked out, the polySia expression is not affected, which suggests that the other polysialyltransferase compensates for the polysialylation[53, 55]. Knocking out both enzymes together affects polysialylation and results in only a 20 % survival rate after birth for four weeks of mice[55]. Double knockout mice confirms the critical role of polySia in embryonic development.

In the human brain, the rate of decrease in polySia expression on cellular surfaces is lower than in murine[31]. It persists till 12 years of age and contributes to plasticity[56]. From age 12 to 80 the expression of polySia remains low but has significant expression in certain brain regions[57]. The areas with significant expression are olfactory bulbs and hippocampus[46]. In addition, polySia NCAM expression has also been shown in substantia nigra[58], amygdala[59], and pons[60]. Its role is diverse; neural cell migration, axonal guidance, fasciculation, myelination, synapse formation, and functional plasticity of the nervous system are all processes in which it is involved[4, 36, 46, 58, 59, 60].

1.3.2.2. PolySia in Reproductive System

The current research about polySia in the human reproductive system is minimal. Its expression has been observed in sperms in sea urchins, and in mammals[61]. PolySia in the sperm of sea urchins has unique functions where it regulates the cellular calcium and the motility of sperm[61, 62]. In sperms of mammals, NCAM and ST8Sia2 have been found to be polysialylated. In addition, the presence of polySia has also been observed in the epithelial cells of epididymis[63]. In females, the trophoblast cells of the placenta also express polySia in the first trimester, which is decreased throughout the course of pregnancy. The expression of polySia is crucial for placental initiation. The invasive cytotrophoblasts (iCTBs), which are a subtype of trophoblasts, play an

important role in placentation. Removing polySia diminishes their migration and invasion, affecting their ability to perform their integral role[64]. In addition, the gestational trophoblastic tumor biopsies demonstrated that both malignant and benign tumors had higher polySia expression than first-trimester placental bed-site of a healthy female[65, 66].

1.3.2.3. PolySia in Immune System

The expression of polySia in the immune system is widespread, with most cell types having some level of polysialylation[36]. However, the proteins which are polysialylated are highly specific to cell type and species. For example, NCAM is the primary polysialylated protein expressed in human natural killer (NK) cells but is not found in mouse equivalents[29]. NCAM is also not expressed in other immune cell types, except for a subset of activated CD8+ T cells[67, 68]. Polysialylated NCAM in NK cells has been proven to control its cytotoxicity. NK cells that are activated exhibit elevated levels of polySia and NCAM[69]. In addition, the CRISPR-Cas9 deletion of NCAM resulted in the reduction of NK cells to kill tumors[70].

In addition to NCAM, two other cell surface proteins have been identified that are polysialylated in the immune system i.e., NRP-2 and CCR7 [71]. NRP-2 is a coreceptor for a wide array of class III semaphorins and vascular endothelial growth factor family proteins. It is expressed in many cell types but has only been shown to be polysialylated in macrophages and dendritic cells[71, 72]. CCR7 is a chemokine receptor that mediates the migration of a wide array of immune cells towards the chemokines C-C chemokine ligand 19 (CCL19) and CCL21. Polysialylation of CCR7 was demonstrated in dendritic cells where it was specifically required for the migration of these cells towards CCL21 but not CCL19[72]. The relative contributions of polysialylated NRP-2 and CCR7 to CCL21-mediated migration is the subject of some debate[71].

Polysialylation of immune cell surface proteins is associated with cell activation. For example, polySia levels increase substantially as NK, dendritic cells, macrophages, and T cells

become activated and/or mature[73, 74]. Similarly, infection of monocyte-derived M2 macrophages with human rhinovirus resulted in the upregulation of ST8Sia4[75]. However, the effect of this increased polySia on immune function is less clear. While polySia may be involved in migration of specific cells to different areas of the body, it also appears to be involved in regulating the immune response. For example, polySia promotes the anti-inflammatory functions of THP-1 macrophages through binding to siglec-11[76]. Similarly, polySia on dendritic cells may play a role in regulating their effect on T cell proliferation and the secretion of proinflammatory cytokines[36, 77]. However, given T cells do not express any siglec receptors[76], the mechanisms by which polySia regulates T cells, are likely to depend on other proteins that have not yet been identified.

1.3.2.4. PolySia in disease

PolySia is a crucial part of physiological and pathological processes and its altered expression levels on cellular surfaces, have been associated with diseases. It has been found associated with different types of cancers specially tumors of the nervous system e.g., neuroblastoma, and glioblastoma etc[50, 51]. NCAM is thought to be the main carrier of polysialylation in most cancers[46]. Higher polySia expression has been found associated with an increase in cancer progression, higher metastasis, and decrease in survival rates in many different polySia expressing cancers[78, 79]. Research is underway to utilize the polySia expression in diagnostics to identify the stages of cancers[80] and to find out therapeutics to regulate the expression of polySia in tumors[81].

Systemic sclerosis (SSc), an autoimmune disorder, has similarities with cancer in terms of angiogenesis, inflammatory responses, immune dysregulations, tissue remodeling, and changes in the extracellular matrix[82]. Recently it was found out that SSc shows dysregulation of polySia cell surface expression in correlations with the severity of the diseases and the highest

polySia concentrations were found in diffuse SSc[83]. Diffuse SSc involves rapid progression of skin fibrosis with extensive skin involvement[5].

Aberrant polySia expression on surface of cells has also been observed in neurodevelopmental, neurodegenerative, and psychiatric disorders. In schizophrenia, a decrease in polySia-NCAM staining was observed in the hypothalamus when compared to the healthy brain[84]. This decrease was not observed in other parts of the brain e.g., amygdala which demonstrated that polySia impairment in schizophrenia is region specific[84, 85]. In addition, bipolar disorder and autism spectrum disorders were also found to have less polySia. This was based on the lower expression of ST8Sia2 when compared to a healthy control[86, 87]. On the contrary, in Parkinson's disease, and in Alzheimer's, the expression of polySia was found to increase especially in the case of Alzheimer's, where its increase was associated with the severity of the disease[88, 89]. It is clear from these studies that determining which proteins are polysialylated and which interact with polySia has the potential to provide mechanistic information about the function of the immune system in both health and disease. However, the properties of polySia can make it challenging to study using traditional methodologies.

1.3.3. Tools to study polysialic acid in complex biological mixtures.

Antibodies have been developed to detect polySia. The most commonly used antibody is mAB735, which is a monoclonal antibody and has a high specificity for polySia and a higher binding affinity with a K_D value of 7×10^{-9} M[90]. It was originally isolated from spleen cells from an autoimmune New Zealand Black (NZB) mouse that was immunized with *Neisseria meningitidis* and *Escherichia coli (E. coli) K1*[91]. To bind, mAB735 often requires a long segment of Sias, and the affinity appears to increase with increasing chain length. The helical segments of longer polySia forms fit into the binding site in the Fab fragment of the antibody[91]. A minimum

of 8 Sias could make the helical structure and could be recognized by mAB735. It is a useful tool in blots and, in enzyme linked immuno-assay (ELISAs) with a secondary horseradish peroxidase (HRP) -linked antibody[91]. Blotting polySia is not without its limitations. Because of its bulky size, variable chain length and variable polysialylated protein levels, it affects protein mobility, successful blotting and antibody recognition[5]. In addition, Serum samples have high concentrations of serum albumin, which distorts sodium dodecyl-sulfate polyacrylamide gel electrophoresis (SDS-PAGE) gels when loaded in sufficient quantities to visualize polySia in an immunoblot[5].

A fluorescent polySia lectin, $EndoN_{DM}$-GFP, is also used to detect and confirm the presence of polySia. It stains polySia on the surface and inside the cells, followed by imaging with florescent microscopy and/or image-cytometry[5, 35]. $EndoN_{DM}$ was produced by making mutations in the two essential amino acids in the catalytic site of EndoN (endosialidase)[35]. EndoN belongs to the category of sialidases that cleaves the α-2,8 linkages within oligoSia and polySia chains. Bacteriophages that infect bacterias encapsulated with polySia, express tail spike proteins that possess sialidase activity that is specific for oligoSia (DP > 5) and polySia. These enzymes are essential for bacteriophages to infect polySia encapsulated bacterias. EndoN, an endosialidase from bacteriophage KF1, has been extensively studied and is widely used in polySia research. It is a homotrimer that can bind to three polySia chains simultaneously. Its double mutant inactive version ($EndoN_{DM}$) is used as polySia lectin as it binds to polySia with great efficiency and specificity through its binding site and it cannot cleave it because of the mutations in the catalytic site[35, 92].

Willis's laboratory has developed an ELISA method that sandwiches polysialylated proteins between the $EndoN_{DM}$-GFP and mAB735 antibody, followed by a secondary antibody

attached to HRP. The entire process can be completed in a day and is highly sensitive in quantifying polySia. Additionally, it is carried out under non-denaturing conditions which is important as polySia is labile in nature[5].

Table 1. Probes to detect polySia.
Anti polySia antibody followed by a secondary HRP linked antibody is primarily used to carry out blots to confirm the presence of polySia. In addition, GFP-EndoN$_{DM}$ is also employed in GFP blots and in ELISAs to detect and quantify polySia. In both cases the EndoN treated sample where polySia is cleaved is used as a negative control.

No.	Type of Probes
1	Anti-polySia antibody (mAB735) followed by a secondary HRP linked antibody (DP>8)
2	GFP-EndoN$_{DM}$, a lectin for polySia and oligoSia (DP>5)

Isolating and enriching polysialylated proteins can enhance the detection sensitivity, particularly for those that are found in low abundance. Furthermore, obtaining purified polySia after release is a crucial prerequisite and a significant step towards achieving precise structural characterization of polySia. Several established techniques for isolation and purification can be utilized for this purpose (Table 2).

A couple of non-specific methods include size exclusion and anion exchange chromatography. In addition, organic solvent precipitations are also used to purify free polySia and polysialylated proteins. Size exclusion chromatography (SEC) is a conventional method to isolate polySia-bound glycoproteins from small molecules. Molecules are separated based on their hydrodynamic volume and molecular size. Porous polymeric resins in the stationary phase of SEC retains smaller molecules and elute them slower while the larger molecules are eluted faster. However, this method could be time-consuming, and compounds of the same molecular weight could not be separated[93]. Anion exchange chromatography involves a column of

positively charged materials that capture negatively charged molecules. A high ionic strength buffer is then used to elute the captured molecules. However, this method cannot distinguish between polysialylated protein, free polySia, and other molecules such as nucleic acids[94]. Chloroform/methanol/aqueous buffer extraction separates polysialylated proteins from membrane lipid content as lipids are dissolved in organic solvent while proteins and peptides are precipitated to form a pellet via centrifugation[95]. Acetone is also used to precipitate polysialylated proteins at low temperatures. However, re-solubilizing the precipitated polysialylated proteins could be challenging[63]. Organic solvent (ethanol) precipitation can also be used for separating free polySia. This is an easy and low-cost method, but ethanol might not be efficient in precipitating polySia with shorter degree of polymerization (DP)[96].

Table 2. ***The extraction and purification methods for polySia bio-conjugates.***
The method type along with its major limitation are outlined. The first four methods included, are non-specific in nature and the final samples end up with impurities. The last two methods where mAb735 is utilized are specific in nature and are dependent on the quality of the antibody used.

No.	Method type	Specificity	Major limitations
1	Size exclusion chromatography	X	Similar sized molecules could not be separated.
2	Anion exchange chromatography	X	Free polySia vs polySia-conjugates could not be seaparated.
3	Organic solvent de-lipidation	X	Contamination and re-solubilization problems.
4	Free polySia precipitation	X	Short chain polySia could not be precipitated.
5	Immuno-affinity chromatography	✓	Costly and dependence on quality of antibody.
6	Bead based extraction	✓	Costly and restricted to low volume samples.
7	Immunoprecipitation	✓	Dependence on quality of antibody and less yield.

Anti-polySia antibody (mAB735) and EndoN_{DM} are employed to purify polysialylated proteins and free polySia and are considered highly specific and efficient tools. These probes are polySia-specific and can be used to coat the stationary phase for immunoaffinity chromatography. For instance, researchers have successfully employed coating with mAB735 to purify peptides-polySia from cell lysates[97]. Additionally, the anti-polySia antibody could function as an immunoprecipitation tool. This method involves incubating the antibody first with biological samples to capture the polysialylated proteins. The protein-antibody complex is then captured with Protein A/G coated beads because of the interaction between protein A/G and Fc region of the antibody. This is followed by washing steps and elution[73]. However, it is important to note that immunoaffinity based purification has some limitations, including its high cost and dependence on the quality of the antibody[98].

PolySia cleavage from glycoproteins is necessary for the analysis of polySia. Both chemical and enzymatic methods can be used for this purpose. However, these techniques carry a significant risk of polymer degradation because of the sensitivity of polySia to chemical hydrolysis outside neutral pH conditions[99]. Chemical approaches include mild hydrolysis and alkaline-based methods. In mild hydrolysis, polySia is separated from the protein in a slightly acidic environment (trifluoroacetic acid, 20 mM, pH 2)[99]. The α-2,6 or α-2,3 Sia-Gal glycosidic bonds between polySia and the underlying glycan are more sensitive to mild acid attack than the polySia itself. Additionally, the lactonization under acidic conditions also contributes to the stability of polySia[99]. However, mild hydrolysis could still cause the cleavage of longer polySia. Enzymatic cleavage of polySia is a more specific method, as a particular enzyme can be used that cleaves a specific bond, such as endo-β-galactosidase, which cleaves the internal β-1,4 galactose linkage (repeating *N*-acetyl-lactose amine)[24]. The released polySia's are labelled with a

fluorochrome and could then be analyzed further with high performance liquid chromatography (HPLC)[24].

HPLC is commonly utilized to detect polySia chains that are linked to a fluorochrome, such as fluorinated boron-dipyrromethene (BODIPY). However, polySia chains with higher DP (which varies based on the type of column) cannot be distinguished and are eluted at the same retention time[98]. In addition, it can also be used to identify polysialylated proteins, provided the protein's molecular weight is low. Mass spectrometry is another option for analyzing shorter polySia chains, but caution must be exercised in selecting the type of ionization used, to prevent the cleavage of polySia chains[98]. Electroscopy ionization (ESI) and matrix assisted laser desorption/ionization (MALDI) are two soft ionization methods that could be adopted but the length of polySia chain could affect its stability under these ionization conditions. It is advised to optimize the method based on the DP of polySia and other experimental conditions.

1.4. Hypothesis

I hypothesis to develop methodologies that will aid in the advancement of polySia research. This would involve extracting polysialylated proteins from biological samples in a relatively pure form, followed by identifying them. Additionally, it would also confirm the presence of receptors for polySia on immune cells.

Chapter 02: Methodology

2.1. Polysialylation of BODIPY-Lactose

2.1.1. BODIPY-GM3 Synthesis

Fluorinated boron-dipyrromethene Lactose (BODIPY-Lac) was added to the reaction mixture to attain a final concentration of 0.1 mM in a total volume of 1000 uL. 4-(2-hydroxyethyl)-1-piperazineethanesulfonic acid (HEPES) buffer of pH 7.5 was included in the mixture at a final concentration of 50 mM, while magnesium chloride and CMP-Sia were added to the mixture at final concentrations of 25 mM and 0.3 mM, respectively. CST-1^{100} enzyme (Table 6-7) was used at a final concentration of 0.05 mg/mL, and alkaline phosphatase was added at a final concentration of 2 ug/mL. The reaction was allowed to proceed overnight at 30 degrees Celsius (°C) and confirmed with thin layer chromatography (TLC) run for 15 minutes in a mixture of ethyl O-acetate, acetic acid, methanol, and water (6:1.5:1.5:1 v/v). The purification process was carried out using a Sep-Pak C18 column that was regenerated with 5 ml of methanol followed by 10 mL of milli-Q water. The GM3 reaction was diluted to 5 mL with milli-Q and injected into the column followed by 10 mL milli-Q water to wash out the unbound material. The sample was then eluted using methanol. The aliquots were concentrated with a vacuum evaporator and confirmed with TLC using a solvent mixture of ethyl O-acetate, acetic acid, methanol, and water (6:1.5:1.5:1 v/v). The aliquots containing GM3 were pooled together, and their concentration was determined based on the absorption of BODIPY.

2.1.2. BODIPY-GD3 Synthesis

BODIPY-GM3 was added to the reaction mixture to attain a final concentration of 0.1 mM in a total volume of 1000 uL. HEPES buffer of pH 7.5 was included in the mixture at a final concentration of 50 mM, while magnesium chloride and CMP-Sia were added to the mixture at

final concentrations of 25 mM and 0.3 mM, respectively. CST-2[101] enzyme (Table 6-7) was used at a final concentration of 0.05 mg/mL, and alkaline phosphatase was added at a final concentration of 2 µg/mL. The reaction was allowed to proceed overnight at 30 °C and confirmed with TLC run for 15 minutes in a mixture of ethyl O-acetate, acetic acid, methanol, and water (6:1.5:1.5:1 v/v). The purification process was carried out using a Sep-Pak C18 column that was regenerated with 5 mL of methanol followed by 10 mL of milli-Q water. The GD3 reaction was diluted to 5 mL with milli-Q and injected into the column followed by 10 mL milli-Q water to wash out the unbound material. The sample was then eluted using methanol. The aliquots were concentrated with a vacuum evaporator and confirmed with TLC using a solvent mixture of ethyl O-acetate, acetic acid, methanol, and water (6:1.5:1.5:1 v/v). The aliquots containing GD3 were pooled together, and their concentration was determined based on the absorption of BODIPY.

2.1.3. BODIPY-GD3 polysialylation

In the final reaction volume of 20 µL, a 1 mM final concentration of BODIPY-GD3 was used, along with Tris buffer of pH 8.8 at a final concentration of 50 mM. Magnesium chloride and CMP-Sia were added at final concentrations of 25 mM and 60 mM, respectively, with bPST-10 at a final concentration of 0.05 mg/mL. The reaction was conducted for 1 hour at 30 °C and was stopped with 50% acetonitrile. Success of the reaction was confirmed with HPLC where 5 µL of 0.3 µM of sample was injected into the DNAPac column PA100 at 0.5 mL/minute at 40°C. Gradient elution was performed over 15 minutes with fluorescent detection of 503 nm, using 0-1 M ammonium acetate pH 8.3 in a constant mobile phase of 20% acetonitrile. For purification, the same process as for GM3 was followed, and the BDP-polySia was eluted with water in the first two aliquots.

2.2. Cloning and Subcloning

The *TurboID* gene was commercially ordered and amplified using PCR with primers *Iw554* and *Iw558* (Table 4). After running the PCR product through gel electrophoresis at 120V for 35 minutes, the gene and *Vek-06* (vector) were both digested with EcoR-1 and Sal-1 (Table 3), and then underwent gel electrophoresis. The resulting bands were purified using a gel purification kit, followed by ligation and transformation into *E. coli* (Table 3). One colony was added into LB media and shaken overnight at 37 °C. The new plasmid (*pTurboID*) was then extracted using a miniprep kit. To make the $EndoN_{DM}$ gene with Nde-1 and Sal-1 cut sites, PCR was conducted with primers *Iw586* and *Iw550*. The gene and *pTurboID* were digested with Nde-1 and EcoR-1, ligated, and transformed. Similar steps were followed for the synthesis of *pGFP-02*, using primers 6 to 8 (Table 3).

Table 3. The cloning/subcloning experimental protocols adapted from NEB website.

PCR		
Component	**Taken**	**Final Concentration**
5X Phusion HF or GC Buffer	10 µL	1X
10 mM dNTPs	1 µL	200 µM
10 µM Forward Primer	2.5 µL	0.5 µM
10 µM Reverse Primer	2.5 µL	0.5 µM
Plasmid DNA	variable	< 50 ng
Phusion DNA Polymerase	0.5 µL	1.0 units/50 µL PCR
Nuclease-free water	to 50 µL	
Thermocycling conditions		
Step	**Temperature**	**Time**
Initial denaturation	98°C	30 seconds
25 cycles	98°C	10 seconds
	55°C	20 seconds

	72°C	20 seconds/kb
Final Extension	72°C	5 minutes
Hold	4°C	
Restriction digest		
Component	**Taken**	**Final Concentration**
Plasmid DNA	1 µg	20 ng/µL
10X NEBuffer	5 µL	1x
Restriction enzyme 1	2.5 µL	12.5 units
Restriction enzyme 2	2.5 µL	12.5 units
Nuclease-free water	to 50 µL	
Incubation at 37°C for 1 hour		
Ligation		
Components	**Taken**	**Final Concentration**
T4 DNA Ligase Buffer (10X)	1 µL	1x
Vector DNA	25 ng total	2.5 ng/µL
Insert DNA	Based on NEB calculator	
T4 DNA Ligase	1 µL	
Nuclease-free water	to 10 µL	
Incubation at 16°C overnight		

2.3. Protein Expression and Purification

A 6 mL culture was inoculated with the desired strain and shaken overnight at 37 °C in the presence of the required antibiotic (100 mg/mL stock), added at 1 µL/mL (Table 6). The next day, the culture was added to 600 mL of LB media along with 600 µL of required antibiotic (100 mg/mL stock) and shaken at 37 degrees Celsius until the optical density (OD) reached 0.3-0.4. Then, 600 µL of IPTG stock at 100 mg/mL was added and the flask was shaken for 22 hours at the required temperature (Table 7). Afterward, the lysogeny broth (LB) media was centrifuged at 6500 relative centrifugal force (RCF) for 10 minutes at 4 °C, and the pellet was stored at -80 °C

overnight. Finally, the previously described protein extraction and purification method was carried out[5] (Table 6).

Table 4. The list of different primers that were used.

#	Primer Number	Primer Sequence	Role
1	Iw 554	ACAGGATCCATCGATGCTTAGGAG	Forward primer for TrbID with Nde1.
2	Iw 558	GCACGTCGACCTATTAAGACCGCAGACT GATTTCTCC	Reverse primer for TrbID with EcoR1.
3	Iw 586	GCTCGAATTCGGAGGCGGTGGAG GCGGTATGGCTAAAGGGGATGGT GT	Forward primer for EndoNDM with 6 Glycine's with EcoR1.
4	Iw 550	GCTGGTCGACTCTAGACTATTACT TCTGTTCAAGAGCAGAAAG	Reverse primer for EndoNDM with Sal1.
5	Iw 611	GCTCCATATGATGCAGTACAAGCT TGCTC	Forward primer for GB1-Seq with Nde1.
6	Iw 612	GCTCGAATTCTGGCGCTGGTGTGG	Reverse primer for GB1-Seq with EcoR1.
7	Iw 615	GCTCGAATTCCCAGGACCCACACCA GCGCCAAGCAGTGGAATGGTGAGC AAGGGCG	Forward primer for Seq-GFP with Nde1.
8	Iw 614	GCTCGTCGACTTACTTGTACAGCT CGTCCATG	Reverse primer for Seq-GFP with EcoR1.

Table 5. The resultant plasmids and the attributes of the final gene.

#	Plasmid Name	Details
1	Trb-EndoNDM	StartCodon-HisTag-ThrombineCutSite-Nde1-Trb-EcoR1-EndoNDM-Sal1-StopCodon.
2	GFP-02	StartCodon-HisTag-ThrombineCutSite-Nde1-GB1-TevCutSite-Seq-Seq-EcoR1-GFP-Sal1-StopCodon.

Table 6. Enlists the details of the enzymes used and the purification columns adapted.

Type	Origin	Antibiotic resistant	Function	Purification method
CST-1	Campylobacter jejune	AmpR	Sialyltransferase	MBP Trap HP
CST-2	Campylobacter jejune	AmpR	Bi-functional Sialyltransferase	Hi Trap DEAE column
HGT-13	Drosophila melanogaster	AmpR	GalNAc transferase	MBP Trap HP
CPG-13	Campylobacter jejune	AmpR	Epimerase	MBP Trap HP
BHV-05	Bovine herpesvirus 4	AmpR	Core-2 synthase	MBP Trap HP
BTS-05	Bibersteinia trehalosi	AmpR	Adds Sia to extended core 2	His Trap HP
bPST-109	Neisseria meningitidis	AmpR	Polysialylation	Heparin HO

Table 7. Enlists the expression conditions for the enzymes used.

Type	Incubation Temperature till OD (0.3-0.4)	Incubation for 22 hours after Post IPTG
CST-1	37°C	25°C
CST-2	37°C	37°C
HGT-13	37°C	20°C
CPG-13	37°C	20°C
DGT-02	37°C	20°C
BHV-05	37°C	20°C
HBGT-21	37°C	20°C
BTS-05	37°C	30°C
bPST-109	37°C	20°C

2.3. GFP-02 core-1 polysialylation

2.3.1. GalNAc addition

GFP-02 was used at a concentration of 0.5 mg/mL in a final volume of 1000 uL, which was adjusted with milli-Q water. HEPES buffer with a pH of 7.5 was added at a final

concentration of 50 mM, and manganese chloride at a final concentration of 25 mM. Enzymes CPG-131[102] and DGT-13[103] (Table 6-7) were included in the solution at a final concentrations of 0.5 mg/mL. Additionally, UDP-GlcNAc was added at a final concentration of 200 μM. The reaction was allowed to run for 4 hours at 30 °C and was confirmed with GalNAc lectin blot.

2.3.2. Gal Addition

To incorporate Gal, to the reaction above DGT-13 (Table 6-7) and UDP-Gal at concentrations of 0.5 mg/ml and 200 μM, respectively were added without prior purification followed by incubation for 4 hrs at 30 °C. The reaction was confirmed via Sia lectin blot.

2.3.3. Sia addition

To add Sia to GFP-2 core-1, ST3Gal1[104] (Table 6-7) was used at a final concentration of 0.5 mg/mL. GFP-02-core-1 was added at a final concentration of 0.5 mg/mL, while CMP-Sia was added at a final concentration of 200 μM. The reaction was carried out in 50 mM HEPES buffer at pH 7.5, and magnesium chloride was added at a final concentration of 0.3 mM followed by incubation for 4 hrs at 30 °C. The reaction was confirmed via Peanut agglutinin (SNA) lectin blot.

2.3.4. 2nd Sia addition

Sialylated GFP-02 was taken and CST-2[101] enzyme was added at a final concentration of 0.05 mg/mL in HEPES buffer of pH 7.5 that was included in the mixture at a final concentration of 50 mM. Alkaline phosphatase was added to the mixture at a final concentration of 2 μg/mL while CMP-Sia was added at the final concentration of 200 μM. Additionally, magnesium chloride was added to the mixture at a final concentration of 25 mM, followed by incubation for 4 hrs at 30 °C. The success of the reaction was confirmed with mass spectrometry.

2.3.5. Polysialylation

GFP-02 diSia was added at a concentration of 0.5 mg/mL to a 50 mM ammonium bicarbonate buffer with a pH of 8.8. Magnesium chloride and CMP-Sia were added at final concentrations of 25 mM and 0.2 mM respectively. CMP-Sia doner sugar was used at a final concentration of 500 μM. After incubation at 30 °C for an hour, the reaction was verified with an anti-polySia blot.

2.4. GFP Core-2 extended polysialylation.

GFP-02 core-2 was created from GFP-02 core-1 through the use of core-2 synthase[103] (Table 6) enzyme at a concentration of 0.05 mg/mL. The reaction conditions remained consistent with Core-1 synthesis, with the exception of CPG-13 and manganese chloride not being added. Confirmation of the reaction was achieved through a 70-minute gel shift assay using a 10% SDS gel run at 200 V. The addition of Gal was performed using the HBGT-21 enzyme at a concentration of 0.05 mg/ml, following similar reaction conditions to those used for the addition of Gal in the core-1 synthesis.

In order to introduce Sialic acid, the enzyme BTS-05 (Table 6) was utilized at a concentration of 0.05 mg/mL while maintaining the same conditions as the CST-1 reaction. Subsequently, the CST-2 and bPST109 reactions were conducted in a similar fashion as previously described for the GFP-02 diSia core-1 polysialylation.

2.5. Cell Culture

The NK-92 cells were cultured in RPMI-1640 medium supplemented with 10% horse serum, 10% fetal bovine serum, 20 mM HEPES (pH 7), 1% penicillin-streptomycin, 200 U/mL interleukin-2 (IL-2), and 1 mM hydrocortisone. Jurkat T cells were grown in RPMI-1640 medium containing 10% fetal bovine serum and 1% penicillin-streptomycin. The chinese

hamster ovary (CHO) cells were kindly provided by Macauley Lab and cultured in DMEM/F12 medium supplemented with 10% fetal bovine serum and 1% penicillin-streptomycin.

2.6. Immunoblotting

The concentration of proteins in the lysates was determined using a bicinchoninic acid (BCA) assay (Pierce). A volume containing 5-16 μg of proteins was taken and an equal volume of 2x loading dye was added followed by heat denaturation for 30 seconds at 95 °C. The proteins were separated using SDS-PAGE gel (200 V for 40 minutes) and then transferred to a PVDF membrane at a voltage of 60 V for 1 hour. The blocking step was carried out in 5% bovine serum albumin (BSA) in phosphate buffered saline with 0.05 % tween (PBST) at room temperature for 1 hour. The anti-polySia antibody (mAB735) and anti-IgG HRP antibodies were used at a dilution factor of 1/1000, and the membrane was washed three times with 10 mL PBST for 10 minutes each in between. Finally, the HRP substrate was added, and the blot was imaged after two minutes.

2.7. Flow Cytometry

One million Jurkat T cells were subjected to centrifugation at 380 RCF for 10 minutes at room temperature. The resulting cell pellet underwent two washes with PBS containing 0.5% BSA. Following this, the cells were blocked for an hour at room temperature via incubation in 1% BSA. The cell pellet was then collected under the same conditions as previously, with a centrifugation time of only 5 minutes. GFP-02 polySia and controls were added at the concentration of 20 μg/mL, and incubation was carried out at room temperature for an hour. The samples were then washed three times using the aforementioned washing conditions. Finally, the pellet was redispersed in 200 μL of PBS, with a final 4',6-diamidino-2-phenylindole (DAPI) dye concentration of 0.1 μg/mL, and the samples were analyzed using an ImageStream MarkII. The

voltage settings were kept at 25 mV and 120 mV to detect DAPI and GFP respectively. The data was analyzed with IDEAS software version 6.0.

2.8. LC-MS Sugar

We used a Vanquish UHPLC System (Thermo Scientific, Germering, Germany) equipped with a Luna Omega 1.6 µm C18 polar reverse-phase analytical column (2.1x50 mm) featuring a 100Å pore size (Phenomenex, Torrance, CA, USA) for HPLC-MS. The column was thermostated at 50°C and mass spectrometric detection was carried out using an Orbitrap Exploris 240 mass spectrometer (Bremen, Germany). The mobile phase was composed of 0.1% FA (formic acid) in water as mobile phase A and 0.1% FA in acetonitrile as mobile phase B. An aliquot of the sample was loaded onto the column at a flow rate of 0.50 -1 mL/min and an initial buffer composition of 100% mobile phase A was maintained for 1.0 min to wash away the buffers. The analytes were separated by using a linear gradient from 0% to 98% mobile phase B over a period of 4.5 minutes, held at 98% mobile phase B for 1 minute and back to 0% mobile phase B in 0.5 minutes. Mass spectras were acquired in both positive and negative mode of ionization. The acquisition parameters were set to Sheath gas 50, Auxiliary gas 10, Sweep Gas 1, Ion transfer tube at 325°C, Vaporizer at 350°C, Spray voltage 3500 V in positive and 2500 V, RF lens 90, MS Scan resolution was set to 120k with a scan range from 200-1600 Da. We used Xcalibur (Ver. 4.6.67.17) (Thermo Fisher Scientific) for data acquisition and FreeStyle 1.8 SP2 (Thermo Scientific) for data analysis. The samples were run by Bela Reiz, Mass Spectrometry Facility at the Department of Chemistry, University of Alberta.

2.9. LC-MS protein

The Vanquish UHPLC System (Thermo Scientific, located in Germering, Germany) was utilized to perform LC-MS. An Aeris 3.6 µm XB-C18 reverse-phase analytical column (2.1x50 mm) with a pore size of 200Å (Phenomenex in Torrance, CA, USA) was used for the analysis. The

column was thermostated at 40°C and mass spectrometric detection was accomplished using an Orbitrap Exploris 240 mass spectrometer in Bremen, Germany. The buffer gradient system consisted of 0.1% FA (formic acid) in water as mobile phase A and 0.1% FA in acetonitrile for mobile phase B. For analyte separation, a sample aliquot was loaded onto the column at a flow rate of 0.50 mL/min, with an initial buffer composition of 99% mobile phase A and 1% mobile phase B. The buffer was kept at 1% mobile phase B for 1.0 mL/min to wash away the buffers. Elution of the analytes was performed by using a linear gradient from 1% to 98% mobile phase B over a period of 5.1 minutes, held at 98% mobile phase B for 0.4 minutes, and then returned to 1% mobile phase B in 0.5 minutes. Mass spectras were acquired in positive mode of ionization, with Sheath gas at 55, Auxiliary gas at 15, Sweep Gas at 1, Ion transfer tube at 350°C, Vaporizer at 375°C, Spray voltage at 3800 V, and RF lens at 100. The MS Scan resolution was set to 120k with a scan range from 700-3200 Da. Data acquisition was performed using Xcalibur by Thermo Fisher Scientific and data analysis was carried out using Spectrus Processor (ACD/Labs in Ontario, Canada). The samples were run by Bela Reiz, Mass Spectrometry Facility at the Department of Chemistry, University of Alberta.

2.9. Cu^{2+} Click Reaction

For the final reaction volume of 1 mL, we utilized concentrations of 1 and 1.5 mM for CMP-Sia-Az and Biotin-S-S-Alkyne, respectively. Our potassium phosphate buffer system was used at a final concentration of 30 mM. Copper sulfate and tris-hydroxy propyl triazolyl methyl-amine (THPTA) were premixed at 2 mM and 50 mM concentrations, respectively, and added to the mixture at final concentrations of 0.25 mM and 1.25 mM, respectively. Sodium ascorbate was added at the final concentration of 5 mM, and the reaction was incubated at 37 °C for two hours. The confirmation was carried out with HPLC in Wakarchuk Lab, using a similar method

to BODIPY-polySia with a 50% gradient concentration over 20 minutes. Detection was carried out at 271 nm for CMP.

2.10. Activity Assays

2.10.1 CST-1, CST-2, and bPST109

The enzyme's glycerol stocks were generously provided by Wakarchuk Lab. To conduct the activity assays, we followed a procedure similar to that outlined in the BODIPY-Lac polysialylation steps, with the exception that the reactions were conducted on a smaller scale (10 µL final reaction volume). The reactions were verified using TLC with the same solvent system as previously described in GM3 synthesis. All glycerol stocks for the remaining enzymes were also provided by Wakarchuk Lab, and their activity assays were conducted in a similar manner to their described reactions but on a smaller scale (10 µL final reaction volume).

2.10.2. Auto-biotinylation Activity Assay

In the PBS buffer, TurboID-EndoN$_{DM}$ was taken at the final concentration of 0.2 mg/mL. ATP and D-biotin were added at final concentrations of 2 mM each. After incubating for 15 minutes at room temperature, the reaction was stopped by adding an equal volume of 2x loading dye and boiling for 5 minutes at 95 °C. This was followed by streptavidin-HRP blot.

2.10.3. Lectin ELISA Assay

The ELISA procedure was conducted following the previously established protocol[5], with slight adjustments made to align with the specific purpose of the experiment. The TurboID-EndoN$_{DM}$ was added to the bottom of 96 well plates at a concentration of 10 µg/mL and allowed to adhere overnight at 4 °C. The wells were then blocked with 5% BSA in PBST. The GFP-EndoN$_{DM}$ was adhered at the same concentration and under similar conditions for the positive

control wells. The rest of the methodology remained consistent with the previously described protocol[5]. Similar protocol was followed for TurboID-scFv.

2.10.4. The Combined Assay

In the PBS buffer, Polysialylated A1AT and TurboID-EndoN$_{DM}$ were incubated for 30 minutes at concentrations of 0.2 and 0.002 mg/mL, respectively. Subsequently, ATP and D-biotin were added at final concentrations of 2 mM each. After incubating for 15 minutes at room temperature, the reaction was stopped by adding an equal volume of 2x loading dye and boiling for 5 minutes at 95 degrees Celsius. This was followed by streptavidin-HRP blot.

Chapter 03: New methodologies to identify polysialylated proteins.

Exploring the role of polySia in immune cells remains a vibrant area of research with several unknowns that necessitate the identification of more polysialylated proteins[36]. However, this identification poses a challenge due to polySia's bulky nature and negative charge at physiological pH[105]. Its susceptibility to hydrolysis, especially at lower pH, further complicates matters, as typical bulk (glyco) protein isolations and analysis methodologies rely on acidic conditions[105]. Also, multiple freeze-thaw cycles as well as boiling lead to its degradation[7]. While immunoprecipitation is a standard method for enriching proteins, polysialylated proteins suffer from high levels of nonspecific interactions under standard immunoprecipitation conditions, which hinders its effectiveness[5]. Vigorous washing conditions are not feasible as they could denature the structure of antibodies, diminishing their binding[5]. As a result, experiments that have used immunoprecipitation to identify polysialylated proteins resulted in numerous hits in the proteomic analysis, which necessitated extensive validation.

To address the difficulties in identifying new polysialylated proteins, the Willis lab developed an alternative method that is based on immobilization of the $EndoN_{DM}$ lectin. This lectin binds polySia with high affinity and is detergent stable, which makes it amenable to stringent washing conditions that could remove non-specifically bound proteins. $EndoN_{DM}$ was expressed with an AviTag on the amino terminus, which allowed for in vitro biotinylation after purification. The biotinylated AviTag- $EndoN_{DM}$ was immobilized on streptavidin beads and then used to capture polysialylated proteins from complex mixtures, including cell lysates and serum, followed by proteomic analysis of the immobilized beads[106]. While the method was highly successful in identifying novel polysialylated proteins, such as Quiescin Sulfhydryl Oxidase 2

(QSOX2), it suffered from a major drawback in that most of the peptides in the spectra were attributed to $EndoN_{DM}$[106]. In order to see peptides corresponding to the polysialylated proteins, a large amount of samples was required, limiting the use of this technology to highly abundant samples. New methodologies that eliminate the presence of $EndoN_{DM}$ in the analysis would substantially improve the sensitivity and reduce the need for large sample volumes.

We developed two distinct approaches for isolating polysialylated proteins, both of which relied on biotinylation of polysialylated proteins. The first method used a proximity labeling approach to biotinylate polysialylated proteins. The second method involved enzymatic transfer of a biotinylated sialic acid to polySia. For both methods, the biotinylated polysialylated proteins could be isolated on streptavidin-agarose beads and identified by mass spectrometry.

3.1. Proximity labeling of polysialylated proteins using TurboID-$EndoN_{DM}$

The first method for isolating polysialylated proteins used the proximity labeling protein TurboID fused to $EndoN_{DM}$ to biotinylate proteins attached to polySia (Figure 4). TurboID is a modified version of BioID, a mutant *E. coli* biotin ligase known for its high level of promiscuity[107]. In the presence of adenine triphosphate (ATP), TurboID triggers the activation of biotin into biotin-adenine monophosphate (biotin-AMP), a compound that exhibits high reactivity towards available lysine residues on proteins within a 10 nm radius[107]. The binding of $EndoN_{DM}$ in the TurboID-$EndoN_{DM}$ fusion protein to polySia would bring TurboID into close proximity to the underlying protein, which would promote their biotinylation after the addition of biotin and ATP. While some degree of indiscriminate biotinylation may occur, judicious selection of controls should result in higher signal from polysialylated proteins.

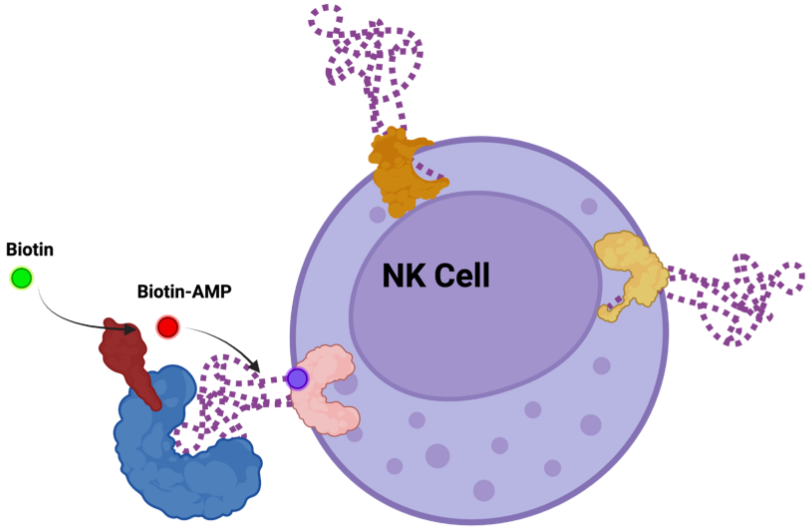

Figure 4. Graphical abstract for proximity labeling method.
The NK cell is shown with surface polysialylated proteins. TurboID-EndoN$_{DM}$ could also be observed bound to polySia, which, upon the addition of ATP and biotin, leads to the biotinylation of unidentified protein(s). The TurboID component of the fused protein is depicted in maroon, while the EndoN$_{DM}$ is shown in blue. The activated biotin is shown in red, ready to interact with an available lysine residue.

To express TurboID-EndoN$_{DM}$, we cloned the genes coding for this protein into an *E. coli* expression vector (Figure 5). The construct consisted of four components: an *N*-terminal HisTag, TurboID, a six-glycine linker, and EndoN$_{DM}$. The HisTag allows for protein purification using a nickel affinity column. The flexible six-glycine linker ensures that the TurboID and EndoN$_{DM}$ domains are properly oriented and flexible for optimal folding and functionality[108]. We expressed the protein in this *E. coli* strain and purified it using Immobilized metal affinity chromatography (IMAC).

To assess the activity of each of the two components of the proteins, two types of activity assays were developed, "The Lectin Assay" for EndoN$_{DM}$ and "The Biotin Assay" for TurboID. Furthermore, a third assay was carried out to evaluate the combined activity of both domains towards the desired goal of biotinylating polysialylated proteins, termed "The Combined Assay."

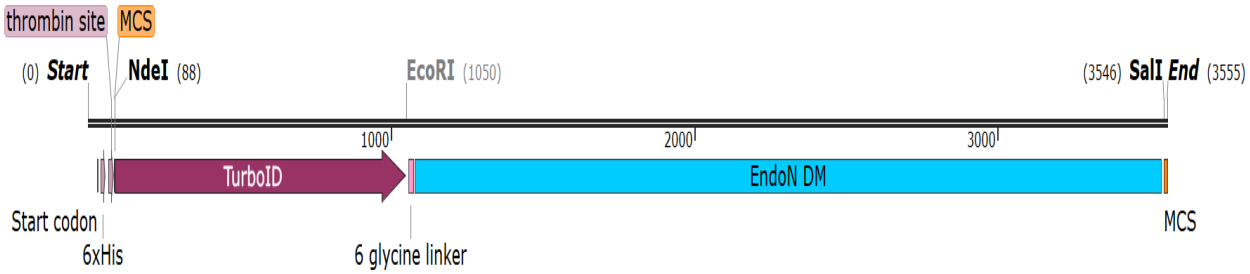

Figure 5. Sequence arrangement of TurboID-EndoN$_{DM}$ and its expression.
The start codon is followed by a HisTag and then a thrombin cut site. At the C-terminus of the thrombin cut site, the TurboID component is attached. Six-glycine linker between TurboID and EndoN$_{DM}$ could also be observed. This image was taken from the Snape Gene file and has been processed to create a figure.

For the lectin assay, we adapted an ELISA-based technique to measure binding of EndoN$_{DM}$ to polySia (Figure 6A)[5]. In this assay, TurboID-EndoN$_{DM}$ was adhered to the wells of a 96-well plate. Colominic acid, a commercially available polySia isolated from *E. coli*, was allowed to bind to the adhered protein. After PBS washing step, the bound polySia was detected using an anti-polySia antibody, followed by a secondary antibody conjugated to HRP which develops a chromophore when 3′-3-5′-5-tetramethylbenzidine (TMB) is added. GFP-EndoN$_{DM}$ was used as a positive control as it binds to polySia[5]. We observed strong signal for this positive control in the presence of colominic acid and very little signal in the absence of colominic acid, as expected (Figure 6B). We also observed strong signal when purified TurboID-EndoN$_{DM}$ was adhered to the plate, indicating that the EndoN$_{DM}$ portion of the protein is functioning as expected.

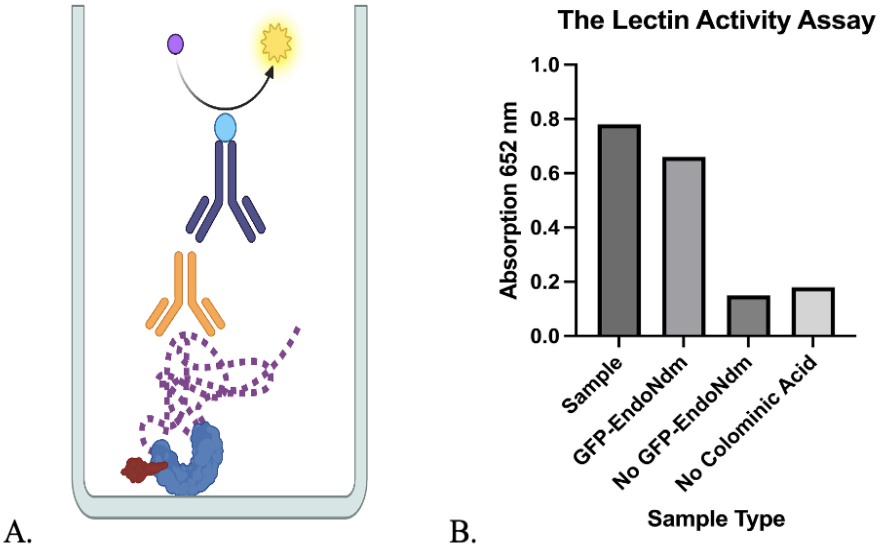

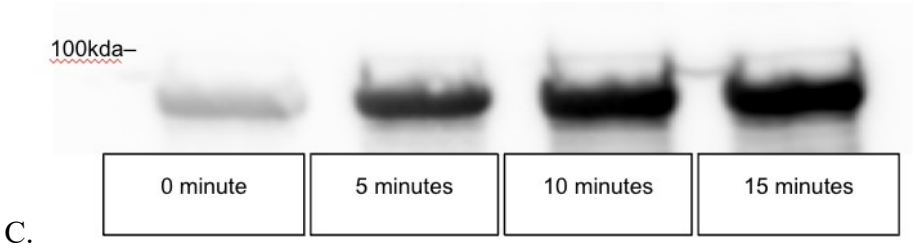

Figure 6. The activity assay for TurboID-EndoN$_{DM}$.
Panel A depicts the ELISA design used, where TurboID-EndoN$_{DM}$ was adhered to the bottom of the well followed by incubation with colominic acid. This was followed by incubation with mAb735 and a secondary HRP-conjugated antibody. In Panel B, the results are illustrated, where both the sample and positive controls display a higher absorbance than the negative controls. This assay was carried out only once. Panel C shows the findings of the biotin assay, where the 0-minute control is the negative control which was taken immediately after adding biotin and was stopped with 50% final concentration of acetonitrile (ACN). The blot shown is the Streptavidin HRP blot.

TurboID is known to autobiotinylate itself, and we took advantage of this feature to determine whether it was active in the TurboID-EndoN$_{DM}$ fusion protein. Biotin and ATP were added to TurboID-EndoN$_{DM,}$ and samples were taken at 0, 5, 10, and 15 minutes. The samples were analyzed by blotting with streptavidin-HRP detection (Figure 6C). At time zero, there was

a small amount of biotinylation, which could be attributed to any autobiotinylation that occurs during protein expression, as *E. coli* contains biotin and ATP in its cytoplasm[109]. In subsequent time points, the signal was substantially increased, indicating that the reaction proceeded and therefore the TurboID domain was active.

The combined assay was designed to confirm the combined activity of both domains of TurboID-EndoN$_{DM}$, i.e., the biotinylation of polysialylated proteins. In this assay, we used a known polysialylated protein to determine if biotinylation is specific to polysialylated proteins. Alpha-1-antitrypsin (A1AT) is a therapeutic glycoprotein with a molecular weight of 52 kDa and three *N*-glycosylation sites. It is naturally glycosylated and contains a mixture of α-2,3/6 linked Sias, which could be leveraged to make polySia enzymatically[110]. The sialyltransferase, CST-2 was used to add an α-2,8-linked Sia primer onto the underlying glycans[111], after which an engineered version of the polysialyltransferase from Neisseria meningitidis was used to synthesize polySia (Figure 7)[112]. To confirm we were successful in making polySia-A1AT, we analyzed the protein by Coomassie gel and anti-polySia immunoblotting (Figure 7). The polysialylated protein was detected as a smear when compared to the negative control, indicating successful polysialylation. Furthermore, a reduction in A1AT concentration and its conversion into its polySia form were also evident in the Coomassie gel. Moreover, an EndoN treated control was also used that specifically removes polySia.

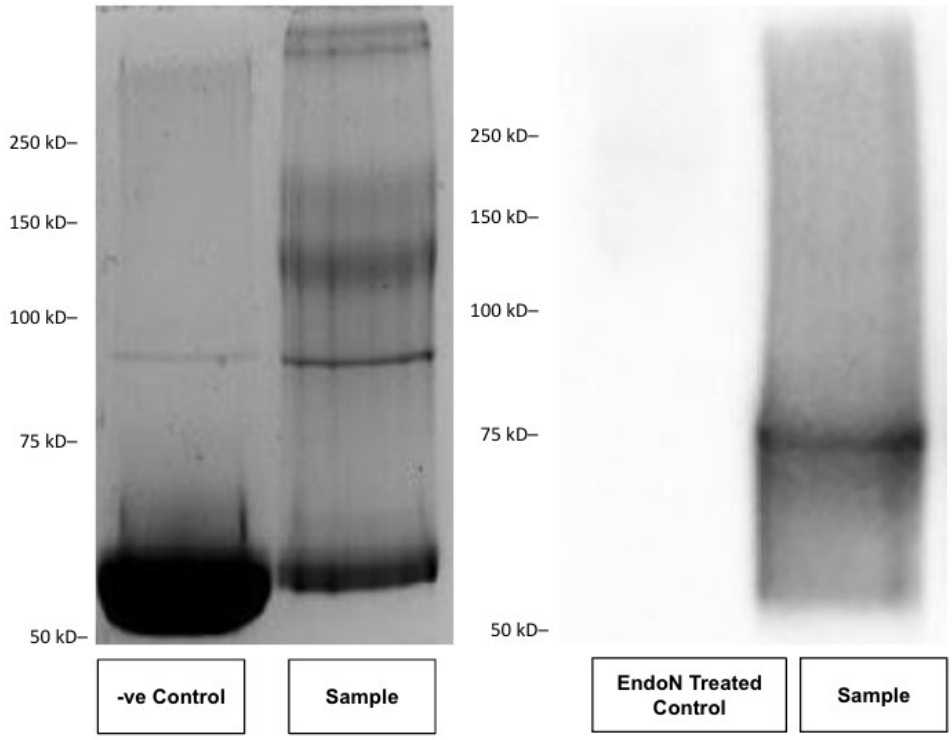

Figure 7. Confirmation of polysialylation of A1AT.
On the left, a Coomassie gel, most of the protein is polysialylated. The negative control is the reaction sample taken out at 0 minutes and stopped with 50% ACN. On the right, the anti-polySia blot confirms further that the polysialylation was successful. The EndoN-treated A1AT polySia is an additional control that further supports the results. The mw of A1AT is 52 kD.

To carry out the combined assay, D-biotin, and ATP were added into a mixture containing polysialylated A1AT and TurboID-EndoN$_{DM}$, which were pre-incubated in a 2:1 concentration, respectively. Biotinylation was assessed using a streptavidin-HRP blot (Figure 8A). It was observed that biotinylation for A1AT-polySia could not be detected above 52 kDa in the sample lane. Moreover, there were no noticeable differences in biotinylation between the sample and the EndoN-treated control. Additionally, autobiotinylation of TurboID-EndoN$_{DM}$ was consistent among all lanes except for the one where no biotin was added. Some degree of biotinylation was also seen here, which may be explained by biotinylation that occurred during the expression of the TurboID-EndoN$_{DM}$ in *E. coli*[107]. The extent of the polySia chain on A1AT

exhibits considerable variation, and it is spread across a wider area on the Coomassie gel. Consequently, this could potentially result in a diminished signaling level that may go undetected in the presence of autobiotinylation of TurboID-EndoN$_{DM}$. We concluded that the higher autobiotinylation of TurboID-EndoN$_{DM}$ could potentially mask the detection of A1AT biotinylation. To determine if decreasing the concentration of TurboID-EndoN$_{DM}$ could improve the results, we redid the experiment and decreased the concentration of TurboID-EndoN$_{DM}$ by 100x while kept the concentration of A1AT-polySia the same (Figure 8B). Unfortunately, there was no difference in biotinylation.

Table 8. The combined assay, sample controls and expected results.

No.	A1AT polySia	TurboID-EndoN$_{DM}$	EndoN	D-biotin	Expected biotinylation	Observed biotinylation
1	✓	✓	✓	✓	X	✓
2	✓	X	X	X	X	X
3	✓	✓	✓	X	X	✓
4	X	✓	✓	✓	X	✓

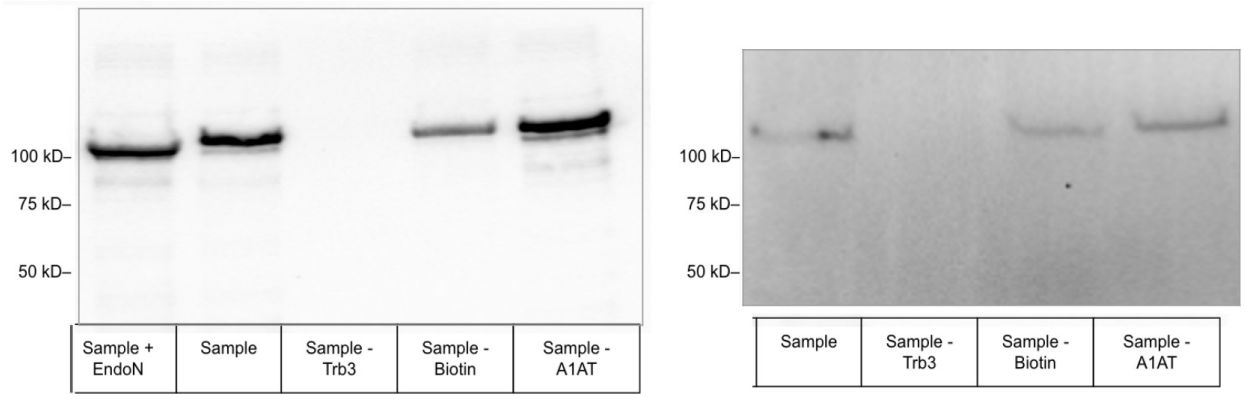

A B

Figure 8. The combined assay results.

In Panel A, the biotin blot is shown when polysialylated A1AT and TurboID-EndoN$_{DM}$ were used in the concentration ratios of 2:1. No band was detected in any of the samples above 52 kD for the A1AT-polySia. Furthermore, no difference was observed between the EndoN treated and untreated samples. In Panel B, the blot is shown when the concentration of TurboID-EndoN$_{DM}$ was reduced by 100x while concentration of A1AT-polySia was kept same. The mw of TurboID-EndoN^{DM} is 110 kD.

3.2. TurboID-scFv

Analysis of the EndoN$_{DM}$ structure revealed numerous exposed lysine residues that could potentially utilize the activated biotin and thus prevent labelling of A1AT. To address the issue of numerous exposed lysine residues, EndoN$_{DM}$ was replaced with scFv, a fusion protein of the variable regions of the heavy (VH) and light chains (VL) of mAB735[113]. ScFv is smaller in size than EndoN$_{DM}$ and has fewer lysine residues so it may both bring the TurboID enzyme closer to the polysialylated protein and also increase the chances of biotinylation.

A plasmid construct was designed to fuse scFv with TurboID. The TurboID-scFv construct mirrored the design of TurboID-EndoN$_{DM}$, where EndoN$_{DM}$ was replaced with scFv. Activity assays were carried out as previously described, with ELISA trials using 10 and 100 μg/mL concentrations of TurboID-scFv (Figure 9). The ELISA demonstrated that the lectin component was active and could bind to colominic acid. However, the biotin activity assay demonstrated that TurboID-scFv was autobiotinylated to a higher degree than TurboID-EndoN$_{DM}$ during its expression (Figure 9B Top), suggesting it may be difficult to detect newly biotinylated proteins in the reactions. Unsurprisingly, the combined assay yielded similar results to TurboID-EndoN$_{DM}$, where no increase in signal was observed in the presence of polysialylated protein. We concluded that the proximity labelling strategy would not be successful in specifically labelling polysialylated proteins.

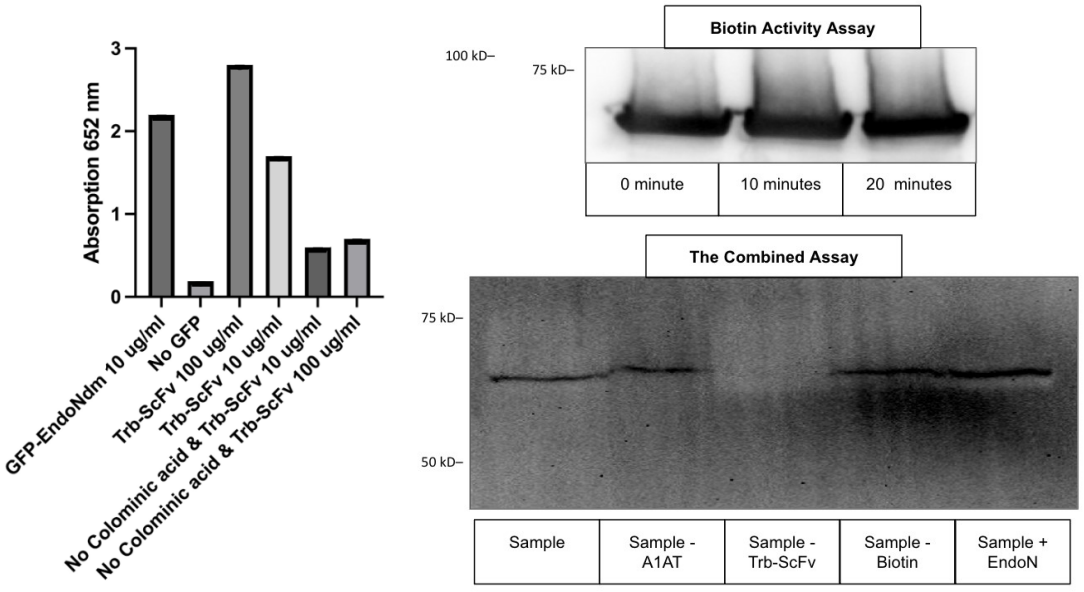

A **B**

Figure 9. The activity assays for TurboID-scFv.
Panel A displays the results for the lectin assay which was performed once. Two different concentrations were tested, and binding to colominic acid was observed when compared to the controls. In Panel B, top, shows the results for the autobiotinylation assay, and the blot below displays the results of the combined assay. The mw of scFv is 63.9 kD.

3.3. Enzymatic biotinylation of polysialic acid using a modified donor sugar.

Our second strategy for isolating polysialylated proteins involves the transfer of biotinylated Sia to the polySia chains using a polysialyltransferase enzyme. We used the Neisseria meningitidis polysialyltransferase that was previously engineered for improved stability (bPST109)[112]. This enzyme normally transfers CMP-Sia to any α-2,8 linked Sia. Modified donors where the 5-acetyl moiety were replaced with a 5-azido moiety have been used extensively with eukaryotic sialyltransferases and would provide a convenient handle for attachment of biotin to polySia (and potentially shorter oligoSia)-containing proteins.

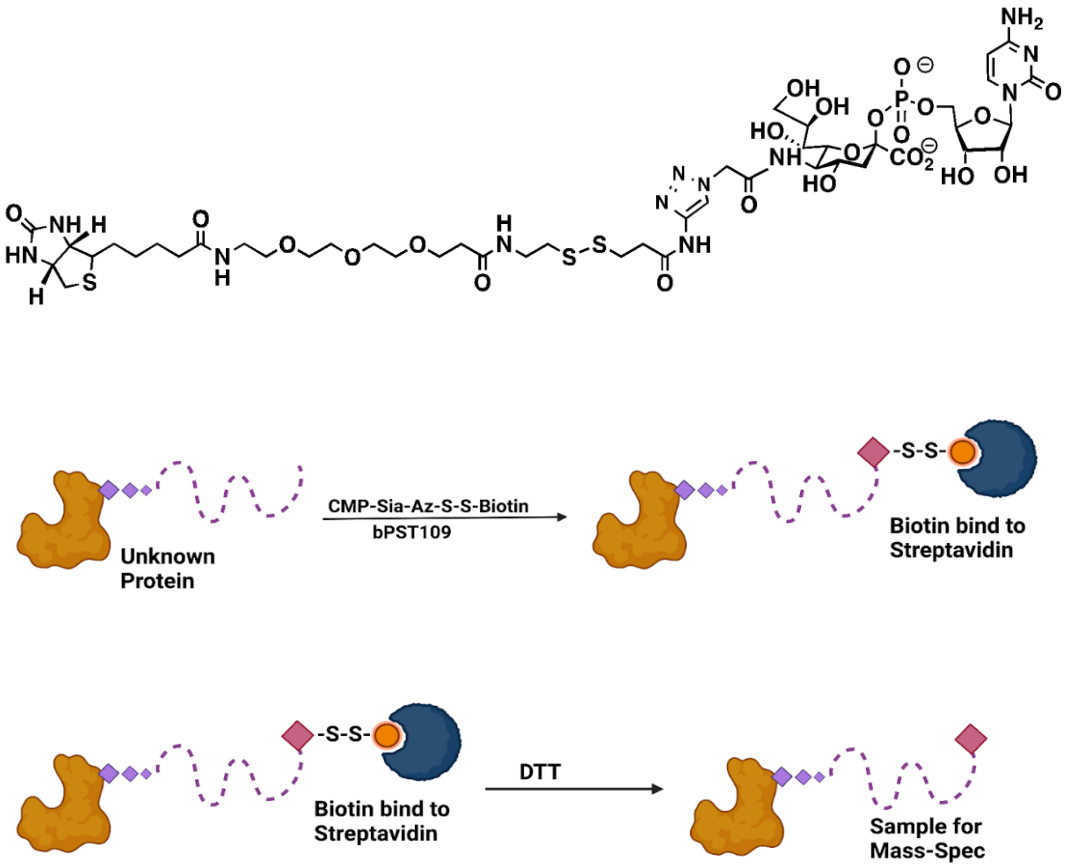

Figure 10. The chemical structure of CMP-Sia-S-S-Biotin and the Graphical Abstract for the method.
The chemical structure of CMP-Sia-S-S-Biotin is shown at the top where on the right-side CMP could be observed, bind to the hydroxyl group at carbon number 2 of Sia. The Sia is attached to biotin through a spacer arm which contains a disulfide linkage. The figure below is the graphical abstract depicting how this method would work. The CMP-Sia-S- S-Biotin (pink diamond) is first enzymatically added to the polySia chain. Streptavidin beads are used to separate the protein-polySia-Biotin, followed by the reduction of the disulfide bond. The samples are then sent for mass spectrometry analysis.

By using a biotin handle that is attached via a disulfide linker, we could isolate the polysialylated proteins on streptavidin-agarose beads and then reduce the disulfide linker to release the proteins for subsequent proteomic analysis (Figure 10). The synthesis of CMP-Sia-S-S-Biotin was achieved through a Cu^{2+}-based click reaction using CMP-SiaAz and biotin-S-S-

alkyne. Successful completion of the reaction was verified using HPLC analysis (Figure 11A). A CMP-SiaAz only sample and a reaction mixture without CMP-SiaAz were used as negative controls, represented by black and blue chromatograms, respectively. The reaction product is represented by the red chromatogram, and a noticeable shift in the chromatogram when compared to the black chromatogram, confirms the success of the reaction. The blue chromatogram indicates the impurities in the reaction sample. The product was purified using a DEAE column and verified using HPLC analysis (Figure 11B).

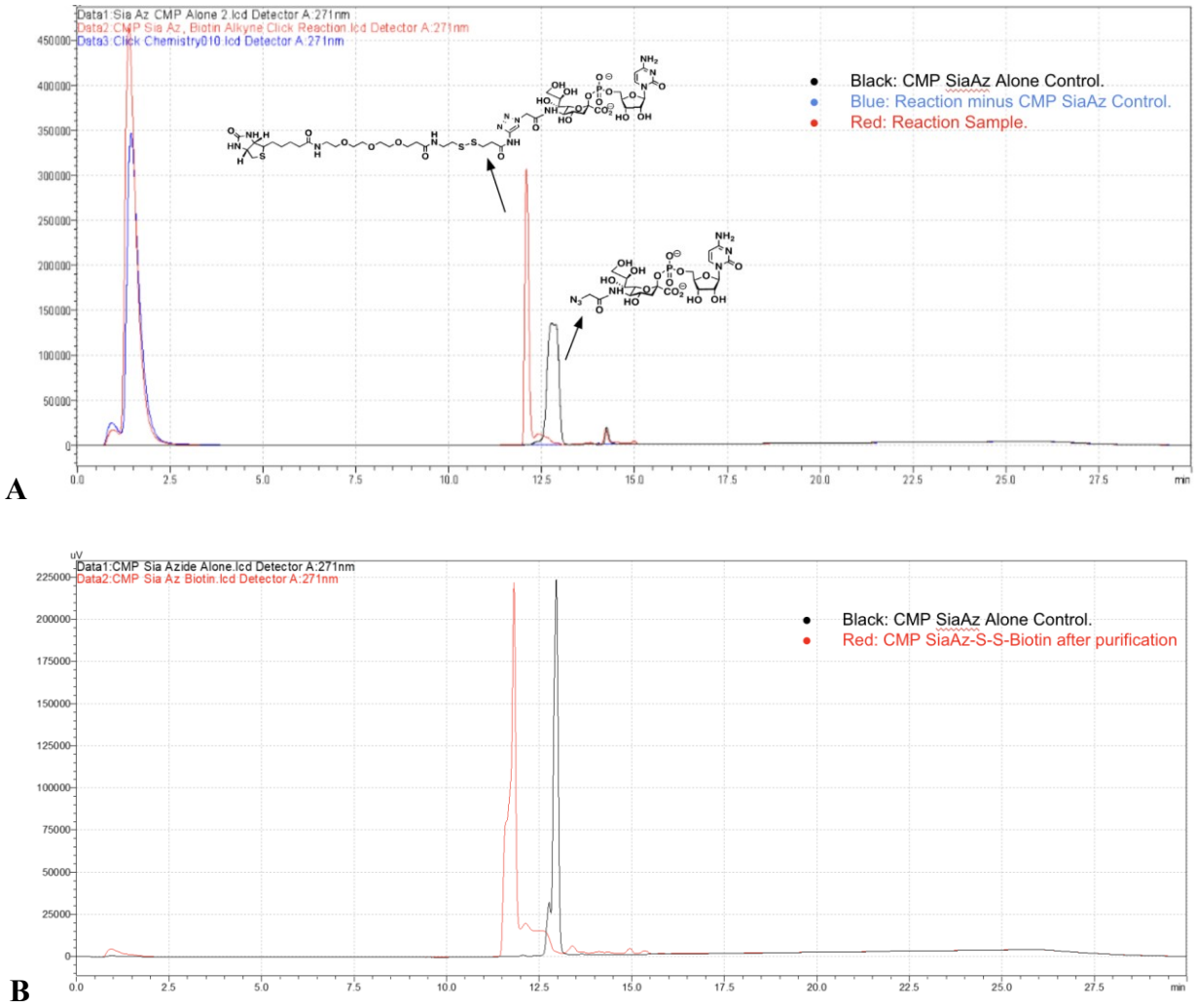

Figure 11. HPLC chromatograms confirming the synthesis and purification of CMP-Sia-S-S-Biotin.

Panel A confirms that the reaction was successful; it shows red, black, and blue chromatograms for CMP-SiaAz, reaction sample, and negative control (Reaction minus CMP-SiaAz), respectively. Panel B confirms the success of purification; it shows the chromatograms in red and black for CMP-SiaAz (control) and the purified CMP-Sia-S-S-Biotin, respectively. It is obvious that the peak at a retention time of less than 2.5, representing the impurities, has disappeared.

We analyzed the product, CMP-Sia-S-S-Biotin with LC-MS (Figure 12). In total four peaks are displayed, each representing a distinct form of CMP-Sia-S-S-Biotin generated through electroscopy ionization (ESI). Peak 3 corresponds to CMP-Sia-S-S-Biotin, while peak 4 reveals it with an additional oxygen resulted from ionization[114]. Moreover, peaks 1 and 2 represent Sia-S-S-Biotin (with cleaved CMP) with and without an additional oxygen, respectively. The molecular weights are shown in Table 9. The additional oxygen is commonly observed as an oxygen adduct, influencing the mass of the analytes and ultimately impacting the chromatograms[114]. Though ESI is a soft ionization technique, it could also result in the breakdown of certain bonds within the analytes. The ionization process could cleave off the CMP at the phosphate backbone, or it could also break the susceptible sites within CMP, producing fragments[115]. The free CMP is more polar than CMP-Sia- S-S-Biotin, and it would interact more with DNAPac columns than CMP-Sia-S-S- Biotin. The chromatogram (Figure 11) does not reveal the presence of free CMP in the sample, so we concluded that the CMP-Sia- S-S-Biotin was intact in the final sample.

Table 9. The corresponding mass/charge of peaks that appeared in mass spectra.

No.	Mass/charge (Z=1)	Represents	Peak no
1	996.3477	Sia-S-S-Biotin	1
2	1012.3425	Sia-S-S-Biotin with additional oxygen	2
3	1301.3883	CMP-Sia-S-S-Biotin	3
4	1317.3831	CMP-Sia-S-S-Biotin with additional oxygen	4

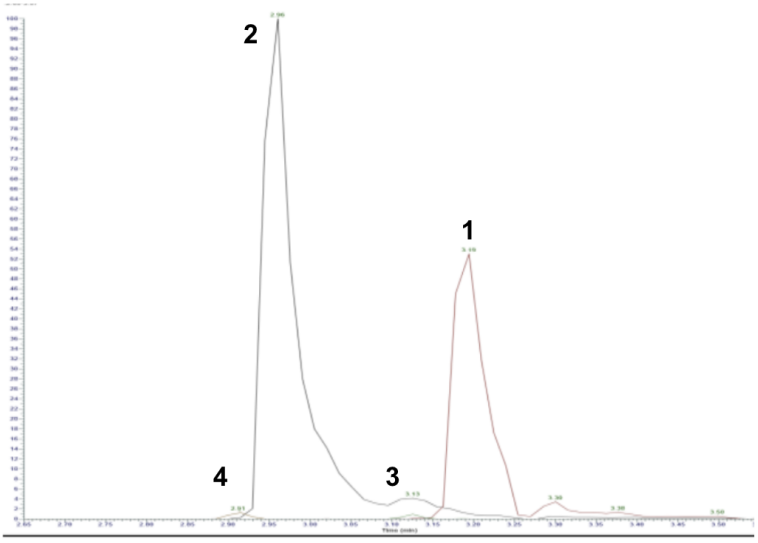
2
1
4
3

A

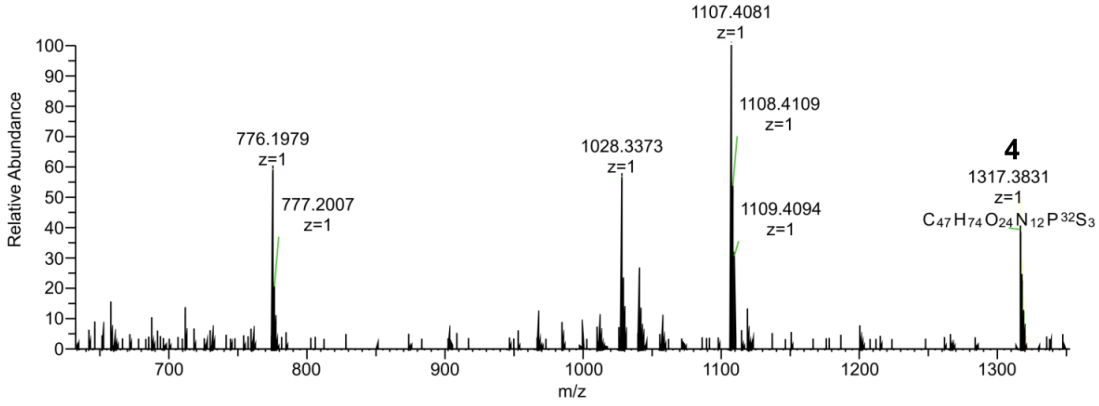
1107.4081
z=1
1108.4109
z=1
776.1979
z=1
1028.3373
z=1
4
1317.3831
z=1
C47H74O24N12P32S3
777.2007
z=1
1109.4094
z=1
Relative Abundance
m/z

B

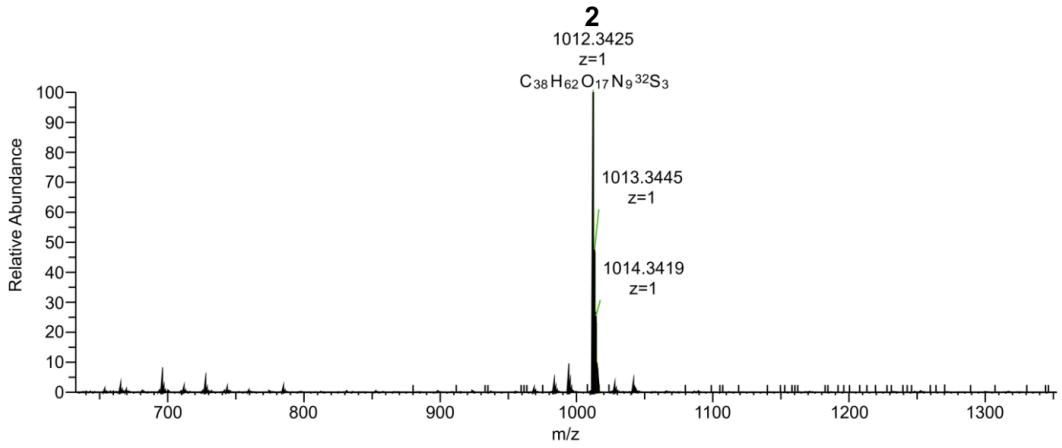
2
1012.3425
z=1
C38H62O17N9 32S3
1013.3445
z=1
1014.3419
z=1
Relative Abundance
m/z

C.

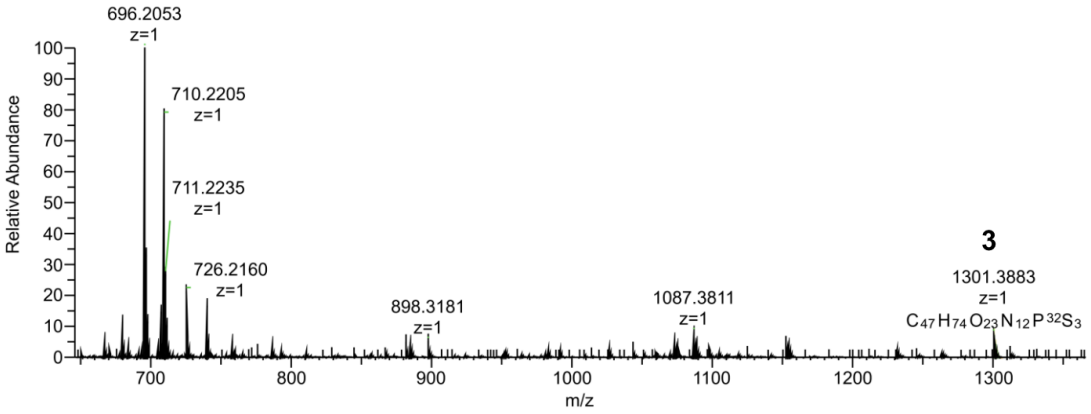

D

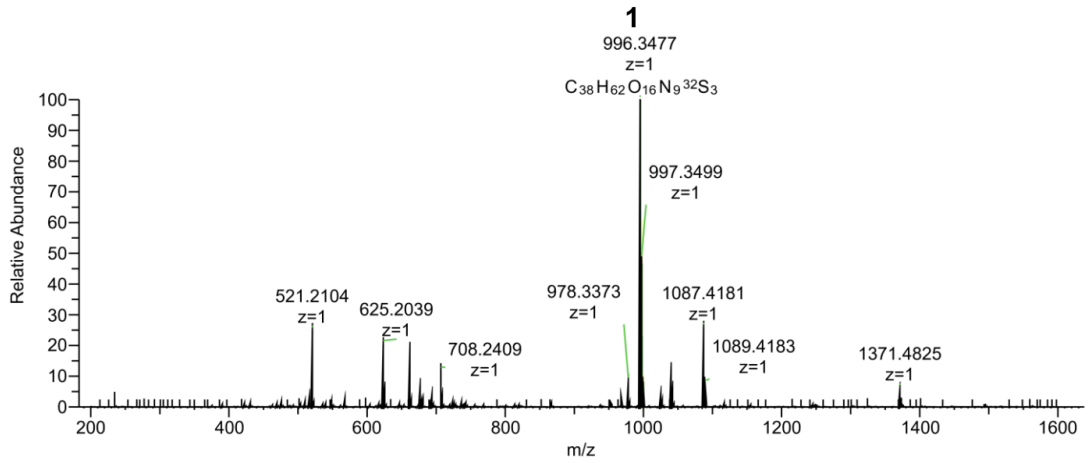

E

Figure 12. LC chromatogram and mass spectra for CMP-Sia-S-S-Biotin.
Panel A exhibits the LC chromatogram where four peaks could be observed. Peaks 3 and 4 represent CMP-Sia-S-S-Biotin, without and with an additional oxygen, respectively. Peaks 1 and 2 represent Sia-S-S-Biotin, without and with an additional oxygen, respectively. The four mass spectras in panel B-E could also be observed confirming the presence of four versions of CMP-Sia-S-S-Biotin under ESI conditions. The respective m/e is shown in table 9.

The next step involved confirming whether the disulfide bond could be broken using a reducing agent. To test this, we treated CMP-Sia-S-S-Biotin with dithiothreitol (DTT) and analyzed the resulting samples with HPLC before and after DTT treatment. Two controls were also used: CMP-Sia-Az and CMP-Sia-Az-Biotin (Figure 13A). The blue chromatogram

represents the resulting sugar after the disulfide bond cleavage. It appeared at a different retention time than CMP-SiaAz due to the triazole ring formed by the Cu^{2+}-based click reaction that remains attached after the disulfide bond reduction. A tiny peak at the start of the chromatogram could potentially indicate the cleaved biotin moiety as it is non-polar and would not stick to the DNAPac column.

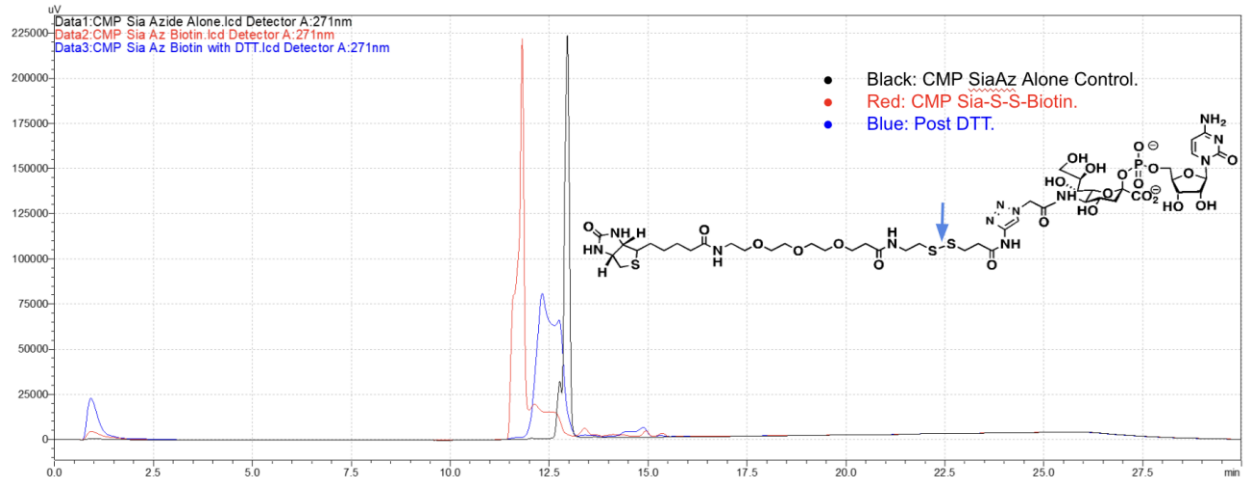

A

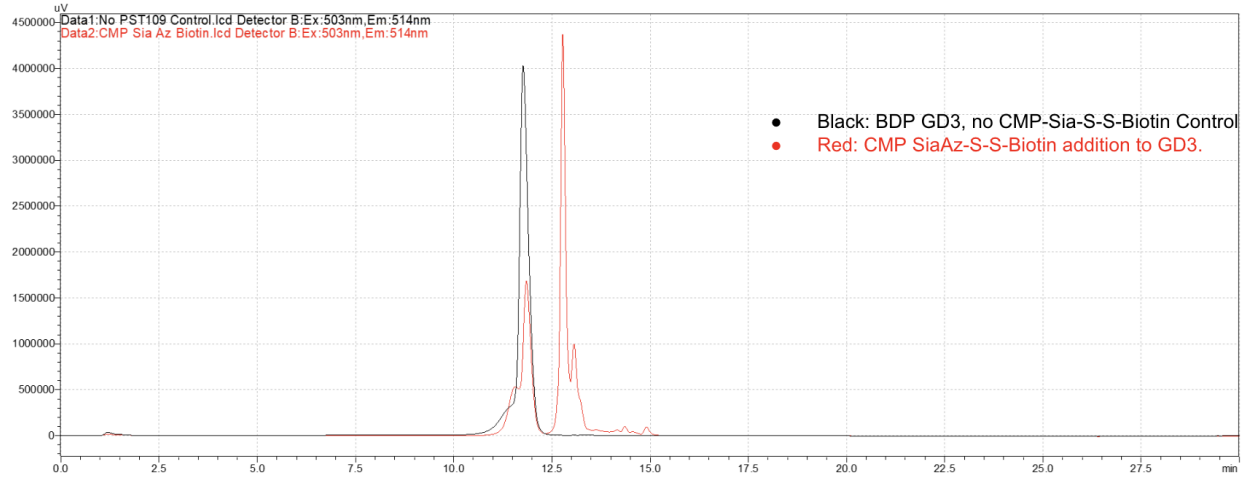

B

Figure 13. HPLC chromatograms confirming the DTT reduction and bPST-109 reaction. Panel A displays chromatograms colored in black, red, and blue, which correspond to CMP-SiaAz, CMP-Sia-S-S-Biotin, and CMP-Sia-S-S-Biotin treated with DTT, respectively. The structure of CMP-Sia-S-S-Biotin is also shown with an arrow pointing to the disulfide bond.

Panel B displays the chromatograms before and after the bPST109 enzymatic reaction where the decrease in the concentration of BODIPY-GD3 (black) and the appearance of new peak (red) confirms the success of the reaction.

To confirm the enzyme's ability to transfer CMP-Sia-S-S-Biotin to a substrate, a bPST-109 enzymatic reaction was carried out using BODIPY-GD3 as a synthetic acceptor (Figure 13B). A noticeable shift was observed when comparing the red and black chromatograms, indicating that bPST-109 can utilize CMP-Sia-S- S-Biotin as a donor sugar.

To determine whether we could transfer CMP-Sia-S-S-Biotin to polySia on the surface of mammalian cells, followed by isolation of the polysialylated protein, we used the NK-92 cell line due to its known NCAM polySialylation[116] (Figure 14).

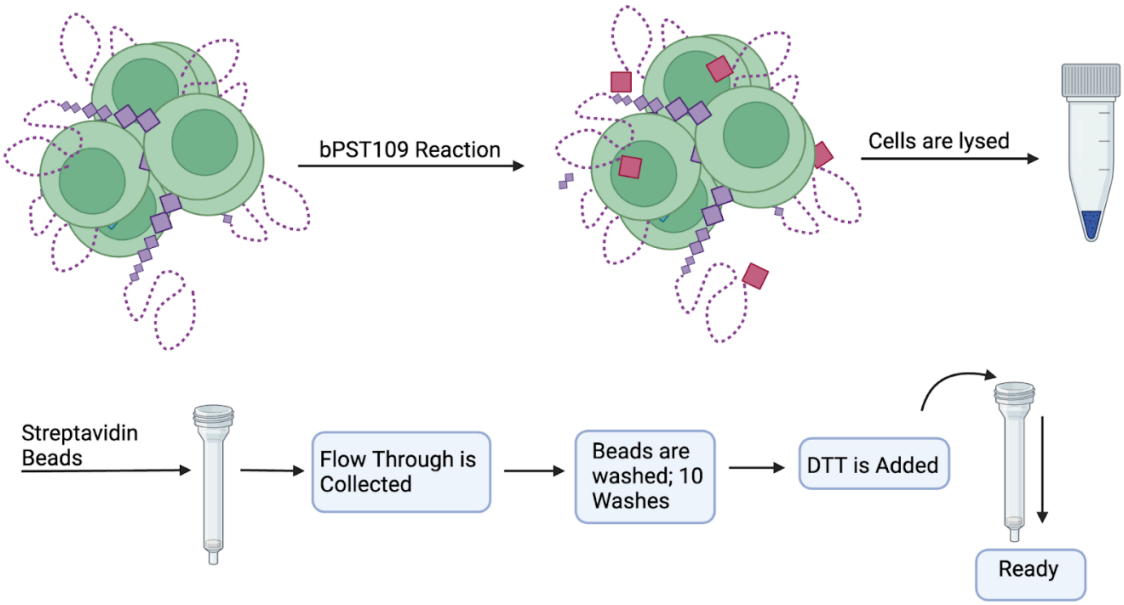

Figure 14. Graphical representation of the CMP-Sia-S-S-Biotin-based method in cells. The NK-92 cells are depicted in green, showcasing the presence of polySia in purple. A pink diamond is used to represent the CMP-Sia-S-S-Biotin, which is added to the cell surface's polySia. Streptavidin HRP blot confirms the success of the enzymatic reaction. The sample is rotated with streptavidin beads, which are then added to the column and washed 4x with 1% SDS in PBS and 10x with PBS to remove impurities. The beads with attached polySia are transferred

to a new tube and treated with DTT, resulting in the removal of streptavidin from protein polySia, which is then sent for mass spectrometry.

We first confirmed the addition of CMP-Sia-S-S-Biotin to the polySia chains on NCAM using a streptavidin-HRP blot (Figure 15A). The biotinylated polySia NCAM was rotated with streptavidin beads and added to the column, and the flow through was collected. An anti-polySia blot confirmed that the polySia was indeed bound to the beads, with only a minuscule amount remaining in the flow-through (Figure 15B). Furthermore, a negative control was similarly carried out without CMP-Sia-S-S-Biotin, and the blot showed that all of the polySia NCAM could be found in the flow-through (Figure 15B).

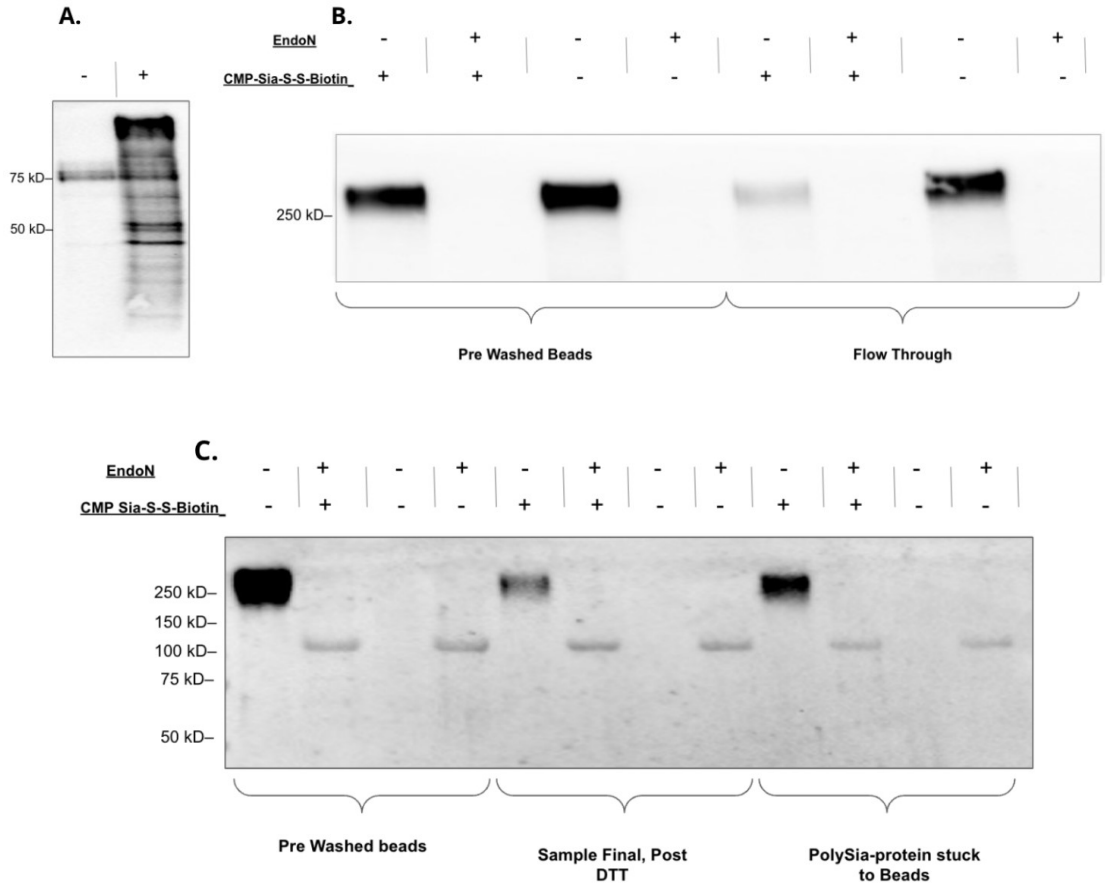

Figure 15. Confirmation blots for CMP-Sia-S-S-Biotin based method in a cell line.

Panel A shows a biotin blot where the biotinylation could be observed against the control. Panel B depicts an anti-polySia blot which shows that most of the polysialylated proteins are attached to streptavidin beads. On the contrary, the majority of polySia could be observed in the flow-through for the control. Lastly, Panel C shows the efficiency of DTT to release polysialylated protein from streptavidin beads. DTT failed to remove polysialylated proteins from streptavidin beads. EndoN treated samples are negative controls where EndoN has been used to remove polySia.

To release the polysialylated proteins from the beads, we treated the sample with DTT to reduce the disulfide bonds. To assess the efficacy of this release, we performed an anti-polySia immunoblot on the eluate and the material remaining associated with the beads post-elution (Figure 15C). While some polysialylated protein eluted from the beads after DTT treatment, we were surprised to find that the majority of polySia remained associated with the beads. To determine if the DTT reductions conditions could be improved upon, we measured the elution of polySia with higher concentrations of DTT and longer incubations but were not able to substantially improve the elution (Figure 16).

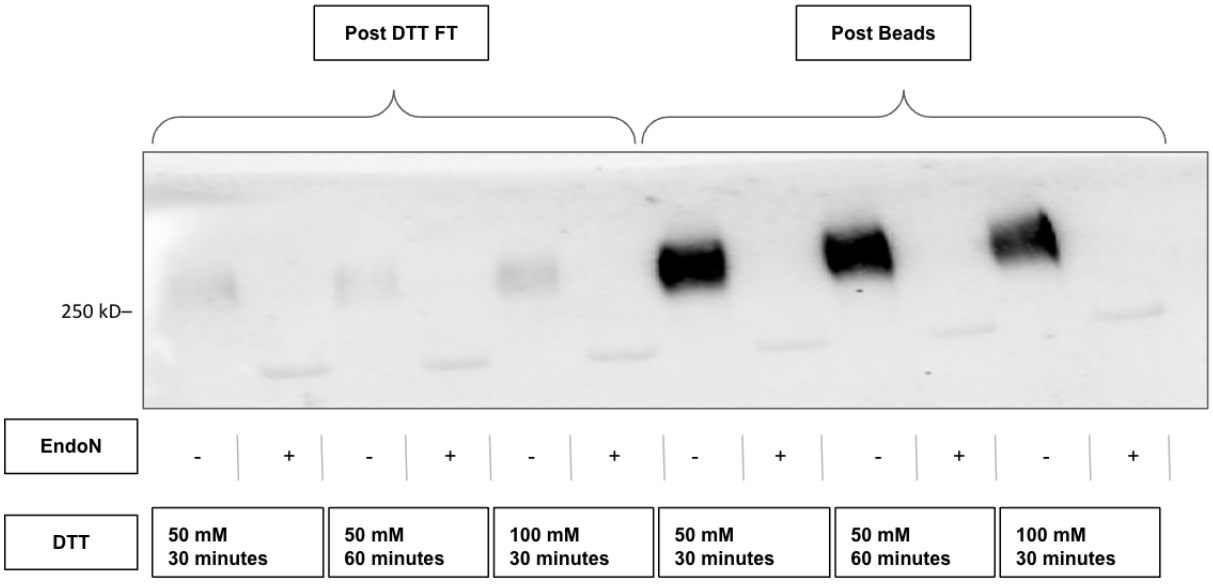

Figure 16. Anti-polySia blot with different DTT conditions to reduce the disulfide bond.

DTT at the final concentration of 50 mM was tried for 30 and 60 minutes at room temperature but no difference was observed. Increasing the DTT concentration to 100 mM increased the reduction slightly but was not significant. EndoN treated samples are negative controls where EndoN has been used to remove polySia.

We next evaluated whether tris(2-carboxyethyl)phosphine (TCEP) would be more effective in releasing the polysialylated proteins, as TCEP outperforms DTT, particularly under acidic conditions, and has a wider pH range[117]. However, TCEP's larger size may pose a greater challenge in reaching the disulfide bond due to steric hindrance. Unfortunately, treatment with TCEP also did not achieve the desired release of polysialylated proteins (Figure 17).

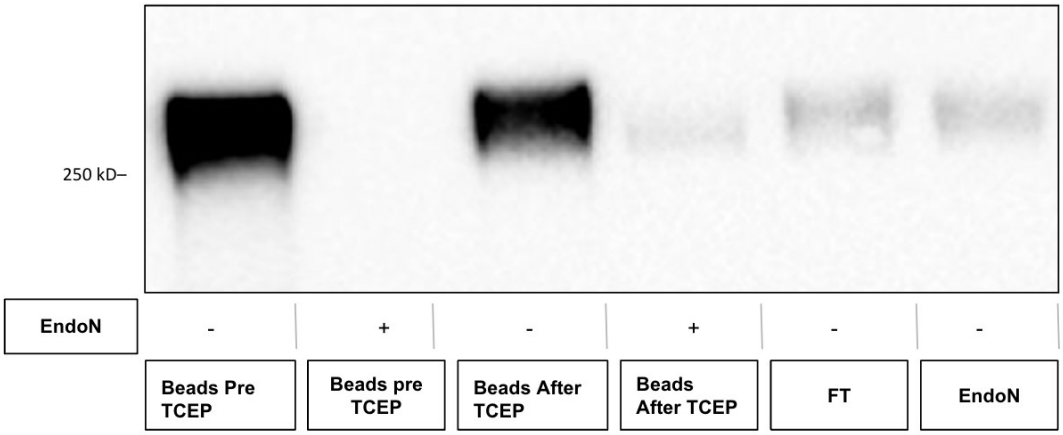

Figure 17. Anti-polySia blot when TCEP was utilized to release polysialylated protein. When the Beads after TCEP and flow through (FT) were compared, no significant differences were observed. EndoN treated samples are negative controls where EndoN has been used to remove polySia.

To confirm that the biotinylation reagent did actually contain a reducible linker, biotinylated sample from NK-92 cells was treated with β-mercaptoethanol, DTT, and TCEP at incubation temperatures of 50, 60, and 70 degrees Celsius for 30 minutes. Three samples in PBS incubated under similar conditions were used as controls to ensure that the removal of polySia was due to the DTT and not the higher temperature. An additional sample in PBS was kept at

room temperature for 30 minutes and was used as a positive control, while a sample without CMP-Sia-S-S-Biotin was used as a negative control. A streptavidin blot confirmed that all reduction conditions worked when compared to the controls, proving that the disulfide bond is present and can be reduced under standard conditions (Figure 18).

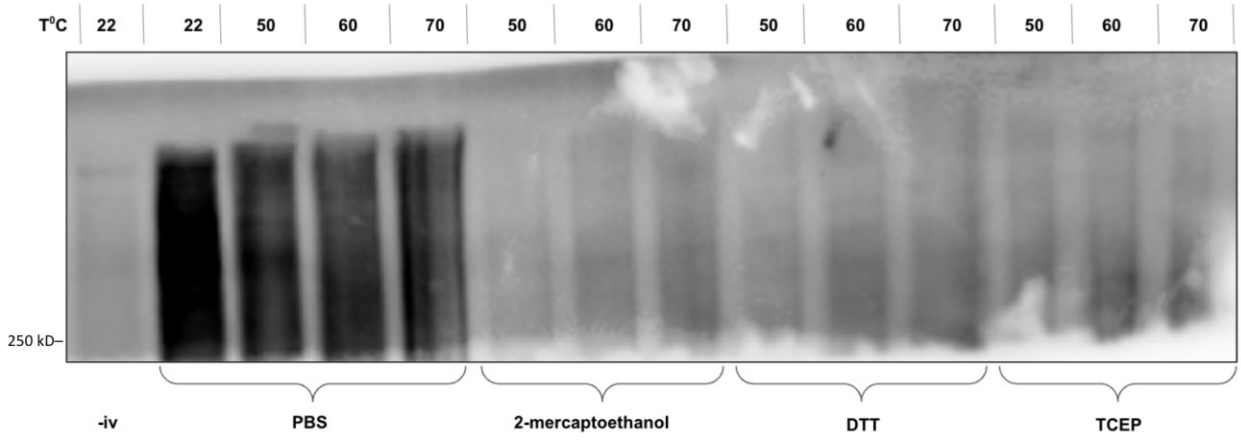

Figure 18. Biotin blot for different reducing conditions confirming the presence of disulfide bond.
The 2-mercaptoethanol, DTT, and TCEP reactions were tried at three different temperatures: 50, 60, and 70 degrees Celsius for 30 minutes. Controls include sample with and without CMP-Sia-S-S-Biotin in PBS kept at room temperature for 30 minutes. Three additional controls with CMP-Sia-S-S-Biotin in PBS, kept at 50, 60 and 70 degrees Celsius were also employed. All of the reduction conditions worked.

Given that the reducing conditions proved effective when the streptavidin beads were not attached but did not have the same success when the beads were present, we wondered if the lack of elution could be attributed to the non-specific binding of NCAM to the streptavidin. NCAM is a single pass membrane protein and also contains numerous disulfide bonds, which may expose internal hydrophobic areas of the protein upon treatment with reducing agents[118]. In order to investigate the potential non-specific binding of NCAM to streptavidin beads, we attempted the same process with artificially polysialylated GFP. GFP is a soluble protein that contains only a

single disulfide bonds so should be more resistant to treatment with reducing agents[119]. We expressed GFP fused to a peptide containing two glycosylation sequences and then enzymatically polysialylated the protein in vitro (see Chapter 4). When we isolated biotinylated GFP polySia on streptavidin-agarose and then treated with the same reducing conditions, we observed that GFP polySia was successfully eluted from the beads (Figure 19). We therefore concluded that this strategy for immobilization of polysialylated proteins followed by reduction to release the proteins would not be as useful as we expected as most of the polysialylated proteins are likely membrane proteins and would potentially behave similar to NCAM by sticking to the beads.

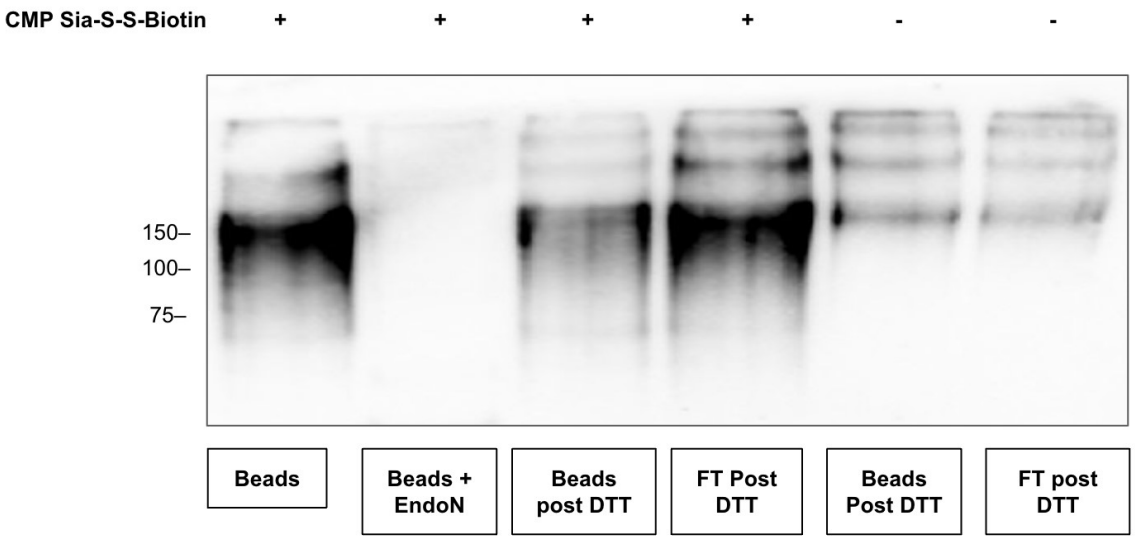

Figure 19. Confirmation of release with DTT when GFP-polySia is used as an alternative. The anti-polySia blot confirm that the GFP-polySia is released from the beads when treated with DTT. This could be observed be comparing beads, pre and post DTT. Most of the GFP-polySia is in the post DTT flow through. The MW of GFP is 38 kD (without polysialylation).

Chapter 04. Development of methodologies to visualize polySia receptors on immune cells.

PolySia possesses the capability to capture biological molecules, function as a ligand, and as a receptor that influences biological responses in both health and diseases[9,10], for instance it binds to BDNF, CCL21 and catecholamines[23,45]. When polySia was immobilized, it bound to both heparin sulfate (HS) and BDNF but when HS and BDNF were immobilized, the polySia could not bind to immobilized BDNF while it did to HS[46]. This could potentially suggest that the site used by BDNF to bind to polySia may already be inaccessible since it was likely utilized during immobilization. This could potentially mean that the binding of BDNF could be a specific ligand-receptor based interaction. In support of these findings, a couple of receptors have been identified that binds to polySia i.e., siglec-11 and siglec-16. Depending upon which receptor is involved, polySia interaction could results in inhibition or activation. For example, binding of polySia to siglec-11 leads to the inhibition of microglial cells, whereas binding to siglec-16 causes activation of tissue macrophages[47,48].

It is possible that immune cells have more polySia receptors on their surfaces due to polySia's immunomodulatory properties. To verify the existence of these receptors, we have been working on creating a fluorescent ligand that could potentially bind to the unknown receptor(s) and allow for detection through flow cytometry or fluorescent microscopy. Our initial attempt at creating a fluorescent ligand, BODIPY-Lactose-polySia, resulted in non-specific internalization when incubated with Jurkat T cells. As a result, we developed a new ligand by polysialylating green fluorescent protein (GFP) and incubating it with Jurkat T cells. While this modified method showed some promise, further refinement is necessary for optimal results.

4.1. Visualization of receptors with BODIPY-polySia

To detect polySia receptors on immune cells, we first synthesized polySia on a BODIPY fluorochrome. Our hypothesis was that cells with polySia receptor(s) would bind to BODIPY-polySia and would potentially produce higher fluorescence, either on the cell surface or inside it, compared to the control. For control purposes, colominic acid, a commercial polySia from *E.coli* was used in excess to outcompete the BODIPY-polySia, resulting in a decrease in fluorescence. Furthermore, we varied the concentration of colominic acid to observe a concentration-dependent decrease in BODIPY fluorescence.

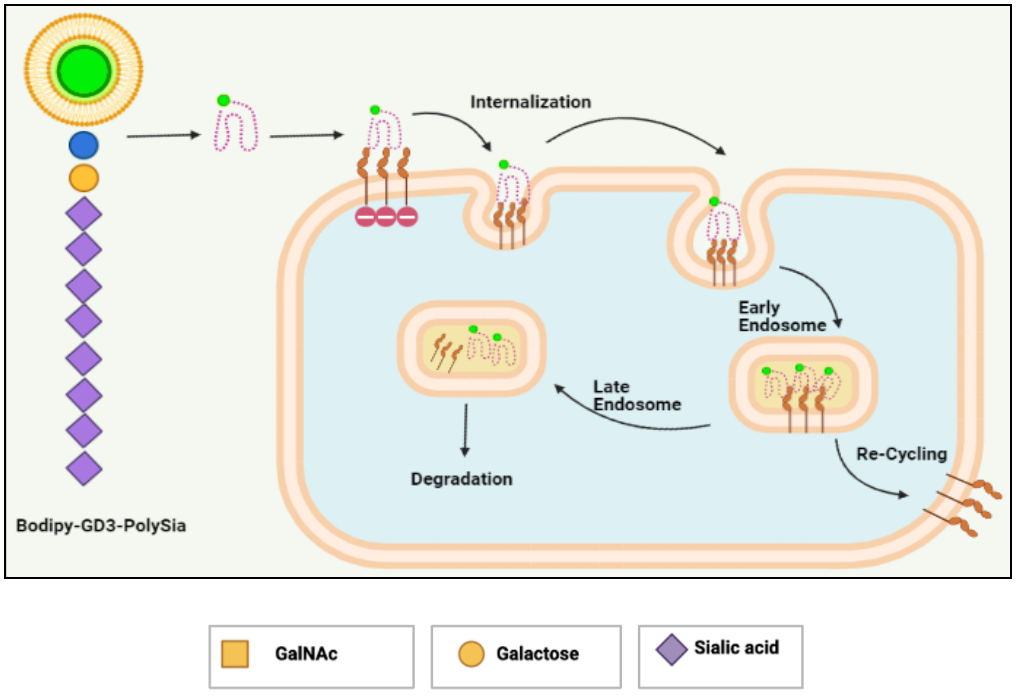

Figure 20. Graphical abstract for the method utilizing BODIPY-polySia.
The cell shown represents a Jurkat T cell expressing receptors for polySia. The BODIPY-polySia in green with purple diamond could be observed that interacts with unknown receptors and is internalized. The BODIPY fluorescence could be confirmed with flow cytometry and/are with fluorescent microscopy.

We built polySia on BODIPY using lactose as a starting disaccharide as we have sialyltransferases that can build polySia on lactose. β-D-Lactose-Ethyl-Azide (β-D-Lac-N_3) was first coupled to BODIPY-alkyne and purified by Sep-Pak C18 column. Enzymes CST-1 and CST-2 were utilized to covalently add the first and second Sias to BODIPY-Lac resulting in the synthesis of BODIPY-GM3 and BODIPY-GD3, respectively. The reactions were confirmed through a TLC (Figure 21A). By adding Sia to BODIPY-Lac, the resultant BODIPY -GM3 becomes more polar and cover less distance on TLC when compared to BODIPY-Lac. This is evident when comparing the dots on TLC for BODIPY-Lac and BODIPY-GM3 (Figure 21A). Additionally, CST-2 enzymatic reaction adds α-2,8 Sia (could be more than one Sia) to BODIPY-GM3 producing a more polar product, which has more interaction with TLC than BODIPY-GM3. This is noticeable when comparing BODIPY-GM3 and BODIPY-GD3 (Figure 21A).

After undergoing purification with the Sep-Pak C18 column, the polysialylation reaction was carried out using the bPST109 enzyme. Confirmation with TLC was not possible due to the higher polarity of polySia, and the sample was instead analyzed with HPLC using DNAPac column with detection at 503 for BODIPY (Figure 21B-D). The control sample that contained BODIPY-GD3 only, appeared at a retention time of 12.5 minutes in the form of a single peak (Figure 21B). The chromatogram after the bPST109 reaction displayed a decrease in the BODIPY-GD3 peak at the retention time of 12.5, with its conversion appearing in the form of new peaks (Figure 21C). Each shifted peak indicates the addition of one Sia. In addition to the peak for BODIPY-GD3 at 12.5 retention time, 26 peaks could be distinguished, with the 26th confirming the addition of 28^{th} Sia. The higher polySia chain could not be resolved with this method and appeared in the form of a single broad peak at the very end.

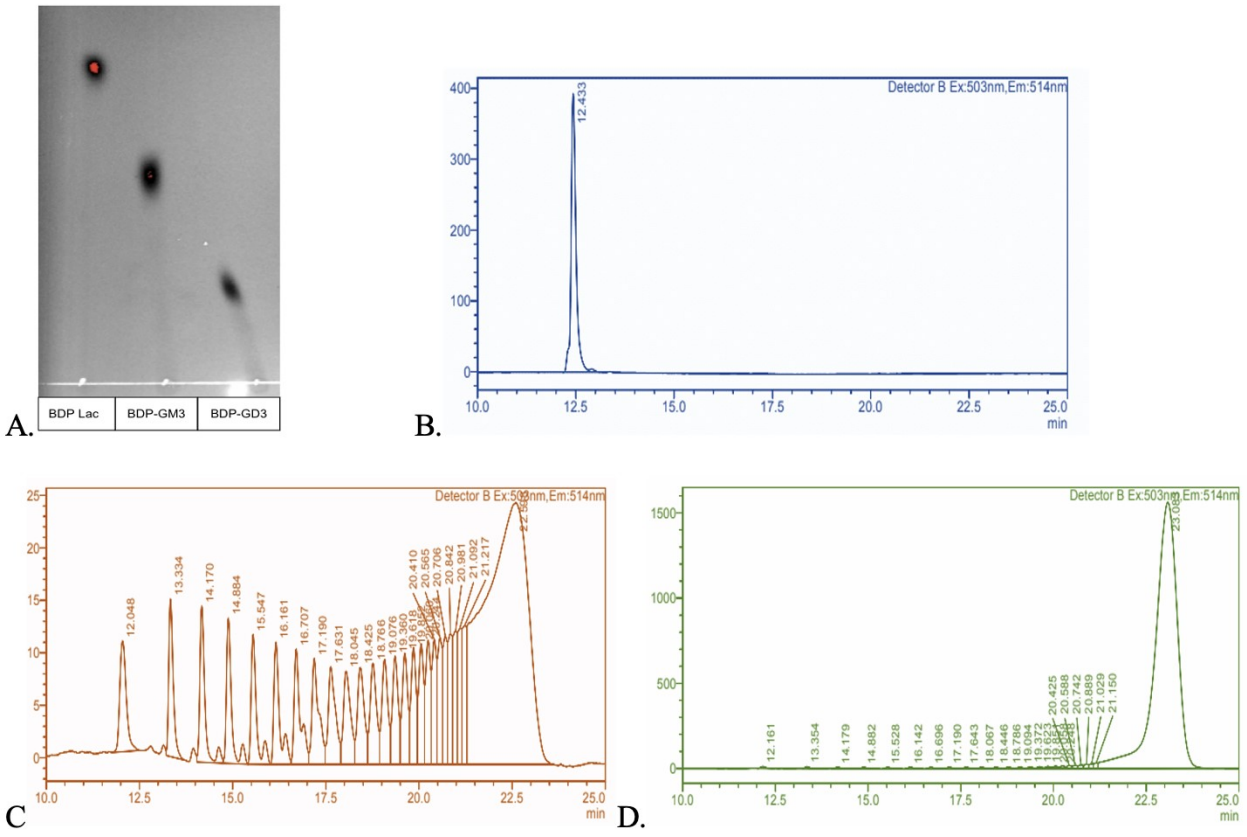

Figure 21. The polysialylation of BODIPY-Lactose.
In Panel A, TLC shows BODIPY-Lac, BODIPY-GM3 from BODIPY-GD3. Panel B displays the chromatogram for the negative control of the bPST109 reaction, wherein CMP-Sia was not added. Panels C and D showcase the pre- and post-purification stages of BDP-polySia, respectively.

In order to purify the BODIPY-polySia, we utilized the Sep-Pak C18 column. It was expected that the polySia chains due to their hydrophilicity, would be eluted in the flow-through. We concentrated all of the aliquots and confirmed the purification of BODIPY polySia through HPLC in each fraction. The aliquots containing the BODIPY polySia were pooled together, concentrated and analyzed with HPLC (Figure 21D). Evidently, the purification process was effective.

Table 10. The details of different controls and sample for the BODIPY-polySia method.

No.	BODIPY-GD3	BODIPY-polySia	Colominic acid	Expected fluorescence	Observed fluorescence
1	20 µM	X	X	✓	✓
2	X	20 µM	X	X	✓
3	X	20 µM	500 µM	X	✓
4	X	20 µM	1000 µM	X	✓

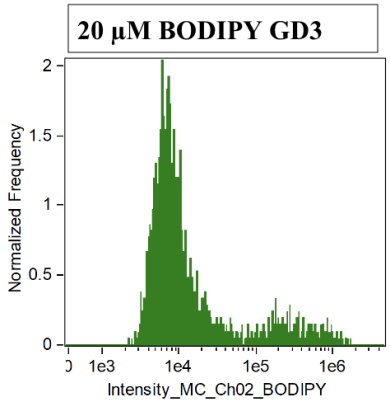

Intensity_MC_Ch02_BODIPY

Population	Count	%Gated	Median
focused & cells	2077	100	7987.14

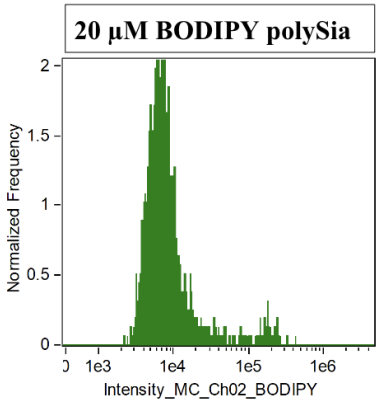

Intensity_MC_Ch02_BODIPY

Population	Count	%Gated	Median
focused & cells & R2	1566	100	6982.88

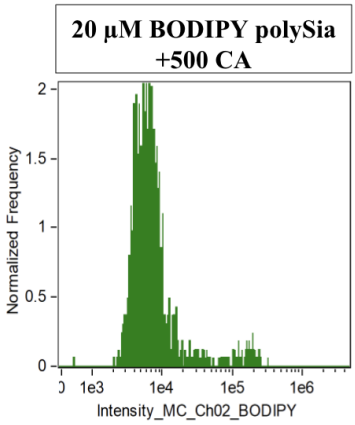

Intensity_MC_Ch02_BODIPY

Population	Count	%Gated	Median
focused & cells & R2	1633	100	6124.62

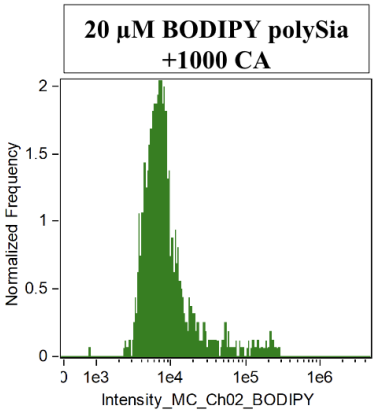

Intensity_MC_Ch02_BODIPY

Population	Count	%Gated	Median
focused & cells & R2	1603	100	7136.77

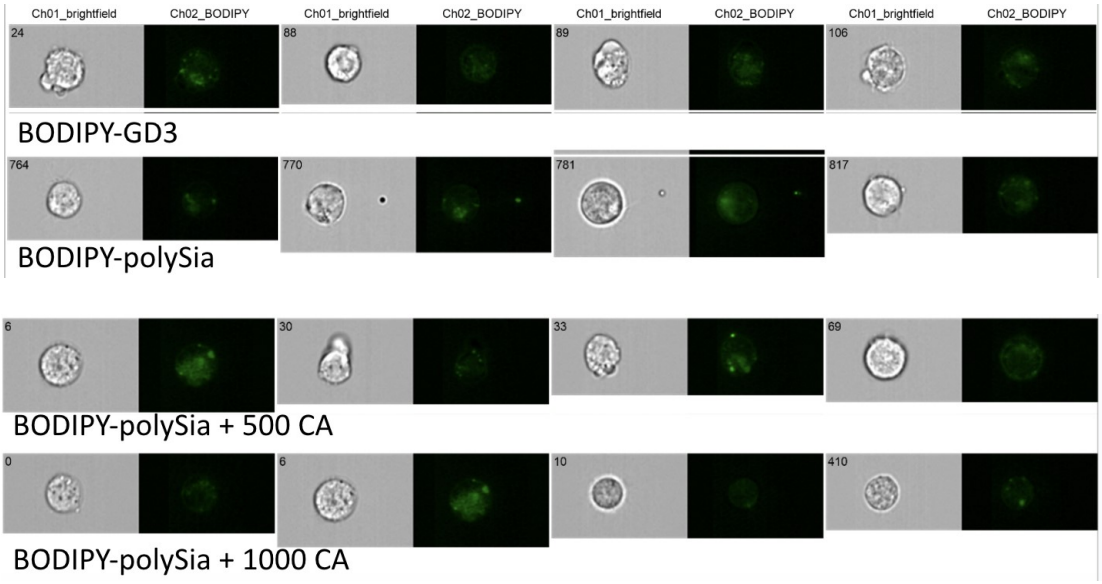

Figure 22. The flow cytometry results for the BDP polySia method.
A single sample was utilized at a concentration of 20 uM, accompanied by a negative control of BDP-GD3 at an equivalent concentration. No discernible variance was noted. The two supplementary negative controls involving colominic acid also failed to produce the expected outcomes. The images of cells were also produced with IDEAS software after the samples were analyzed with ImageStreamer cytometer. CA: colominic acid.

To determine whether BODIPY polySia could bind to T cells in a polySia-dependent manner, we examined its interactions with Jurkat T cells at room temperature. Jurkat T cells are immortalized T lymphocytes, acquired from the peripheral blood of a 14-year-old boy with T cell leukaemia[120]. We also conducted three control treatments (Table 10). We analyzed the samples using an image flow cytometer and found no significant difference in median fluorescence between the sample and controls. The green color BODIPY was present throughout the cell cytoplasm, indicating nonspecific internalization of BODIPY polySia (Figure 22). The fluorescence remained unchanged despite testing various other conditions (Table 11) and lowering the incubation temperature. To prevent nonspecific internalization, we decided to use a macromolecule, e.g., fluorescent protein polySia, which would also provide a more natural experimental condition.

Table 11. Different conditions that were used to optimize the procedure and to avoid non-specific internalization of the fluorescent ligand.

No.	**Different experimental conditions used.**
1	Different time points from 15 minutes to 2 hours.
2	Different concentrations of BODIPY-polySia; 20, 50 and 100 µM.
3	Different temperature: room temperature, 4 and 37 degrees Celsius.
4	Different blocking conditions.
5	Different cell lines; Jurkat T, NK-92 and CHO cells.
6	Different instruments: imageStreamer cytometer and fluorescent microscopy.

4.2. Visualization of receptors with GFP-02 polySia

The methodology employed closely resembles that of BODIPY-Lac-polySia (Figure 20), with the exception that polysialylated GFP was utilized as a ligand following polysialylation. To ensure protein stability and solubility in the aqueous reaction environment, we constructed a plasmid featuring HisTag-GB1-Seq-Seq-GFP (Figure 23). GB1, which is the B1 domain of protein G, was incorporated to facilitate stabilization and solubilization by preventing aggregation and aiding in proper folding[121]. The two Sequences consisting of P-G-P-T-P-A-P were inserted twice in a repeating manner between GB1 and GFP (Figure 23). This construct was termed as *GFP-02*.

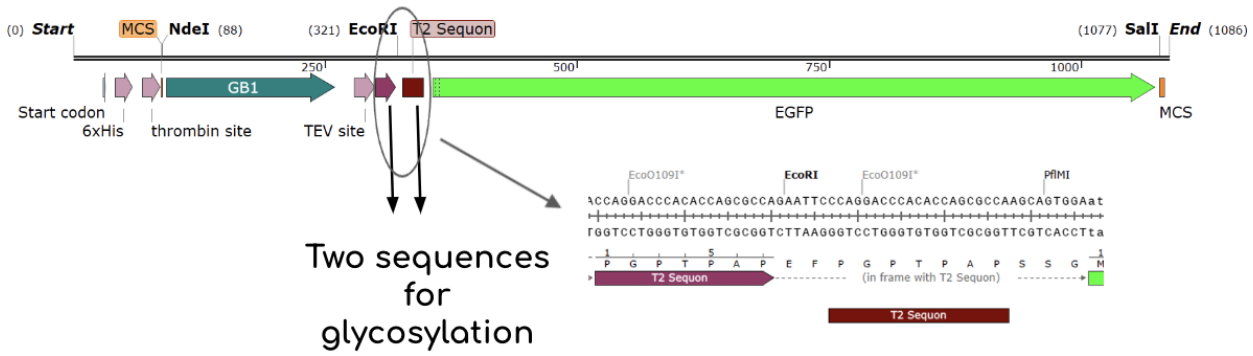

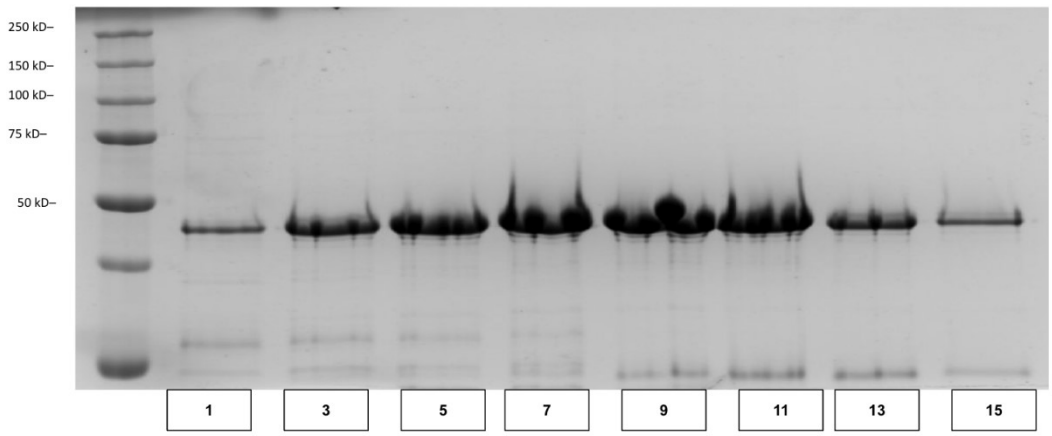

Figure 23. The gene construct for GFP-02 and its expression and purification.
The construct features two glycosylation Sequons positioned between GFP and GB1. Additionally, a HisTag is located at the N terminus. A TEV cut site is also present between GB1 and the first sequence. The panel at the bottom shows its purification. The mw of GFP-02 is 38.3 kD.

The GFP-02 protein was successfully expressed and purified using a nickel affinity column (Figure 23). To add GalNAc to the threonine's hydroxyl functional group, a test enzymatic reaction was carried out where two enzymes - GalNAcT and CPG-13 were used. UDP-GlcNAc was converted to UDP-GalNAc by CPG-13, an epimerase, while GalNAcT covalently added GalNAc to threonine. The reaction was confirmed by using GalNAc lectin blot. Once the optimal GalNAc addition was reached, the reaction was scaled up, and GFP-02-GalNAc from the test reaction was used as the positive control (Figure 24). The same blot was also imaged with the GFP channel to validate the experiment, especially the negative control. The 0-minute negative control was obtained from the reaction sample at zero minutes and stopped with heat inactivation in 1x loading dye.

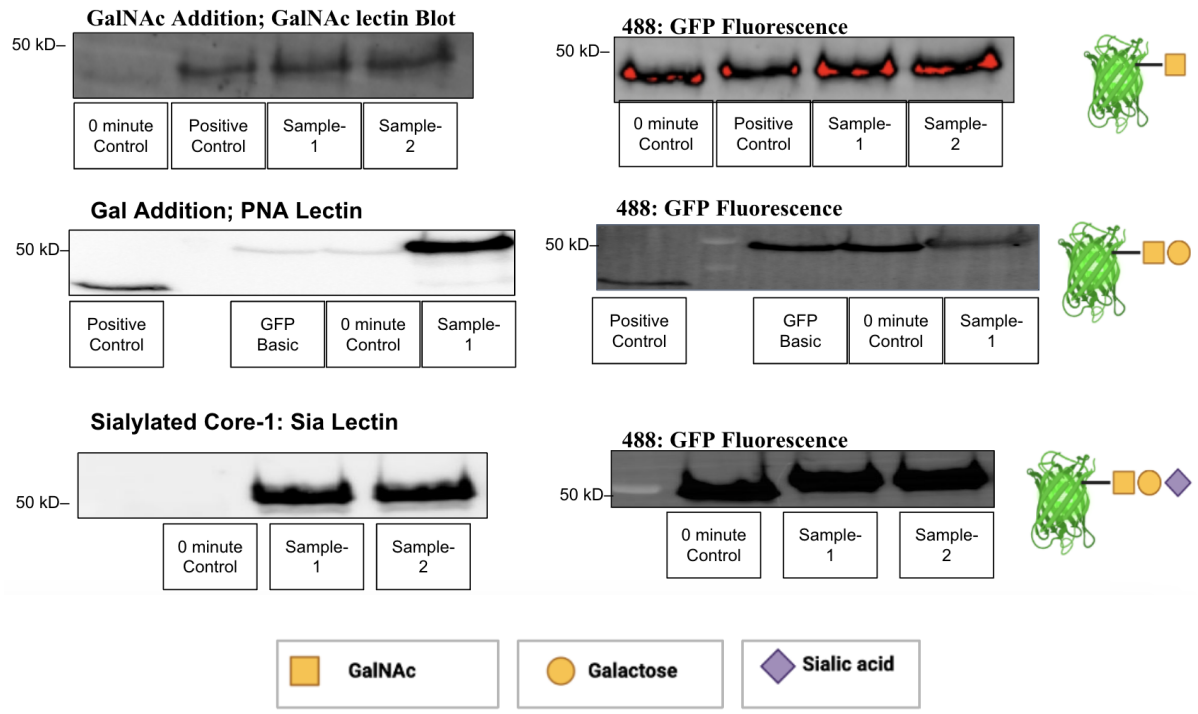

Figure 24. The confirmation blots for GalNAc, Gal, and Sia addition.
The GalNAc lectin blot was used to confirm the addition of GalNAc. For the confirmation of Gal and Sia addition, PNA and Sia lectin blots were used respectively. The blots were also imaged with GFP channel. The structures of the resultant glycosylated proteins are shown on the right sides. The mw of GFP-02 is 38.3 kD.

Following the addition of Gal through the use of enzyme DG-02, a PNA lectin blot was carried out to verify the success of the reaction (Figure 24). MPS-142 was utilized as a positive control, being 50% *O*-glycosylated. In addition, two negative controls were used, with GFP basic representing non-glycosylated GFP-02. The reaction sample underwent purification before the addition of Sia with enzyme ST3Gal1. The success of the reaction was confirmed with a Sia-lectin blot (Figure 24).

Following the purification process utilizing HisTag, the reaction advanced towards the CST-2 enzymatic reaction, successfully incorporating α-2,8 Sia onto the terminal α-2,3 Sia. Verification of the reaction was conducted using mass spectrometry (Figure 25 and Table 12). The non-glycosylated GFP-02 is represented by Peak A with a mw of 38307 Da. Peak B

represents the product after the ST3Gal1 reaction, with evidence of three glycosylation sites, as the difference between Peak A and Peak B is 1972 Da, which is equivalent to three times the mass of GalNAc-Gal-Sia. Peaks C and D represent the additional Sias that were added by CST-2 enzymatic reaction.

Table 12. The mass of the relevant possibilities based on mass spectrometry data.

No.	Peak letter	Peak represents	Mass (Da)	Difference
1	A	GFP-02, before glycosylation.	38307	
2	B	GFP-02, with three “sialylated core-1” added.	40279	1972
3	C	One additional Sia.	40572	293
4	D	One additional Sia.	40860	288

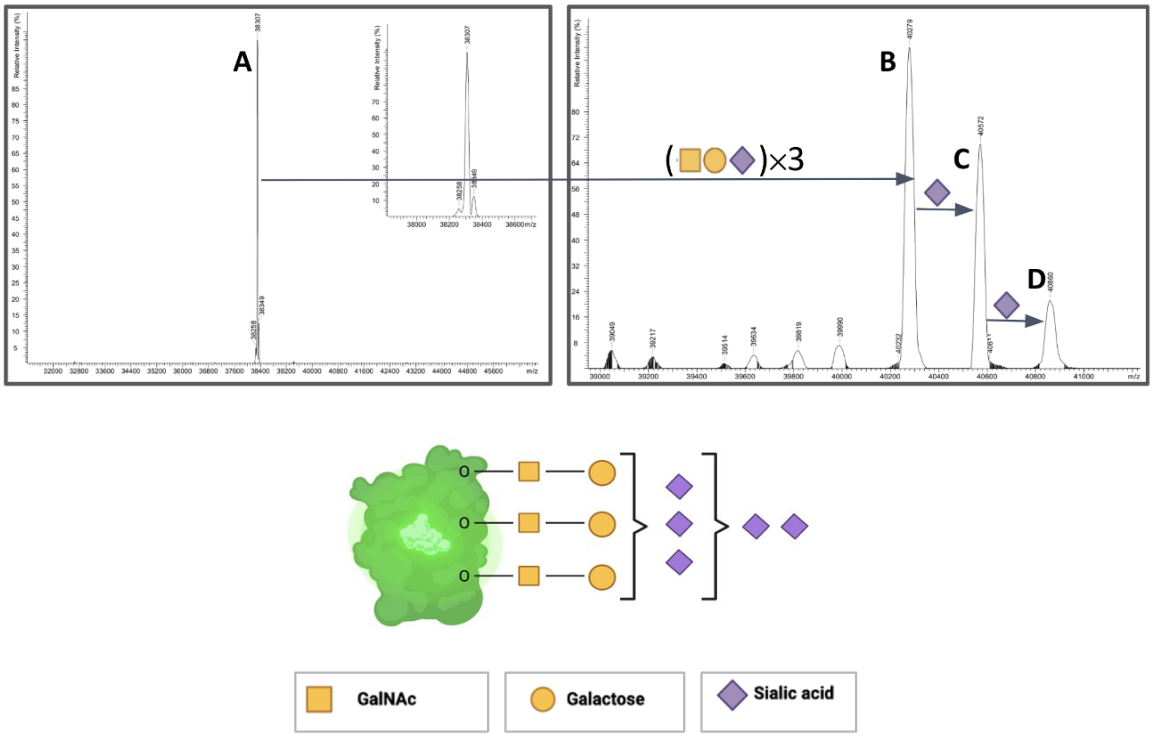

Figure 25. The mass spectra and the possible structure after the CST-2 reaction.
Capital letters have been used to represent the peaks. The detail of each peak is mentioned in Table 12. The expected structure after the CST-2 reaction is also shown.

Following the successful confirmation of the CST-2 reaction, the enzymatic reaction of bPST-109 was carried out. To serve as a negative control, an additional sample without the addition of CMP-Sia was used. The reaction was verified through Coomassie gel and with anti-polySia blot (Figure 26).

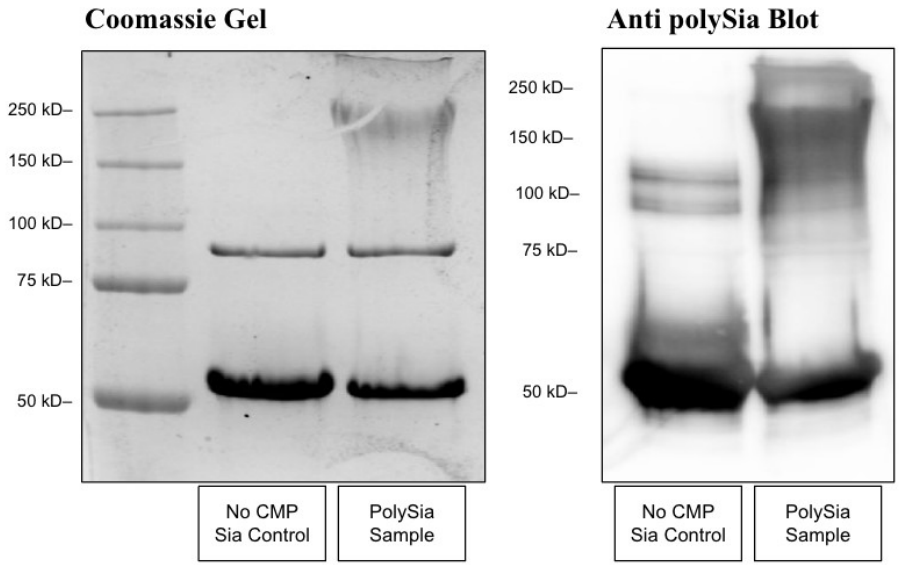

Figure 26. The confirmation of bPST-109 enzymatic reaction.
On the left side, a Coomassie gel is showing the success of polysialylation. On the right side, an anti-polySia blot is given which supports similar findings. The No CMP-Sia control is when CMP-Sia was not added to the sample.

To separate the polysialylated GFP-02 from its non-polysialylated counterpart, the reaction sample was run through the Superdex-75 column (Figure 27). The resultant polysialylated GFP-02 aliquots were then pooled and concentrated, and their concentration was measured via the BCA assay. Similarly, the non-glycosylated GFP-02 and GFP-02-diaSia were also passed through the Superdex-75 column, and their respective aliquots were pooled and concentrated.

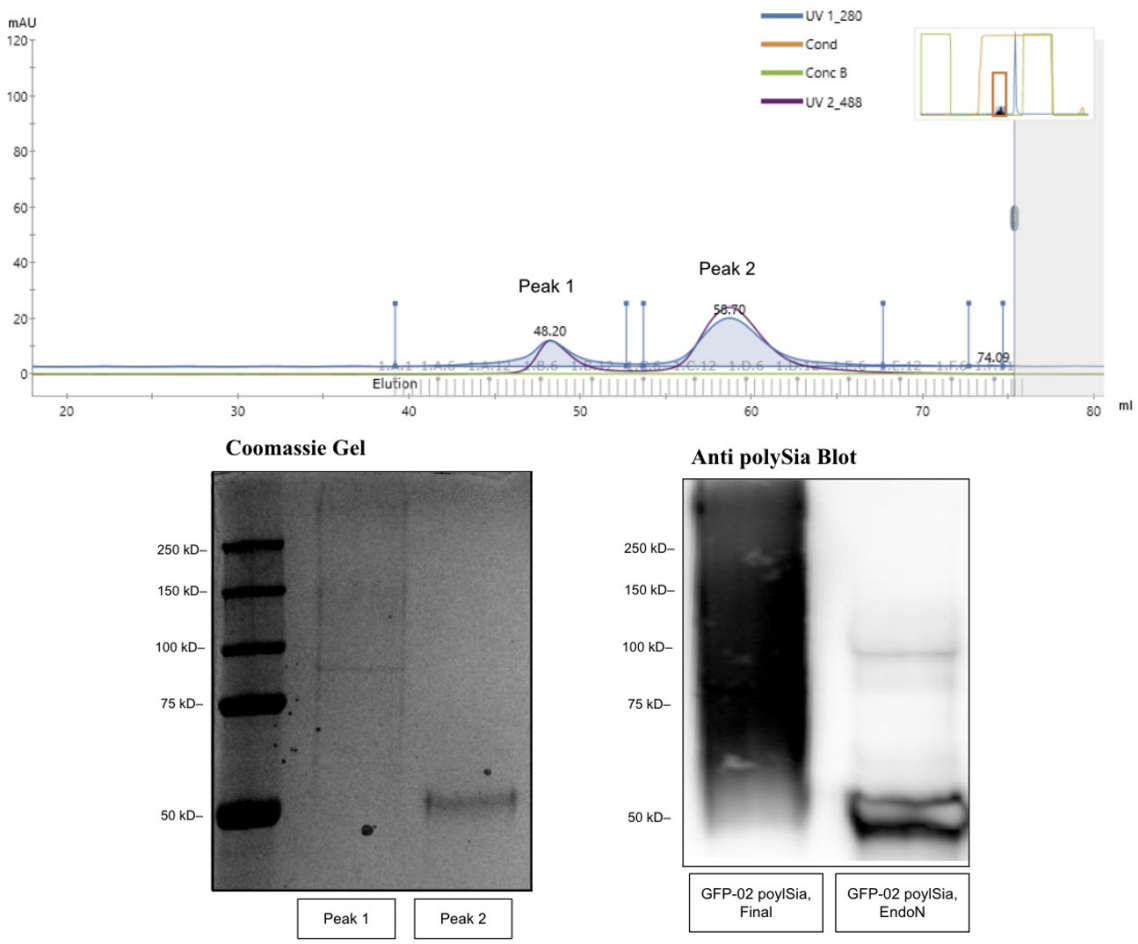

Figure 27. The purification of GFP-02 polySia.
Two detection methods were used during the purification, channel -280 for the protein and channel-488 for the GFP fluorescence. The Coomassie gel and anti-polySia blot are also shown confirming the successful purification of GFP-02 polySia. The sample used for anti-polySia blot were taken after concentrating the aliquots from peak 1.

The GFP-02 polySia underwent incubation with Jurka T cells and was subsequently examined through flow cytometry. Three negative controls were also utilized (Table 13). We anticipated that the sample would exhibit higher GFP fluorescence, but adding colominic acid would outcompete the ligand, reducing GFP fluorescence. We employed a GFP-02 diSia control to eliminate the possibility of diSia interactions, while the No GFP-02 control was utilized to

adjust autofluorescence. The flow cytometry chromatograms show that GFP-02 polySia resulted in higher fluorescence compared to the controls "No GFP-02" and "GFP-02 diSia" (Figure 28A). Furthermore, the addition of colominic acid shifted the peak backward towards the earlier stages of the analysis. The images of individual cells captured by imageStreamer showed similar results (Figure 28B). No visible fluorescence was observed on or inside the cells for “No GFP-02 Control” and “GFP-02 diSia”. However, when the cells were treated with GFP-02 polySia, fluorescence was detected. The addition of colominic acid, eliminated the fluorescence, except for a few cells. It appears that GFP-02 polySia is potentially interacting with unidentified receptors, resulting in an increase in fluorescence and the excess colominic acid is competing for receptor binding, resulting in a decrease in fluorescence but this needs to be explored further.

Table 13. The flow cytometry sample arrangement for the GFP-02 polySia method.

No.	Sample treatment type	Concentration	Expected fluorescence	Observed fluorescence
1	GFP-02, non-glycosylated	20 µM	X	X
2	GFP-02 diSia	20 µM	X	X
3	GFP-02 polySia	20 µM	✓	✓
4	GFP-02 polySia + colominic acid	20+250 µM	X	X

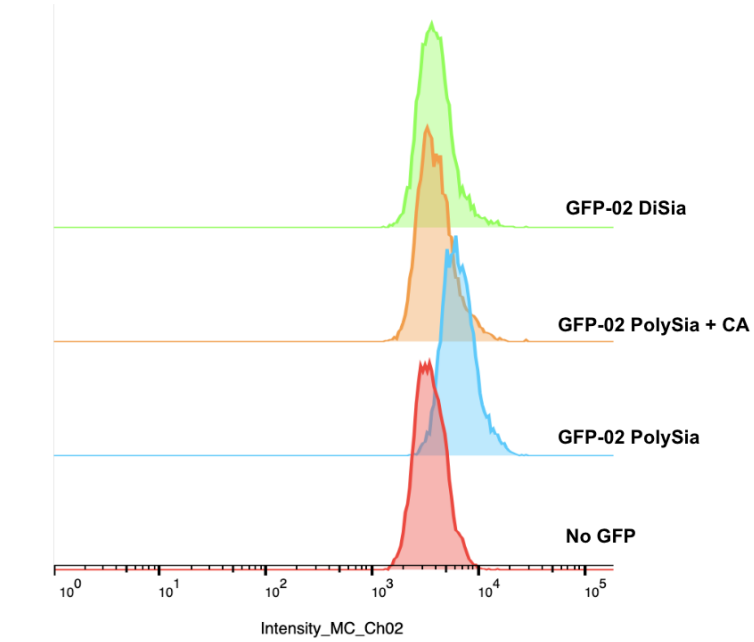

A.

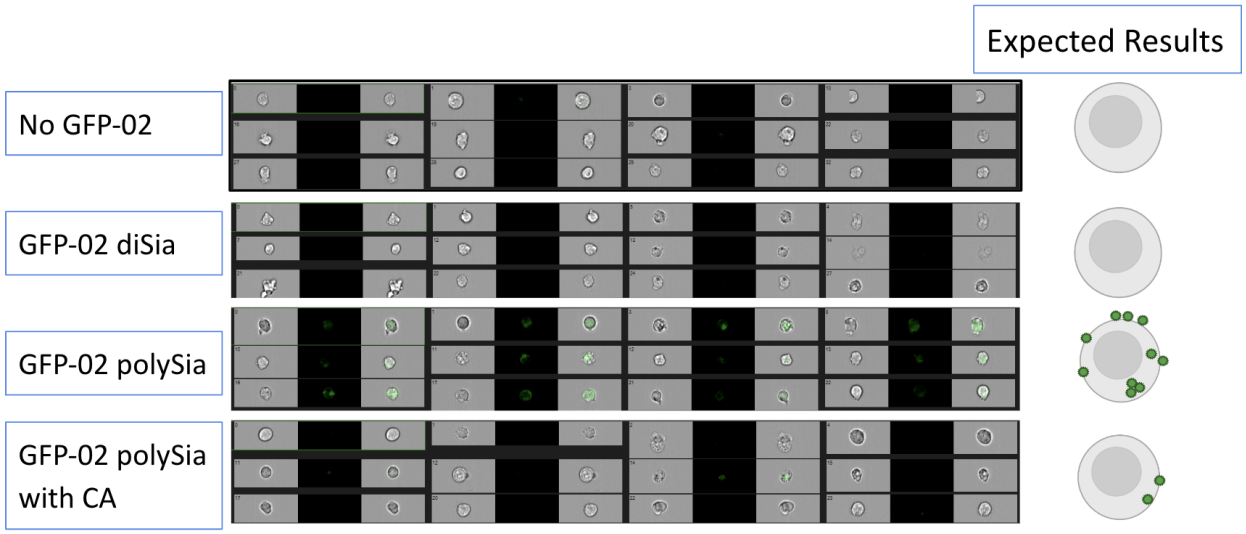

B

Figure 28. The flow cytometry results for the GFP-02 polySia fluorescence when incubated with Jurkat T cells.

The sample details are shown with its respective chromatograms. The GFP-02 polySia resulted in higher fluorescence when compared to negative controls and a clear shift could be observed in panel A. The images of the cells could also be observed in panel B with higher green color fluorescence in GFP-02 polySia treated sample against the controls. CA: colominic acid.

The experiment was conducted multiple times using a fresh batch of GFP-02 polySia, but the results were not reproduced. Furthermore, the experiment was performed on CHO cells with siglec-11 receptors and with NK-92 cells, but no variance between the sample and negative controls was observed. Upon examination of the sample batches, it was discovered that the CST-2 reaction could potentially influence the outcomes. In the latest batches, there was minimal to no presence of the third peak (Peak D) for Sia (α-2,8 Sia) (Figure 29). This led to the hypothesis that this additional Sia could lead to an extra polySia chain(s) which would result in higher avidity.

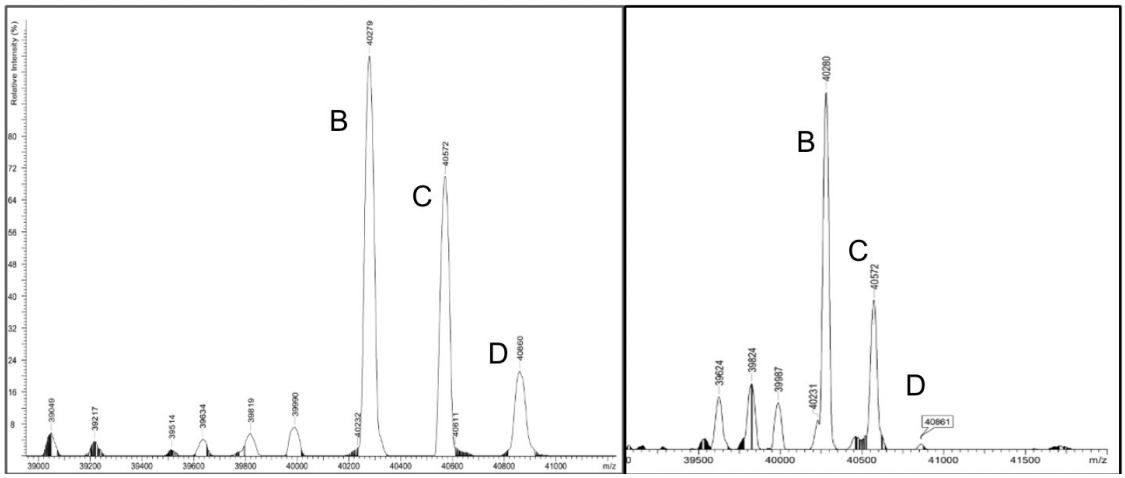

Figure 29. The mass spectras from two different batches of CST-2 reactions.
Two mass spectras separated by a bold line in the middle are shown for the 1st and 2nd batches (left to right). Peak A representing the non-glycosylated GFP-02 is not shown here. The details of peak B and C are shown in Table 12. It could be observed the peak D representing the addition of 2nd α-2,8 Sia, is absent in the 2nd batch.

Despite experimenting with different conditions to enhance the success of CST-2 reaction, the attempts were unsuccessful. It has been shown that CST-2 prefers Gal attached to GlcNAc through β-1,4[122]. In core-1, Gal is attached to GalNAc via β-1,3, while in core-2 structure, Gal is attached to underlying GlcNAc via β-1,4 (Figure 30)[122]. To enhance peak D, a

core-2 structure was synthesized. This approach would also be more cost-effective since a majority of the GFP could undergo polysialylation.

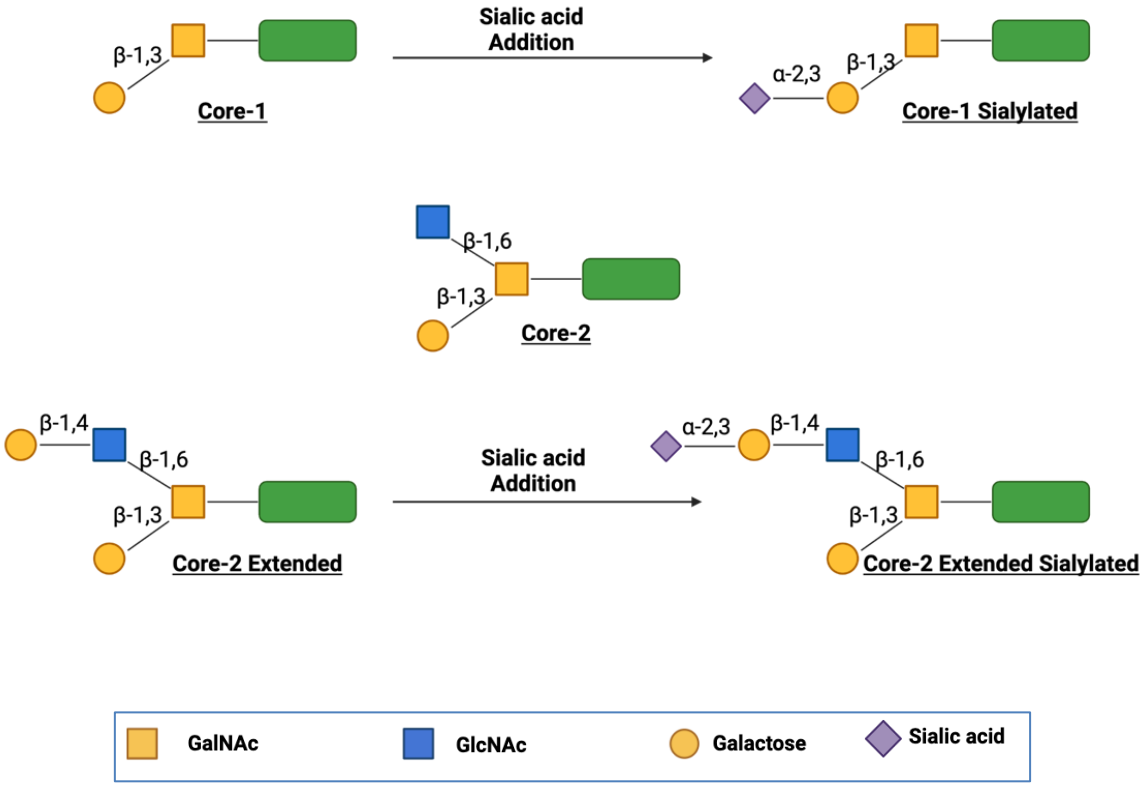

Figure 30. The structure of core-1, core-2, and their Sialylated versions
In core 1, the GalNAc is attached to the hydroxyl functional group of threonine/serine through an alpha linkage. In addition, Gal is attached to GalNAc through a β-1,3 linkage. Core-2 is synthesized when GlcNAc is attached to core-1 through β-1,6, while the addition of Gal to core-2 through β-1,4 results in the synthesis of extended core-2. The Sialic acid is attached through α-2,3 in both cases. The green color rectangle represents a generic protein with an *O*-glycosylation site.

The core-2 structure was synthesized by first making core-1. The reactions were confirmed with gel shift assays (Figure 31). Clear shifts could be observed with the addition of each sugar when compared to the controls. To core-1, GlcNAc was added enzymatically via

core-2 synthase, and a shift in the band confirmed the success of the reaction (Figure 31). Finally, the HBGT21 enzyme was utilized to add Gal, producing extended Core-2.

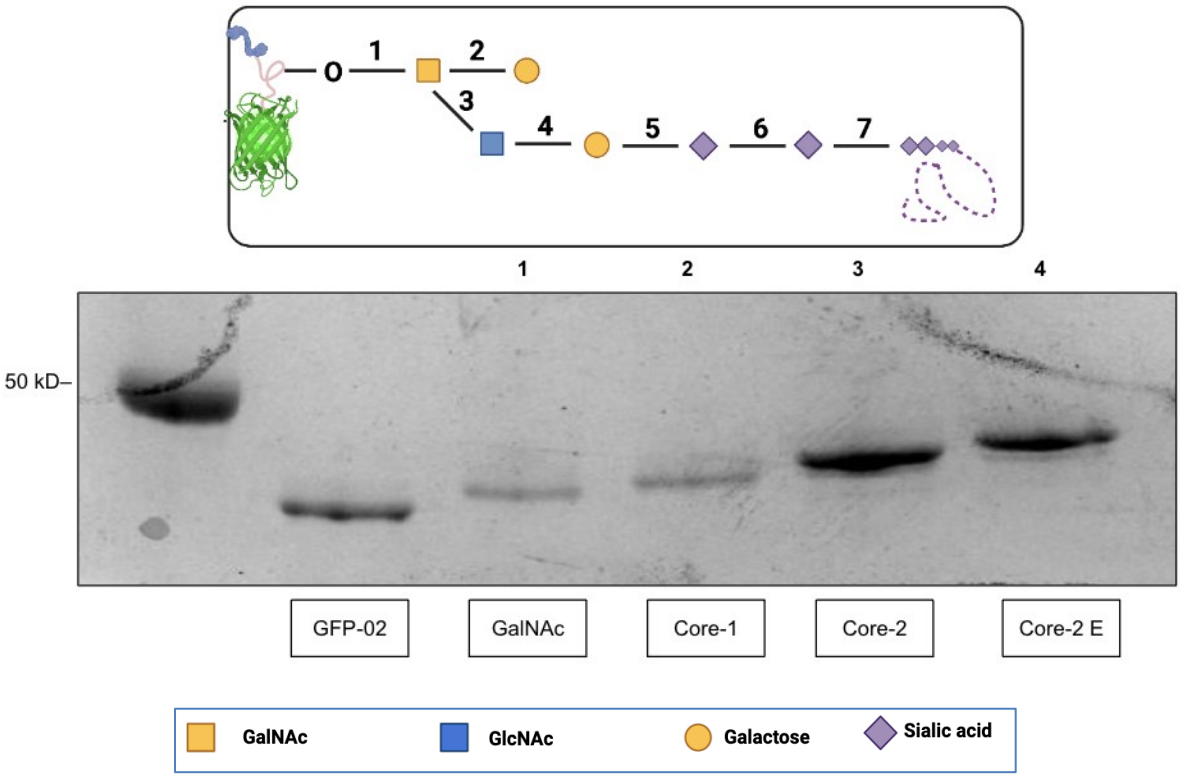

Figure 31. Gel shift assay confirming the success of the addition of different sugars to make extended core-2.
The upper panel displays the proposed arrangement to synthesize and polysialylate the extended core-2 structure, utilizing seven specific enzymes: GalNAcT (1), DGT-13 (2), BHV05 (3), HBGT-21 (4), BTS-05 (5), CST-II (6), and bPST109 (7). The details of enzymes are included in chapter 2. With the addition of each sugar, there was a noticeable shift, indicating the successful completion of steps 1 to 4.

Next in the process was sialylation, which involved using enzyme BTS-05 to add Sia to the β-1,4 linked galactose in the extended core-2. The gel shift assay confirms the addition of Sia (Figure 32). This was followed by a CST-2 which was also successful as could be confirmed with shifts in bands. However, both reactions were not entirely successful and resulted in

multiple bands with varying degrees of glycosylation. The protein was then purified and subjected to a polysialylation enzymatic reaction using bPST109. The results were exceptional, with nearly all of the protein undergoing polysialylation (Figure 32).

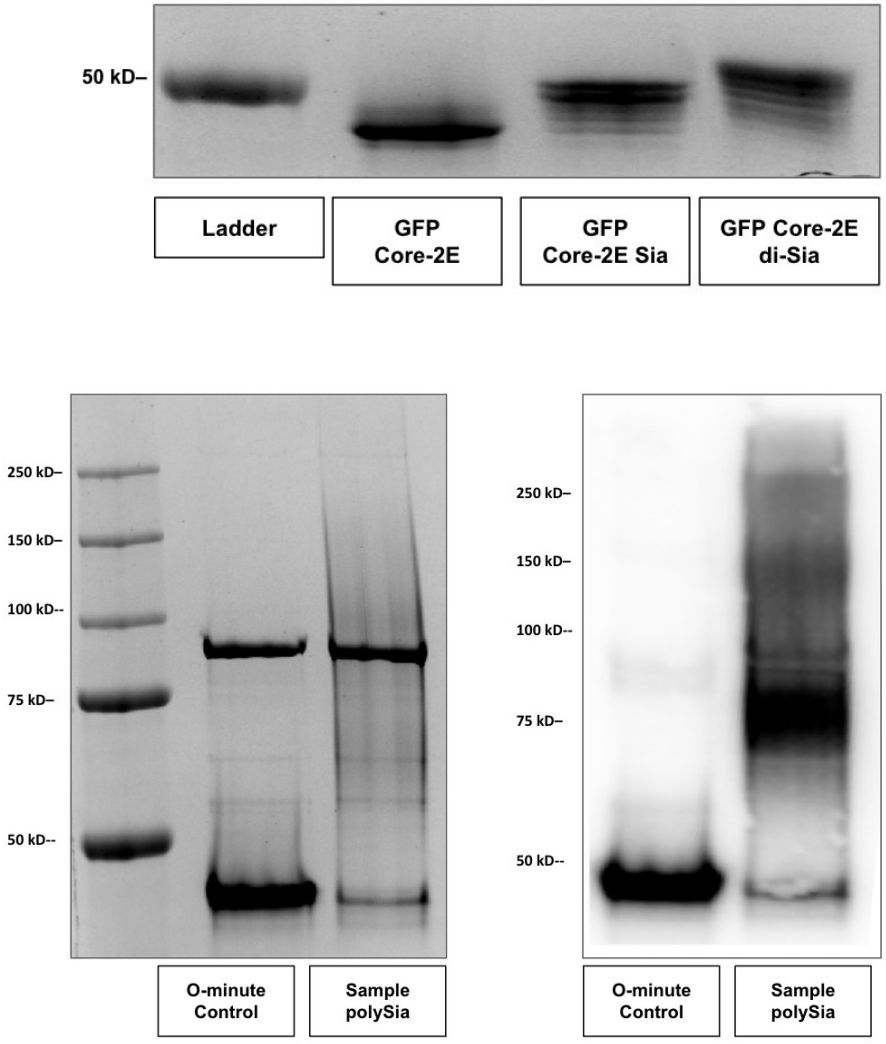

Figure 32. The CST-1, CST-2, and bPST-109 reactions.
Panel A, the gel shift assay validates the positive outcomes of both BTS-05 and CST-2 reactions. Notably, the bands exhibit clear shifts that indicate different degrees of sialylation. Panel B, a Coomassie gel on the left and an anti-polySia blot on the right with a 0-minute negative control are presented for bPST-109 reaction, successfully affirming the polysialylation process.

Chapter 5: Discussion

In our research to identify polysialylated proteins, we tried two methods: proximity labeling using TurboID-EndoN$_{DM}$ and enzymatic biotinylation of polySia using CMP-Sia-S-S-Biotin. However, we encountered issues with the former due to autobiotinylation, which could mask the detection of biotinylation of the targeted polysialylated protein. Decreasing the concentration of TurboID-EndoN$_{DM}$ could not improve the results and even at 100:1 of A1AT polySia to TurboID-EndoN$_{DM}$ concentration the, autobiotinylation persisted. We attempted to address this problem by replacing the lectin segment with a smaller scFv lectin, but this resulted in even higher autobiotinylation which happened during its expression in *E.coli*.

To avoid autobiotinylation, we suggest using ascorbate peroxidase (apex) -based proximity labelling(Figure 33)[123]. Apex-2 has the advantage of remaining inactive unless exposed to H_2O_2 and becomes active for less than a millisecond upon exposure. In addition, the labelling process can also be better controlled by stopping it with a quenching buffer[123]. This approach could potentially help us recover more polysialylated proteins with streptavidin beads for further analysis.

The second method utilized CMP-Sia-S-S-Biotin, a modified Sialic acid that showed some potentials for future experiments. It was synthesized through a click reaction between CMP-SiaAz and disulfide alkyne. The enzymatic addition of CMP-Sia-S-S-Biotin to polySia NCAM proceeded as planned, except for the part that involved the cleavage of disulfide bond that would potentially get rid of attached biotin-streptavidin. The reduction of disulfide bond is necessary for producing samples free of streptavidin beads as previously, Willis lab developed a method based on immobilization of the EndoN$_{DM}$ lectin. The biotinylated AviTag- EndoN$_{DM}$ was immobilized on streptavidin beads and then used to capture polysialylated proteins. The method

had a major drawback in that most of the peptides in the mass spectra were attributed to $EndoN_{DM}$ lectin, which made the method less sensitive[106].

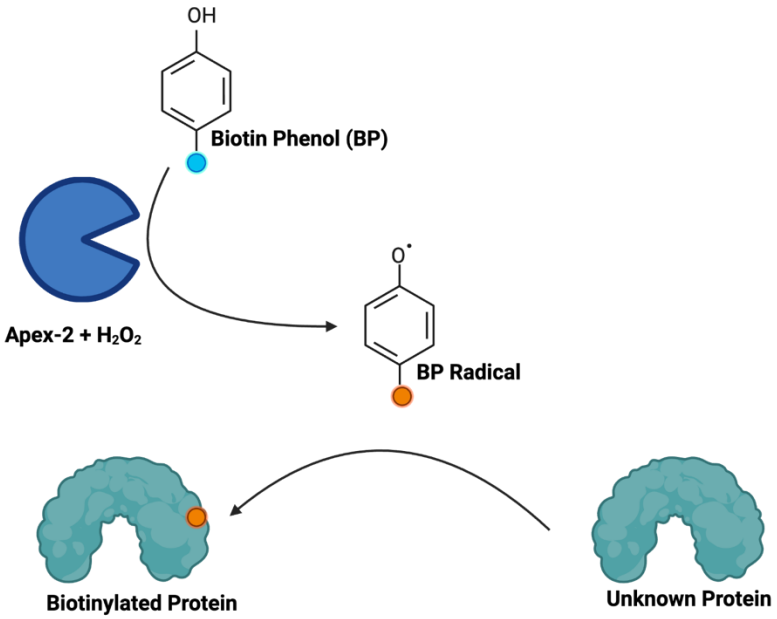

Figure 33. The Apex-2 biotinylation.
The Apex-2, in the presence of H_2O_2 produces biotin phenol radical that biotinylates the available protein in its vicinity.

Several attempts were made to detach the biotin-streptavidin from polysialylated NCAM by reducing the disulfide bond. Unfortunately, all the attempts turned out to be unsuccessful. A streptavidin blot showed that a sample that was not treated with streptavidin-beads and when incubated with DTT resulted in the removal of biotin. We wondered if the lack of elution could be attributed to non-specific binding of NCAM to the streptavidin. NCAM is a single pass membrane protein and also contains numerous disulfides, which may expose internal hydrophobic areas of the protein upon treatment with reducing agents. To confirm this hypothesis, GFP-02 polySia was used as an alternative. It only contains a single disulfide bond

and when we isolated biotinylated GFP-02 polySia on streptavidin-beads and then treated with the same reducing conditions, we observed that GFP-02 polySia was successfully eluted from the beads. We therefore concluded that this strategy for immobilization of polysialylated proteins followed by reduction to release the proteins would not be as useful as we expected in determining the identity of new polysialylated proteins as most are likely membrane proteins and would likely behave similar to NCAM by sticking to the beads. But the method did get rid of the lectin, $EndoN_{DM}$, it is advised to analyze the samples with mass spectrometry and compare the findings to the lectin method. It may also be worth trying a different linker, such as a photocleavable linker or one that can be cleaved with mild acidic conditions[124]. However, it is crucial to note that any strategy would have to account for bPST109 acceptance.

The GFP-02 diSia samples when sent for mass spectrometry, revealed the presence of three glycosylation sites, although only two glycosylation sequences were inserted. All threonine-containing sequences were analyzed for Isoform-Specific O-Glycosylation Prediction (IsoGlyP) values and yielded low results, leaving the origin of the third site unclear. To address this, a TEV cut site between GB1 and Sequons could be cleaved to figure out if the third site is in GB1 or in the remaining part of the protein (Seq-Seq-GFP). Alternatively, using different primers, new constructs could be developed to isolate different parts of the construct and identify which third threonine is getting glycosylated. Once the threonine is identified, could be confirmed with single site mutagenesis kit followed by its glycosylation and analysis with proteomics. In fact, generating various fragments of the construct utilizing primers may not be the most effective approach. While a particular fragment may not undergo glycosylation independently, it could, when part of the complete construct and vice versa. Thus, the optimal strategy is to polysialylate the protein first, then cleave it at the TEV site, and subsequently run it

on a Coomassie gel to identify which segment has the additional glycosylation site. This course of action would decrease the number of threonine residues that require further analysis through single site-directed mutagenesis.

Initially, different versions of the GFP construct were tested, one of which included a single sequone consisting of HisTag-GB1-Seq-GFP. Surprisingly, this specific construct did not undergo glycosylation. However, upon adding a second sequone, both the newly added sequone, and the first sequone got glycosylated. Additionally, a third glycosylation site also appeared. Previous studies have established that proline can increase the likelihood of threonine glycosylation at various positions (-9, -7, -6, -5, -3, -1, +2, +3, +6, +7, and +9)[125]. In our construct, there are two threonine residues, one in the GB1 region and the other in the GFP region, that fall within this range and could potentially undergo glycosylation. However, further investigation is required to validate this possibility.

When GFP02 core-1 polySia was incubated with Jurkat T cells initially, it should some potential initially, but the results could not be reproduced. The higher fluorescence resulting from GFP-02 polySia led to a shift in the peak compared to the negative controls. More importantly, the addition of colominic acid caused a backward shift. Unfortunately, no more ligand was available from the same batch and when the experiment was repeated with new batches of GFP polySia, it did not yield similar results. The old and new GFP-02 polySia batches were compared, and it was observed that the CST-2 reaction was not as successful in the later batches as in the first batch. Only one additional peak was observed after the CST-2 enzymatic reaction, which could potentially result in the synthesis of one polySia chain and could affect the avidity of the ligand. It was decided to create a core-2 structure. This would potentially result in more than one polySia chain and could lead to a ligand with higher avidity. The core-2 structure

was synthesized, and the reaction yielded promising results. However, neither reaction, BTS-05 nor CST-2, went to completion as multiple bands were observed. It is difficult to predict the structure even with mass spectrometry analysis, as the CST-2 has the potential to add more than one α-2,8 Sia. Additionally, it could also add one or more Sias on the galactose that is part of the core-1 branch of the underlying glycan.

The GFP-02 core-2 polySia is ready for testing with a cell line. Thanks to the kind support of the Macauley lab, we have access to CHO cells, both with and without the siglec-11 receptor. We also have a cell line that carries a mutated version of Siglec-11 with an arginine mutation that is known to be crucial for Sia interactions[18]. By incubating the GFP-02 core-2 polySia with these cell lines, we may potentially develop a reliable method to visualize and confirm the presence of polySia receptors (Figure 34). However, it is important to note that CHO cells also express polySia on their surfaces, which could influence the GFP-02 core-2 polySia's interaction with siglec-11. To account for this, we could optimize the magnetic-Beads-EndoN-based method discovered by Willis' Lab to remove polySia prior to testing[106].

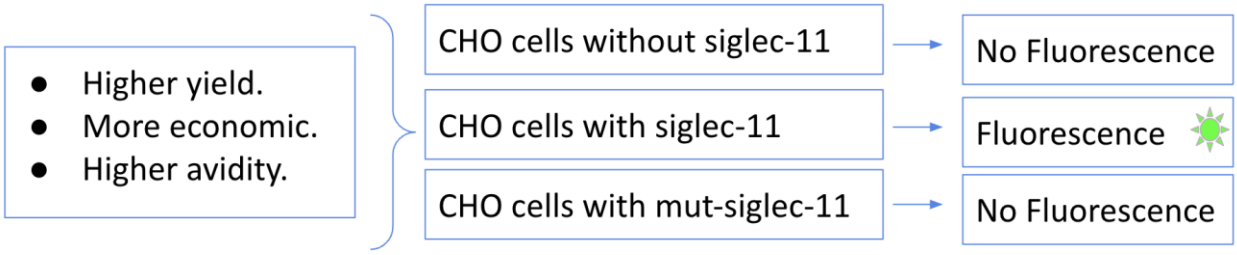

Figure 34. Cho cells expressing siglec-11 could be used to confirm that the method is working. On the left side the new GFP-02 core-2 polySia has been described which has the potential of higher avidity and is more economical as the reactions are more efficient and most of the protein gets polysialylated. In the middle CHO cells with different version of siglec-11 are included while on the right side the expected results are shown.

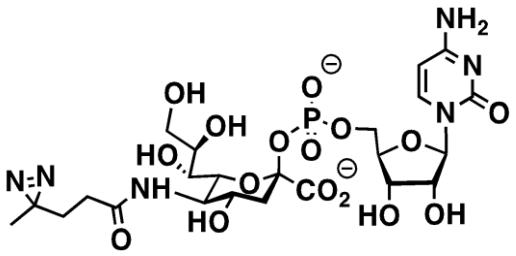

Figure 35 The structure of Sia-Diazirine

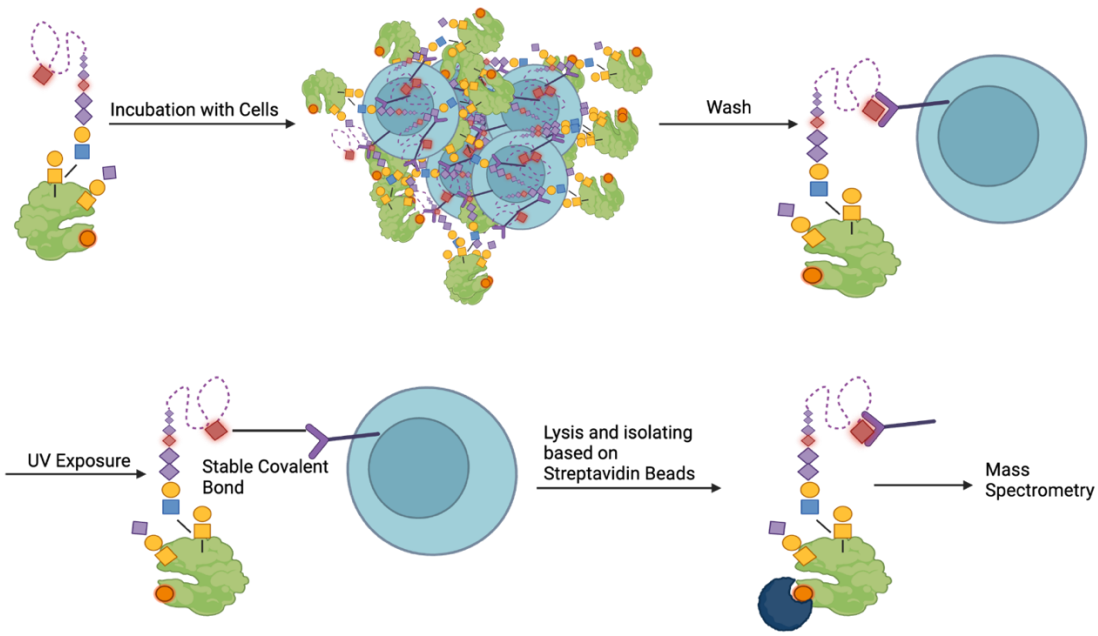

Figure 36. Proposed method involving Sia diazirine could be used to extract polySia receptors.

The Sia diazirine is enzymatically added to the polySia chain on a protein with biotinylated AviTag. Diazirine could potentially make a covalent bond when exposed to UV light and the biotin could be utilized to extract the protein with streptavidin beads followed by analysis with mass spectrometry.

Once the presence of receptor(s) is confirmed, additional research could be conducted to identify them. To discover polySia receptors, a polysialylated AviTag protein may be created

using a mixture of CMP-Sia and CMP-Sia-diazirine (Figure 35). CMP-Sia-diazirine is a modified Sia containing a diazirine group at carbon-5. Under ultraviolet light, the diazirine loses nitrogen gas and converts into a carbene ion, which could interact with polySia receptor(s) and could form a stable covalent bond[126]. The resulting protein-polySia-receptor conjugate could be isolated on streptavidin-agarose beads, and mass spectrometry analysis could be utilized to identify the attached protein(s) (Figure 36). The identified receptor(s) could then be validated in T and NK cells lacking these receptors, which can be generated through siRNA or CRISPR-Cas9 techniques. Alternatively, the receptor(s) could also be overexpressed.

To summarize, we have established the foundation for two techniques that has the potential to contribute to the advancement of polySia research. With the development of two probes, we can tackle two of the most crucial aspects of polySia research: the identification of polysialylated proteins and receptors for polySia. The discovery of these proteins can potentially provide valuable insights into the role of polySia in both health and disease, paving the way for new breakthroughs and developments.

.....

Bibliography

[1] Vakari.A, "Evolutionary forces shaping the Golgi glycosylation machinery: why cell surface glycans are universal to living cells," *Cold Spring Harbor perspectives in biology,* vol. 3, no. 6, 06/01/2011 2011, doi: 10.1101/cshperspect.a005462.

[2] Varki.A, "Glycan-based interactions involving vertebrate sialic-acid-recognizing proteins," (in En), *Nature,* BriefCommunication vol. 446, no. 7139, pp. 1023-1029, 2007-04-25 2007, doi: doi:10.1038/nature05816.

[3] Rambourg.A and Leblond. CP, "Electron microscope observations on the carbohydrate-rich cell coat present at the surface of cells in the rat," *The Journal of cell biology,* vol. 32, no. 1, 1967 Jan 1967, doi: 10.1083/jcb.32.1.27.

[4] Thiesler.H, Gretenkort.L,and Hildebrandt.H, "News and Views on Polysialic Acid: From Tumor Progression and Brain Development to Psychiatric Disorders, Neurodegeneration, Myelin Repair and Immunomodulation," *Frontiers in cell and developmental biology,* vol. 10, 04/04/2022 2022, doi: 10.3389/fcell.2022.871757.

[5] Tajik. A, Phillips. KL, Nitz. M, and Willis. LM, "A new ELISA assay demonstrates sex differences in the concentration of serum polysialic acid," *Analytical biochemistry,* vol. 600, 07/01/2020 2020, doi: 10.1016/j.ab.2020.113743.

[6] Falconer. RA, and Petrson. LH, "Polysialyltransferase: a new target in metastatic cancer," *Current cancer drug targets,* vol. 12, no. 8, 2012 Oct 2012, doi: 10.2174/156800912803251225.

[7] F. Lehmann, E. Tiralongo, and J. Tiralongo, "Sialic acid-specific lectins: occurrence, specificity and function," (in En), *Cellular and Molecular Life Sciences CMLS,* ReviewPaper vol. 63, no. 12, pp. 1331-1354, 2006-04-05 2006, doi: doi:10.1007/s00018-005-5589-y.

[8] Katja.M, Ostertag. E, and Stehle. T, "The polyfunctional polysialic acid: A structural view," *Carbohydrate research,* vol. 507, 2021 Sep 2021, doi: 10.1016/j.carres.2021.108376.

[9] Varki.A, "Chemical Diversity in the Sialic Acids and Related α-Keto Acids: An Evolutionary Perspective," (in en), research-article January 4, 2002 2002, doi: 10.1021/cr000407m.

[10] Shyamamsree. G, PMC, "Sialic acid and biology of life: An introduction," (in English), *Sialic Acids and Sialoglycoconjugates in the Biology of Life, Health and Disease,* pp. 1-61, 2024.

[11] Varki.A, Schnaar.R.L, and Schauer.R, "Sialic Acids and Other Nonulosonic Acids," (in en), Text 2017 2017, doi: https://www.ncbi.nlm.nih.gov/books/NBK453082/.

[12] Lewis, X. Chen, R. L. Schnaar, and A. Varki, "Sialic Acids and Other Nonulosonic Acids," Text 2022 2022, doi: https://www.ncbi.nlm.nih.gov/books/NBK579976/.

[13] Tanner. ME, "The enzymes of sialic acid biosynthesis," *Bioorganic chemistry,* vol. 33, no. 3, 2005 Jun 2005, doi: 10.1016/j.bioorg.2005.01.005.

[14] Wayne K. Chou, Stephan Hinderlich, a. Werner Reutter, and Martin E. Tanner*, "Sialic Acid Biosynthesis: Stereochemistry and Mechanism of the Reaction Catalyzed by the Mammalian UDP-N-Acetylglucosamine 2-Epimerase," (in en), research-article February 6, 2003 2003, doi: 10.1021/ja021309g.

[15] Pilatte.Y, Bignon.J and Lambre.CR "Sialic acids as important molecules in the regulation of the immune system: pathophysiologicai implications of sialidases in immunity." (accessed.

[16] Markus.A. *et al.*, "Sialic acid is a critical fetal defense against maternal complement attack," *The Journal of clinical investigation,* vol. 129, no. 1, 01/02/2019 2019, doi: 10.1172/JCI99945.

[17] R. L. Schnaar, R. Gerardy-Schahn, and H. Hildebrandt, "Sialic Acids in the Brain: Gangliosides and Polysialic Acid in Nervous System Development, Stability, Disease, and Regeneration," (in en), *https://doi.org/10.1152/physrev.00033.2013*, review-article 2014 Apr 01 2014, doi: 10.1152/physrev.00033.2013.
[18] Vikari. A, "Sialic acids as ligands in recognition phenomena," *FASEB journal : official publication of the Federation of American Societies for Experimental Biology,* vol. 11, no. 4, 1997 Mar 1997, doi: 10.1096/fasebj.11.4.9068613.
[19] Fraschilla.I, and Pillai.S, "Viewing siglecs through the lense of tumor immunology **https://doi.org/10.1111/imr.12526**
[20] Morel.M, and Pochard.P, "Frontiers | Abnormal B cell glycosylation in autoimmunity: A new potential treatment strategy," 2024, doi: doi:10.3389/fimmu.2022.975963.
[21] Zhang. Y, Wang. R, F. Y, and Ma. F, "The role of sialyltransferases in gynecological malignant tumors," *Life sciences,* vol. 263, 12/15/2020 2020, doi: 10.1016/j.lfs.2020.118670.
[22] Wurzner. R, "Evasion of pathogens by avoiding recognition or eradication by complement, in part via molecular mimicry," *Molecular immunology,* vol. 36, no. 4-5, 1999 Mar-Apr 1999, doi: 10.1016/s0161-5890(99)00049-8.
[23] Colley. KJ, Kitajima. K, and Sato. C, "Polysialic acid: biosynthesis, novel functions and applications," *Critical reviews in biochemistry and molecular biology,* vol. 49, no. 6, 2014 Nov-Dec 2014, doi: 10.3109/10409238.2014.976606.
[24] Nakata. D and Troy. FA, "Degree of polymerization (DP) of polysialic acid (polySia) on neural cell adhesion molecules (N-CAMS): development and application of a new strategy to accurately determine the DP of polySia chains on N-CAMS," *The Journal of biological chemistry,* vol. 280, no. 46, 11/18/2005 2005, doi: 10.1074/jbc.M508762200.
[25] Sato. C and Kitajima. K, "Disialic, oligosialic and polysialic acids: distribution, functions and related disease," *Journal of biochemistry,* vol. 154, no. 2, 2013 Aug 2013, doi: 10.1093/jb/mvt057.
[26] Angata. K and Fukuda. M, "Polysialyltransferases: major players in polysialic acid synthesis on the neural cell adhesion molecule," *Biochimie,* vol. 85, no. 1-2, 2003 Jan-Feb 2003, doi: 10.1016/s0300-9084(03)00051-8.
[27] Varbanov. H *et al.*, "Rescue of synaptic and cognitive functions in polysialic acid-deficient mice and dementia models by short polysialic acid fragments," *Neurobiology of disease,* vol. 180, 2023 May 2023, doi: 10.1016/j.nbd.2023.106079.
[28] Liao. H, Klaus. C, and Neumann. H, "Control of Innate Immunity by Sialic Acids in the Nervous Tissue," *International journal of molecular sciences,* vol. 21, no. 15, 07/31/2020 2020, doi: 10.3390/ijms21155494.
[29] Hildebrandt. H, Muhlenhoff. M, and G.-S. R, "Polysialylation of NCAM," *Advances in experimental medicine and biology,* vol. 663, 2010 2010, doi: 10.1007/978-1-4419-1170-4_6.
[30] Soroka. V, Kasper. C, and Poulsen. FM, "Structural biology of NCAM," *Advances in experimental medicine and biology,* vol. 663, 2010 2010, doi: 10.1007/978-1-4419-1170-4_1.
[31] Hildebrandt. H, Muhlenhoff. M, and G.-S. R, "Dissecting polysialic acid and NCAM functions in brain development," *Journal of neurochemistry,* vol. 103 Suppl 1, 2007 Nov 2007, doi: 10.1111/j.1471-4159.2007.04716.x.
[32] Quartu.M, Serra, MP, Boi. M, Ibba.C, and Del Fiacco.M, "Polysialylated-neural cell adhesion molecule (PSA-NCAM) in the human trigeminal ganglion and brainstem at prenatal and adult ages," (in En), *BMC Neuroscience,* OriginalPaper vol. 9, no. 1, pp. 1-13, 2008-11-06 2008, doi: doi:10.1186/1471-2202-9-108.

[33] Rollenhagen. M *et al.*, "Polysialic acid on neuropilin-2 is exclusively synthesized by the polysialyltransferase ST8SiaIV and attached to mucin-type o-glycans located between the b2 and c domain," *The Journal of biological chemistry,* vol. 288, no. 32, 08/09/2013 2013, doi: 10.1074/jbc.M113.463927.

[34] Muhlenhoff. M, Rollenhagen. M, Werneburg, and Hildebrandt. H, "Polysialic acid: versatile modification of NCAM, SynCAM 1 and neuropilin-2," *Neurochemical research,* vol. 38, no. 6, 2013 Jun 2013, doi: 10.1007/s11064-013-0979-2.

[35] Hunter. C, Derksen. T, Karathra. K, Baker. K, and Willis. L.M, "A new strategy for identifying polysialylated proteins reveals they are secreted from cancer cells as soluble proteins and as part of extracellular vesicles," (in en), 2022-09-02 2022, doi: 10.1101/2022.09.01.506237.

[36] Villanueva-Cabello. TM, Valenzuela. LD,*et al*, "Polysialic Acid in the Immune System," *Frontiers in immunology,* vol. 12, 02/11/2022 2022, doi: 10.3389/fimmu.2021.823637.

[37] Werneburg. S *et al.*, "Polysialylation and lipopolysaccharide-induced shedding of E-selectin ligand-1 and neuropilin-2 by microglia and THP-1 macrophages," *Glia,* vol. 64, no. 8, 2016 Aug 2016, doi: 10.1002/glia.23004.

[38] Close. BE and Collry. KJ, "In vivo autopolysialylation and localization of the polysialyltransferases PST and STX," *The Journal of biological chemistry,* vol. 273, no. 51, 12/18/1998 1998, doi: 10.1074/jbc.273.51.34586.

[39] Yang. P, Major. D, and Rutishauser. U, "Role of charge and hydration in effects of polysialic acid on molecular interactions on and between cell membranes," *The Journal of biological chemistry,* vol. 269, no. 37, 09/16/1994 1994.

[40] Jakobsson. E, Schwarzer. D, Jokilammi. A, and Finne. J, "Endosialidases: Versatile Tools for the Study of Polysialic Acid," *Topics in current chemistry,* vol. 367, 2015 2015, doi: 10.1007/128_2012_349.

[41] Jhonson. CP, Fujimoto. I, Rutishauser. U, *et al*, "Direct evidence that neural cell adhesion molecule (NCAM) polysialylation increases intermembrane repulsion and abrogates adhesion," *The Journal of biological chemistry,* vol. 280, no. 1, 01/07/2005 2005, doi: 10.1074/jbc.M410216200.

[42] Seidenfaden.R, Krauter.K, Schertzinger.F, Gerardy-Schahn.R, and Hildebrandt.H, "Polysialic Acid Directs Tumor Cell Growth by Controlling Heterophilic Neural Cell Adhesion Molecule Interactions," (in EN), research-article 2003-8-1 2003, doi: 10.1128/MCB.23.16.5908-5918.2003.

[43] Storms. SD and Rutishauser. U, "A role for polysialic acid in neural cell adhesion molecule heterophilic binding to proteoglycans," *The Journal of biological chemistry,* vol. 273, no. 42, 10/16/1998 1998, doi: 10.1074/jbc.273.42.27124.

[44] Kanato.Y, *et al*, Graduate School of Bioagricultural Sciences and Bioscience and Biotechnology Center, Nagoya 464-8601, Japan, K. Kitajima, N. U. Graduate School of Bioagricultural Sciences and Bioscience and Biotechnology Center, Nagoya 464-8601, Japan, C. Sato, and N. U. Graduate School of Bioagricultural Sciences and Bioscience and Biotechnology Center, Nagoya 464-8601, Japan, "Direct binding of polysialic acid to a brain-derived neurotrophic factor depends on the degree of polymerization," *Glycobiology,* vol. 18, no. 12, pp. 1044-1053, 2024, doi: 10.1093/glycob/cwn084.

[45] Bax. M, Van-Vliet. SJ, Litjens. M, and Van-Kooyk. Y, "Interaction of polysialic acid with CCL21 regulates the migratory capacity of human dendritic cells," *PloS one,* vol. 4, no. 9, 09/14/2009 2009, doi: 10.1371/journal.pone.0006987.

[46] Sato. C and Kitajima. K, "Polysialylation and disease," *Molecular aspects of medicine,* vol. 79, 2021 Jun 2021, doi: 10.1016/j.mam.2020.100892.

[47] Neumann.H, Shahraz.A, and Burgdorf.S, "Neuroprotective Effects of Polysialic Acid and SIGLEC-11 in Activated Phagocytic Cells," (in eng), Thesis 2016-03-30 2016, doi: urn:nbn:de:hbz:5n-43063.

[48] Lin. CH, Yeh. YC, and Yang. KD, "Functions and therapeutic targets of Siglec-mediated infections, inflammations and cancers," *Journal of the Formosan Medical Association = Taiwan yi zhi,* vol. 120, no. 1 Pt 1, 2021 Jan 2021, doi: 10.1016/j.jfma.2019.10.019.
[49] Schwarz. F *et al.*, "Paired Siglec receptors generate opposite inflammatory responses to a human-specific pathogen," *The EMBO journal,* vol. 36, no. 6, 03/15/2017 2017, doi: 10.15252/embj.201695581.
[50] Valentiner. U, Muhlenhoff. M, Lehmann. U, Hildebrandt. H, and Schumacher. U, "Expression of the neural cell adhesion molecule and polysialic acid in human neuroblastoma cell lines," *International journal of oncology,* vol. 39, no. 2, 2011 Aug 2011, doi: 10.3892/ijo.2011.1038.
[51] Rosa. P *et al.*, "Polysialic Acid Sustains the Hypoxia-Induced Migration and Undifferentiated State of Human Glioblastoma Cells," *International journal of molecular sciences,* vol. 23, no. 17, 08/24/2022 2022, doi: 10.3390/ijms23179563.
[52] Kurosawa. N, Yoshida. Y, Kojima. N, and Tsuji. S, "Polysialic acid synthase (ST8Sia II/STX) mRNA expression in the developing mouse central nervous system," *Journal of neurochemistry,* vol. 69, no. 2, 1997 Aug 1997, doi: 10.1046/j.1471-4159.1997.69020494.x.
[53] Oltmann.-N. I *et al.*, "Impact of the polysialyltransferases ST8SiaII and ST8SiaIV on polysialic acid synthesis during postnatal mouse brain development," *The Journal of biological chemistry,* vol. 283, no. 3, 01/18/2008 2008, doi: 10.1074/jbc.M708463200.
[54] Brennaman. LH, and Maness. PF, "Developmental regulation of GABAergic interneuron branching and synaptic development in the prefrontal cortex by soluble neural cell adhesion molecule," *Molecular and cellular neurosciences,* vol. 37, no. 4, 2008 Apr 2008, doi: 10.1016/j.mcn.2008.01.006.
[55] Weinhold. B *et al.*, "Genetic ablation of polysialic acid causes severe neurodevelopmental defects rescued by deletion of the neural cell adhesion molecule," *The Journal of biological chemistry,* vol. 280, no. 52, 12/30/2005 2005, doi: 10.1074/jbc.M511097200.
[56] Hildebrandt. H and Dityatev. A, "Polysialic Acid in Brain Development and Synaptic Plasticity," *Topics in current chemistry,* vol. 366, 2015 2015, doi: 10.1007/128_2013_446.
[57] Bonfanti. L, "PSA-NCAM in mammalian structural plasticity and neurogenesis," *Progress in neurobiology,* vol. 80, no. 3, 2006 Oct 2006, doi: 10.1016/j.pneurobio.2006.08.003.
[58] Aaron. LI and Chesselet. MF, "Heterogeneous distribution of polysialylated neuronal-cell adhesion molecule during post-natal development and in the adult: an immunohistochemical study in the rat brain," *Neuroscience,* vol. 28, no. 3, 1989 1989, doi: 10.1016/0306-4522(89)90015-8.
[59] Nacher. J, Lanuza. E, and McEvan. BS, "Distribution of PSA-NCAM expression in the amygdala of the adult rat," *Neuroscience,* vol. 113, no. 3, 2002 2002, doi: 10.1016/s0306-4522(02)00219-1.
[60] Shahbazian. S, Bokiniec. P, Berning. BA, McMullan. S, and Goodchild. AK, "Polysialic acid in the rat brainstem and thoracolumbar spinal cord: Distribution, cellular location, and comparison with mouse," *The Journal of comparative neurology,* vol. 529, no. 4, 2021 Mar 2021, doi: 10.1002/cne.24982.
[61] Miyata.S, Sato.C, and and Kitajima.K, "Glycobiology of Polysialic Acids on Sea Urchin Gametes." (accessed.
[62] Kitazume.S *et al.*, "Identification of polysialic acid-containing glycoprotein in the jelly coat of sea urchin eggs. Occurrence of a novel type of polysialic acid structure.," (in English), *Journal of Biological Chemistry,* vol. 269, no. 36, pp. 22712-22718, 1994/09/09 1994, doi: 10.1016/S0021-9258(17)31704-0.

[63] Simon. P *et al.*, "Polysialic acid is present in mammalian semen as a post-translational modification of the neural cell adhesion molecule NCAM and the polysialyltransferase ST8SiaII," *The Journal of biological chemistry,* vol. 288, no. 26, 06/28/2013 2013, doi: 10.1074/jbc.M113.451112.
[64] Velicky. P, Knofler. M, and Pollheimer. J, "Function and control of human invasive trophoblast subtypes: Intrinsic vs. maternal control," *Cell adhesion & migration,* vol. 10, no. 1-2, 03/03/2016 2016, doi: 10.1080/19336918.2015.1089376.
[65] Mastersteck. CM, Kedersha. NL, Drapp. DA, Tsui. TG, and Colley. KJ, "Unique alpha 2, 8-polysialylated glycoproteins in breast cancer and leukemia cells," *Glycobiology,* vol. 6, no. 3, 1996 Apr 1996, doi: 10.1093/glycob/6.3.289.
[66] Hromatka. B. S, *et al.*, "Polysialic acid enhances the migration and invasion of human cytotrophoblasts," *Glycobiology,* vol. 23, no. 5, pp. 593-602, 2024, doi: 10.1093/glycob/cws162.
[67] Winther. M, Berezin. V, and Walmod. PS, "NCAM2/OCAM/RNCAM: cell adhesion molecule with a role in neuronal compartmentalization," *The international journal of biochemistry & cell biology,* vol. 44, no. 3, 2012 Mar 2012, doi: 10.1016/j.biocel.2011.11.020.
[68] Larochelle. C *et al.*, "Melanoma cell adhesion molecule identifies encephalitogenic T lymphocytes and promotes their recruitment to the central nervous system," *Brain : a journal of neurology,* vol. 135, no. Pt 10, 2012 Oct 2012, doi: 10.1093/brain/aws212.
[69] Rosenstock. P, Bork. K, and Horstkorte. R, "Sialylation of Human Natural Killer (NK) Cells is Regulated by IL-2," *Journal of clinical medicine,* vol. 9, no. 6, 06/11/2020 2020, doi: 10.3390/jcm9061816.
[70] Rosenstock.P and Kaufmann.T, "Sialic Acids and Their Influence on Human NK Cell Function," (in en), *Cells,* Review vol. 10, no. 2, p. 263, 2021-01-29 2021, doi: 10.3390/cells10020263.
[71] R.-G. A, D.-M. C, and V. MA, "Polysialic acid is required for neuropilin-2a/b-mediated control of CCL21-driven chemotaxis of mature dendritic cells and for their migration in vivo," *Glycobiology,* vol. 21, no. 5, 2011 May 2011, doi: 10.1093/glycob/cwq216.
[72] Rey.-Gallardo. A *et al.*, "Polysialylated neuropilin-2 enhances human dendritic cell migration through the basic C-terminal region of CCL21," *Glycobiology,* vol. 20, no. 9, 2010 Sep 2010, doi: 10.1093/glycob/cwq078.
[73] Drake. PM *et al.*, "Polysialic acid, a glycan with highly restricted expression, is found on human and murine leukocytes and modulates immune responses," *Journal of immunology (Baltimore, Md. : 1950),* vol. 181, no. 10, 11/15/2008 2008, doi: 10.4049/jimmunol.181.10.6850.
[74] Kiermaier. E *et al.*, "Polysialylation controls dendritic cell trafficking by regulating chemokine recognition," *Science (New York, N.Y.),* vol. 351, no. 6269, 01/08/2016 2016, doi: 10.1126/science.aad0512.
[75] Rajput.C, Walsh. M. P, Eder B. N, Metitiri.B. N, Popova. A. P, and Hershenson. M. B, "Rhinovirus infection induces distinct transcriptome profiles in polarized human macrophages," (in en), *https://doi.org/10.1152/physiolgenomics.00122.2017,* research-article 2018 May 01 2018, doi: 10.1152/physiolgenomics.00122.2017.
[76] Shahraz.A *et al.*, "Anti-inflammatory activity of low molecular weight polysialic acid on human macrophages," (in En), *Scientific Reports,* OriginalPaper vol. 5, no. 1, pp. 1-17, 2015-11-19 2015, doi: doi:10.1038/srep16800.
[77] Liu.J, Zhang.X, Cheng.Y, and Cao.X, "Dendritic cell migration in inflammation and immunity," (in En), *Cellular & Molecular Immunology,* ReviewPaper vol. 18, no. 11, pp. 2461-2471, 2021-07-23 2021, doi: doi:10.1038/s41423-021-00726-4.

[78] Dobie.C and Skropeta.D, "Insights into the role of sialylation in cancer progression and metastasis," (in En), *British Journal of Cancer,* ReviewPaper vol. 124, no. 1, pp. 76-90, 2020-11-04 2020, doi: doi:10.1038/s41416-020-01126-7.
[79] Li. X *et al.*, "Polysialic acid-functionalized liposomes for efficient honokiol delivery to inhibit breast cancer growth and metastasis," (in EN), research-article 2023-12-31 2023, doi: 227606048.
[80] Soukhtehzari.S, Berish.R.B, Fazli.L, Watson P. H, and Williams K. C, "The different prognostic significance of polysialic acid and CD56 expression in tumor cells and lymphocytes identified in breast cancer," (in En), *npj Breast Cancer,* OriginalPaper vol. 8, no. 1, pp. 1-11, 2022-07-02 2022, doi: doi:10.1038/s41523-022-00442-w.
[81] Kloos. A *et al.*, "PolySia-Specific Retargeting of Oncolytic Viruses Triggers Tumor-Specific Immune Responses and Facilitates Therapy of Disseminated Lung Cancer | Cancer Immunology Research | American Association for Cancer Research," 2015, doi: 10.1158/2326-6066.CIR-14-0124-T.
[82] Maria.A.T.j, Guilpain. P, *et al,* "Intriguing Relationships Between Cancer and Systemic Sclerosis: Role of the Immune System and Other Contributors," 2019, doi: doi:10.3389/fimmu.2018.03112.
[83] Khan. L *et al.*, "The cancer-associated glycan polysialic acid is dysregulated in systemic sclerosis and is associated with fibrosis," *Journal of autoimmunity,* vol. 140, 09/22/2023 2023, doi: 10.1016/j.jaut.2023.103110.
[84] Gilabert.-Juan. J, Varea. E, and Nacher. J, "Alterations in the expression of PSA-NCAM and synaptic proteins in the dorsolateral prefrontal cortex of psychiatric disorder patients," *Neuroscience letters,* vol. 530, no. 1, 11/14/2012 2012, doi: 10.1016/j.neulet.2012.09.032.
[85] Varea. E *et al.*, "Expression of PSA-NCAM and synaptic proteins in the amygdala of psychiatric disorder patients," *Journal of psychiatric research,* vol. 46, no. 2, 2012 Feb 2012, doi: 10.1016/j.jpsychires.2011.10.011.
[86] Hane. M, Kitajima. K, and Sato. C, "Effects of intronic single nucleotide polymorphisms (iSNPs) of a polysialyltransferase, ST8SIA2 gene found in psychiatric disorders on its gene products," *Biochemical and biophysical research communications,* vol. 478, no. 3, 09/23/2016 2016, doi: 10.1016/j.bbrc.2016.08.079.
[87] Angata. K *et al.*, "Sialyltransferase ST8Sia-II assembles a subset of polysialic acid that directs hippocampal axonal targeting and promotes fear behavior," *The Journal of biological chemistry,* vol. 279, no. 31, 07/30/2004 2004, doi: 10.1074/jbc.M403429200.
[88] Murray. HC *et al.*, "Distribution of PSA-NCAM in normal, Alzheimer's and Parkinson's disease human brain," *Neuroscience,* vol. 330, 08/25/2016 2016, doi: 10.1016/j.neuroscience.2016.06.003.
[89] Perry. EK, Jhonson. M, and Attems. J, "Neurogenic abnormalities in Alzheimer's disease differ between stages of neurogenesis and are partly related to cholinergic pathology," *Neurobiology of disease,* vol. 47, no. 2, 2012 Aug 2012, doi: 10.1016/j.nbd.2012.03.033.
[90] Sato. C, Kitajima. k, "Structural Analysis of Polysialic Acid | SpringerLink," 2024, doi: 10.1007/978-4-431-77924-7_21.
[91] Nagae. M *et al.*, "Crystal structure of anti-polysialic acid antibody single chain Fv fragment complexed with octasialic acid: insight into the binding preference for polysialic acid," *The Journal of biological chemistry,* vol. 288, no. 47, 11/22/2013 2013, doi: 10.1074/jbc.M113.496224.
[92] Jokilammi.A, "InactIve endosIalIdase-based detectIon of bacterIal and oncofetal PolysIalIc acId." (accessed.
[93] Berek. D, "Size exclusion chromatography--a blessing and a curse of science and technology of synthetic polymers," *Journal of separation science,* vol. 33, no. 3, 2010 Feb 2010, doi: 10.1002/jssc.200900709.

[94] Khan.H.U, and Khan.H.U, "The Role of Ion Exchange Chromatography in Purification and Characterization of Molecules," (in en), 2012/11/07 2012, doi: 10.5772/52537.
[95] Svennerholm. L and Fredmann. P, "A procedure for the quantitative isolation of brain gangliosides," *Biochimica et biophysica acta,* vol. 617, no. 1, 01/18/1980 1980, doi: 10.1016/0005-2760(80)90227-1.
[96] Rode. B *et al.*, "Large-scale production and homogenous purification of long chain polysialic acids from E. coli K1," *Journal of biotechnology,* vol. 135, no. 2, 06/01/2008 2008, doi: 10.1016/j.jbiotec.2008.03.012.
[97] Hayrinen. J, Haseley. S, and Vliegenthart. JF, "High affinity binding of long-chain polysialic acid to antibody, and modulation by divalent cations and polyamines," *Molecular immunology,* vol. 39, no. 7-8, 2002 Nov 2002, doi: 10.1016/s0161-5890(02)00202-x.
[98] Guo. X, Elkashef. SM, and Falconer. RA, "Recent advances in the analysis of polysialic acid from complex biological systems," *Carbohydrate polymers,* vol. 224, 11/15/2019 2019, doi: 10.1016/j.carbpol.2019.115145.
[99] Inoue. S and Inoue. Y, "Developmental profile of neural cell adhesion molecule glycoforms with a varying degree of polymerization of polysialic acid chains," *The Journal of biological chemistry,* vol. 276, no. 34, 08/24/2001 2001, doi: 10.1074/jbc.M103336200.
[100] Chiu. CP, Lairson. LL, and wakarchuk. w, "Structural analysis of the alpha-2,3-sialyltransferase Cst-I from Campylobacter jejuni in apo and substrate-analogue bound forms," *Biochemistry,* vol. 46, no. 24, 06/19/2007 2007, doi: 10.1021/bi602543d.
[101] Lee. HJ *et al.*, "Structural and kinetic analysis of substrate binding to the sialyltransferase Cst-II from Campylobacter jejuni," *The Journal of biological chemistry,* vol. 286, no. 41, 10/14/2011 2011, doi: 10.1074/jbc.M111.261172.
[102] UniProt. "gne - UDP-glucose 4-epimerase - Campylobacter jejuni subsp. jejuni serotype O:2 (strain ATCC 700819 / NCTC 11168) | UniProtKB | UniProt.":UniProtKB-UniRule. https://www.uniprot.org/uniprotkb/Q0P9C3/entry (accessed.
[103] UniProt. "C1GalTA - Glycoprotein-N-acetylgalactosamine 3-beta-galactosyltransferase 1 - Drosophila melanogaster (Fruit fly) | UniProtKB | UniProt.":UniProtKB. https://www.uniprot.org/uniprotkb/Q7K237/entry (accessed.
[104] Ortiz.-Soto. ME and Seibel. J, "Expression of Functional Human Sialyltransferases ST3Gal1 and ST6Gal1 in Escherichia coli," *PloS one,* vol. 11, no. 5, 05/11/2016 2016, doi: 10.1371/journal.pone.0155410.
[105] Manzi. AE, Higa. HH, Diaz. S, and Varki. A, "Intramolecular self-cleavage of polysialic acid," *The Journal of biological chemistry,* vol. 269, no. 38, 09/23/1994 1994.
[106] Derksen.T "biotinylated AviTag- EndoNDM - Google Scholar." https://scholar.google.com/scholar?hl=en&as_sdt=0%2C5&q=biotinylated+AviTag-+EndoNDM+&btnG= (accessed.
[107] Branon. TC *et al.*, "Efficient proximity labeling in living cells and organisms with TurboID," *Nature biotechnology,* vol. 36, no. 9, 2018 Oct 2018, doi: 10.1038/nbt.4201.
[108] Rosmalen.M.V, Krom.M, and Merkx.M, "Tuning the Flexibility of Glycine-Serine Linkers To Allow Rational Design of Multidomain Proteins," (in EN), research-article December 7, 2017 2017, doi: 10.1021/acs.biochem.7b00902.
[109] Santala. V and L. U, "Production of a biotinylated single-chain antibody fragment in the cytoplasm of Escherichia coli," *Journal of immunological methods,* vol. 284, no. 1-2, 2004 Jan 2004, doi: 10.1016/j.jim.2003.10.008.
[110] Tonelli. AR, Rouhani. F, and Brantly. ML, "Alpha-1-antitrypsin augmentation therapy in deficient individuals enrolled in the Alpha-1 Foundation DNA and Tissue Bank," *International journal of chronic obstructive pulmonary disease,* vol. 4, 2009 2009, doi: 10.2147/copd.s8577.

[111] Visekruna.T, Ernst.B, and Palcic.M.M, "Sialyltransferases: expression and application for chemo-enzymatic syntheses," (in eng), NonPeerReviewed 2005 2005, doi: urn:urn:nbn:ch:bel-bau-diss73992.
[112] Freiberger. F *et al.*, "Biochemical characterization of a Neisseria meningitidis polysialyltransferase reveals novel functional motifs in bacterial sialyltransferases," *Molecular microbiology,* vol. 65, no. 5, 2007 Sep 2007, doi: 10.1111/j.1365-2958.2007.05862.x.
[113] Somplatzki. S, Muhlenhoff. M, and Boldicke. T, "Intrabodies against the Polysialyltransferases ST8SiaII and ST8SiaIV inhibit Polysialylation of NCAM in rhabdomyosarcoma tumor cells," *BMC biotechnology,* vol. 17, no. 1, 05/12/2017 2017, doi: 10.1186/s12896-017-0360-7.
[114] Hayen.H, Michels.A, and Franzke.J, "Dielectric Barrier Discharge Ionization for Liquid Chromatography/Mass Spectrometry," (in EN), research-article November 13, 2009 2009, doi: 10.1021/ac902176k.
[115] Martin. R. L, Thaysen-Andersena. M, Nicolle H. Packera and Giuseppe Palmisano*bc, "Structural analysis of glycoprotein sialylation – Part I: pre-LC-MS analytical strategies," (in en), 2013/10/28 2013, doi: 10.1039/C3RA42960A.
[116] Rosenstock.P, Bork.K, Massa.C, Selke.P, Seliger.B, and Horstkorte.R, "Sialylation of Human Natural Killer (NK) Cells Is Regulated by IL-2," (in en), *Journal of Clinical Medicine,* Article vol. 9, no. 6, p. 1816, 2020-06-11 2020, doi: 10.3390/jcm9061816.
[117] SANTARINO. I.B, SOLIVEIRA. . C. B, and OLIVEIRA-BRETT. A. M, "Protein reducing agents dithiothreitol and tris(2-carboxyethyl)phosphine anodic oxidation," 2024, vol. 23, pp. 114-117. [Online]. Available: https://pascal-francis.inist.fr/vibad/index.php?action=getRecordDetail&idt=26419931
[118] Pakula. AA and Simon. MI, "Determination of transmembrane protein structure by disulfide cross-linking: the Escherichia coli Tar receptor," *Proceedings of the National Academy of Sciences of the United States of America,* vol. 89, no. 9, 05/01/1992 1992, doi: 10.1073/pnas.89.9.4144.
[119] Krasowska.J, Olasek.M, Bzowska.A, Clark.P.L, and Wielgus-Kutrowska.B, "The comparison of aggregation and folding of enhanced green fluorescent protein (EGFP) by spectroscopic studies. | Spectroscopy: An International Journal | EBSCOhost," vol. 24, no. 3/4, p. 343, 2024, doi: 10.1155/2010/186903.
[120] ATCC, "Jurkat, Clone E6-1 - TIB-152 | ATCC."
[121] Li. H, Wang. HC, and Wang. M, "Configurational entropy modulates the mechanical stability of protein GB1," *Journal of molecular biology,* vol. 379, no. 4, 06/13/2008 2008, doi: 10.1016/j.jmb.2008.04.018.
[122] Audry. M, Jeanneau. C, Imberty. A, and Breton. C, "Current trends in the structure-activity relationships of sialyltransferases," *Glycobiology,* vol. 21, no. 6, 2011 Jun 2011, doi: 10.1093/glycob/cwq189.
[123] Nguyen. TMT, Kim. J, and Lee. M, "APEX Proximity Labeling as a Versatile Tool for Biological Research," *Biochemistry,* vol. 59, no. 3, 01/28/2020 2020, doi: 10.1021/acs.biochem.9b00791.
[124] Leriche. G, Chisholm. L, and Wagner. A, "Cleavable linkers in chemical biology," *Bioorganic & medicinal chemistry,* vol. 20, no. 2, 01/15/2012 2012, doi: 10.1016/j.bmc.2011.07.048.
[125] Christlet. TH and Veluraja. K, "Database analysis of O-glycosylation sites in proteins," *Biophysical journal,* vol. 80, no. 2, 2001 Feb 2001, doi: 10.1016/s0006-3495(01)76074-2.
[126] Tanaka. Y and Kohler. JJ, "Photoactivatable crosslinking sugars for capturing glycoprotein interactions," *Journal of the American Chemical Society,* vol. 130, no. 11, 03/19/2008 2008, doi: 10.1021/ja7109772.